

**University of Alberta**

**Practical Use of Multiple Geostatistical Realizations in Petroleum Engineering**

by

**Dawib R. Fenik**

A thesis submitted to the Faculty of Graduate Studies and Research  
in partial fulfillment of the requirements for the degree of

**Master of Science**

**Civil and Environmental Engineering**

©Dawib R. Fenik

Spring 2010

Edmonton, Alberta

Permission is hereby granted to the University of Alberta Libraries to reproduce single copies of this thesis and to lend or sell such copies for private, scholarly or scientific research purposes only. Where the thesis is converted to, or otherwise made available in digital form, the University of Alberta will advise potential users of the thesis of these terms.

The author reserves all other publication and other rights in association with the copyright in the thesis and, except as herein before provided, neither the thesis nor any substantial portion thereof may be printed or otherwise reproduced in any material form whatsoever without the author's prior written permission.

## **Examining Committee**

Alireza Nouri, Department of Civil and Environmental Engineering

Sirish L. Shah, Department of Chemical and Materials Engineering

Clayton Deutsch, Department of Civil and Environmental Engineering

Japan Trivedi, Department of Civil and Environmental Engineering

## **Abstract**

Ranking of multiple realizations is an important step when the processing time for a realization is large. This is the case in reservoir flow simulation and in other areas of geology, environmental and even medical applications. Significant uncertainty exists in all reservoirs especially at unsampled locations where the geological heterogeneity and connectivity are impossible to exactly predict between wells. Geostatistical techniques are used to construct models of static properties such as lithofacies, porosity, permeability and residual fluid saturations and provide multiple equally probable realizations of these properties.

The number of realizations that is required for modeling the uncertainty may be large; usually 100 realizations are considered enough to quantify uncertainty. However, this number of realizations is still too high for processing by a flow simulator. This thesis aims at developing a robust and reliable ranking methodology to rank the realizations using a static ranking measure. The outcome is the identification of the high, low, and intermediate ranking realizations for further detailed simulations. The methodology was developed for the steam assisted gravity drainage (SAGD) reservoir application.

This thesis will consider the cumulative oil produced ( $COP_{rate}$ ) and cumulative steam-oil-ratio (CSOR) as the ranking parameters in the flow simulations, hereafter called performance parameter. Connected hydrocarbon volume (CHV) was the parameter that was used in the ranking methodology as the static ranking measure. High calibration between the performance parameters and the CHV would indicate the success of the proposed ranking methodology. The ranking methodology was validated against the results of the flow simulations. The results indicate a mediocre correlation between the SAGD performance parameters and CHV. The ranking methodology was modified by incorporating the average reservoir permeability. Significant improvement in the correlation between the static ranking measure and the SAGD performance parameters resulted.

## **ACKNOWLEDGEMENT**

It is a great pleasure to thank my supervisors Professor Alireza Nouri and Professor Clayton V. Deutsch for all the guidance, support and assistance during the preparation of this thesis at the University of Alberta. This thesis would not have been possible without their constant support and encouragement.

I would like to emphasize special and strong thanks to Dr. Clayton V. Deutsch, Director in the School of Mining and Petroleum Engineering at the University of Alberta and Director of the Centre for Computational Geostatistics (CCG), for his many suggestions and constant support during this research. I must also thank all the students of CCG for their camaraderie.

I would like to express my gratitude to my parents Rahouma and Amna for their love at all times.

Lastly, I acknowledge my wife and daughter Amel for bringing endless happiness to my life and their encouragement throughout my studies.

# Table of Contents

<b>1</b>	<b>INTRODUCTION .....</b>	<b>1</b>
1.1	DESCRIPTION OF THE PROBLEM.....	2
1.2	SIGNIFICANCE OF THE RESEARCH .....	3
1.3	RESEARCH MOTIVATION.....	3
1.4	OVERALL APPROACH.....	4
1.5	RESEARCH OUTLINE .....	5
<b>2</b>	<b>LITERATURE REVIEW AND BACKGROUND .....</b>	<b>6</b>
2.1	LITERATURE REVIEW .....	6
2.1.1	<i>Introduction .....</i>	<i>6</i>
2.1.2	<i>Ranking Methodologies.....</i>	<i>7</i>
2.1.3	<i>Static Measures .....</i>	<i>7</i>
2.1.4	<i>Dynamic Measures .....</i>	<i>8</i>
2.2	RESEARCH BACKGROUND.....	12
2.2.1	<i>SAGD Technique.....</i>	<i>13</i>
2.2.2	<i>Flow Simulation .....</i>	<i>16</i>
2.2.3	<i>Geological Description of Alberta Oil Sands .....</i>	<i>16</i>
2.2.4	<i>Geostatistics .....</i>	<i>20</i>
2.2.5	<i>Ranking Realizations.....</i>	<i>23</i>
<b>3</b>	<b>INPUT DATA GENERATIONS .....</b>	<b>25</b>
3.1	GEOSTATISTICAL MODELS.....	25
3.1.1	<i>Data Generation .....</i>	<i>25</i>
3.1.2	<i>Monte Carlo Simulation.....</i>	<i>26</i>
3.1.3	<i>Normal Score Transformation (NScore).....</i>	<i>29</i>
3.1.4	<i>Sequential Gaussian Simulation (SGS).....</i>	<i>31</i>
3.1.5	<i>Back Transformation .....</i>	<i>37</i>
3.1.6	<i>Sequential Indicator Simulation (SIS).....</i>	<i>41</i>
3.1.7	<i>Merging of the Realizations.....</i>	<i>45</i>
3.2	GENERATING REALIZATIONS .....	46
<b>4</b>	<b>THE RANKING METHODOLOGY .....</b>	<b>48</b>
4.1	INTRODUCTION.....	48
4.2	RANKING METHODOLOGY.....	48

<b>5</b>	<b>VALIDATION OF THE RANKING METHODOLOGY.....</b>	<b>52</b>
5.1	FLOW SIMULATION.....	52
5.2	RESULTS FROM FLOW SIMULATION.....	56
5.3	RANKING USING FLOW SIMULATION RESULTS .....	63
5.4	RESULTS FROM THE RANKING METHODOLOGY .....	65
<b>6</b>	<b>MODIFICATION TO THE RANKING METHOD .....</b>	<b>72</b>
6.1	THE NEED FOR THE MODIFICATION.....	72
6.2	MODIFICATION OF THE METHODOLOGY.....	73
6.3	RESULTS FROM THE MODIFIED RANKING METHOD .....	76
<b>7</b>	<b>CONCLUSIONS AND RECOMMENDATIONS .....</b>	<b>80</b>
7.1	SUMMARY .....	80
7.2	CONCLUSIONS .....	82
7.3	FUTURE WORK.....	84
	<b>REFERENCES .....</b>	<b>85</b>
<b>APPENDIX A</b>	<b>CODE OF CMG-STARS .....</b>	<b>89</b>

## **List of Tables**

Table 2-1: Geological features of Cold Lake in Alberta (National Energy Board, 2000) ...	19
Table 3-1: Mean and variance values for different variables .....	27
Table 5-1: Variables with their values used to simulate SAGD case (CMG) .....	53
Table 5-2: The first 15 ranked realization based on CSOR & COP (CMG results) .....	64
Table 5-3: The first 20 ranked realizations for different window sizes .....	69
Table 5-4: Net cells, connected net cells and CHV for different realizations .....	70

## List of Figures

Figure 2-1: SAGD parallel wells (National Energy Board, 2004) .....	14
Figure 2-2: Injection and production processes (National Energy Board, 2004).....	15
Figure 2-3: Geographical map of the oil sands deposits in Alberta (National Energy Board, 2000).....	17
Figure 2-4: The oil migration from Rocky Mountains to McMurray (National Energy Board, 2004).....	18
Figure 2-5: Northeastern Alberta stratigraphic succession (National Energy Board, 2004) .....	19
Figure 2-6: Factors influencing oil sands projects (National Energy Board, 2006).....	20
Figure 2-7: An example of Probability Density Function (PDF).....	22
Figure 2-8: An example of Cumulative Distribution Function (CDF).....	22
Figure 3-1: Workflow diagram for generating data.....	26
Figure 3-2: The parameter file of MCS with mean and variance for each property in each geological facies .....	28
Figure 3-3: Normal Score Transformation ( <a href="http://www.statios.com/Resources/08-sgsim.pdf">www.statios.com/Resources/08-sgsim.pdf</a> ) 30	
Figure 3-4: Example of NScore transformation for sand porosity (R-5) .....	31
Figure 3-5: The parameter file for sequential Gaussian simulation .....	33
Figure 3-6: Sample sand permeability map simulated by SGS (R-5).....	34
Figure 3-7: Sample shale porosity map simulated by SGS (R-5) .....	34
Figure 3-8: Sample water saturation map in sand simulated by SGS (R-5) .....	35



Figure 3-9: Sample shale permeability map simulated by SGS (R-5).....	35
Figure 3-10: Sample shale porosity map simulated by SGS (R-5) .....	36
Figure 3-11: Sample water saturation map in shale simulated by SGS (R-5) .....	36
Figure 3-12: The parameter file of back transformation from Gaussian unit to original unit .....	38
Figure 3-13: Sample histogram of the back transformation of the sand permeability (R-5) .....	39
Figure 3-14: Sample histogram of the back transformation of the sand porosity (R-5) ..	39
Figure 3-15: Sample histogram of the back transformation of the shale permeability (R-5) .....	40
Figure 3-16: Sample histogram of the back transformation of the shale porosity (R-5) .	40
Figure 3-17: Sample facies map for R-5 .....	43
Figure 3-18: Sample facies map for R-52 .....	43
Figure 3-19: Parameter file of SIS .....	44
Figure 3-20: Sample maps of merged geological facies with reservoir properties (R-5) .	45
Figure 3-21: Sample maps of merged geological facies with reservoir properties (R-52)	46
Figure 3-22: Sample merged generated realizations for use in flow simulation.....	47
Figure 4-1: Example of window size .....	50
Figure 4-2: Directions of line of sight.....	50
Figure 4-3: Parameter file for connected hydrocarbon volume (CHV).....	51
Figure 5-1: Curve of relative permeability to oil and gas .....	54

Figure 5-2: Curve of relative permeability to oil and water .....	54
Figure 5-3: Permeability map as imported to CMG (R-50) .....	55
Figure 5-4: Porosity map as imported to CMG (R-50) .....	55
Figure 5-5: The oil volume per unit area before drainage (R-50) .....	58
Figure 5-6: Oil volume per unit area after 10 years of drainage (R-50) .....	58
Figure 5-7: Temperature distribution after 10 years (R-50) .....	59
Figure 5-8: CSOR, COP and daily OP for R-50.....	59
Figure 5-9: Plot of OOIP vs. realization number (CMG results) .....	60
Figure 5-10: Histogram plot of OOIP (CMG results) .....	60
Figure 5-11: Plot of CSOR vs. realizations number (CMG results) .....	61
Figure 5-12: Histogram plot of CSOR (CMG results) .....	61
Figure 5-13: Plot of COP vs. realizations number (CMG results) .....	62
Figure 5-14: Histogram plot of COP (CMG results) .....	62
Figure 5-15: Correlation between CSOR and COP (CMG results) .....	63
Figure 5-16: Map for calculated CHV to compare with Figure 5-12 (R-50) .....	65
Figure 5-17: Maps of CHV at different window sizes (R-4).....	66
Figure 5-18: Maps of CHV at different window sizes (R-52).....	67
Figure 5-19: Maps of CHV at different window sizes (R-84).....	68
Figure 5-20: Plot of (a) OOIP , (b) COP, (c) CSOR vs. CHV at WS= 50 .....	71
Figure 6-1: Correlation of CHV with COP .....	74

Figure 6-2: Plot of COP with MCHV.....	77
Figure 6-3: Plot of CSOR with MCHV.....	78
Figure 6-4: Plot of COP with CSOR after MCHV .....	79

## **List of Nomenclature and Abbreviations**

### **Abbreviations**

CDF	Cumulative Distribution Function
CHV	Connected Hydrocarbon Volume
CMG	Computer Modeling Group
CNC	Connected Net Cells
CSOR	Cumulative Steam-Oil-Ratio
GSLIB	Geostatistical software library and user's guide
MCS	Monte Carlo Simulation
NC	Net Cells
OOIP	Original Oil In Place
PDF	Probability Distribution Function
SAGD	Steam Assisted Gravity Drainage Process
SCSOR	Stable Cumulative Steam-Oil-Ratio
SGS	Sequential Gaussian Simulation
SIS	Sequential Indicator Simulation
SOR	Steam-Oil-Ratio
WS	Window Sizes

## Symbols

$A$	Area or volume of interest
$F(k)$	Dimensional factor for permeability
$F(x)$	Random function
$i(u, k)$	Indicator of facies category $k$ at location $u$
$K$ (arithmetic)	Arithmetic permeability, mD
$K$ (harmonic)	Harmonic permeability, mD
$K$	Reservoir permeability, mD
$L$	Number of realizations
$m$	Mean of data
$N$	Number of grids
$OP_{rate}$	Oil production rate
$p$	Value of facies proportion
$P_R$	Reservoir pressure, kPa
$P, u, k$	Facies proportion variable for facies category $S_k$ at location $u$
$P_{10}, P_{50}, P_{90}$	Low, intermediate and high probability outcomes
$Prob [A,B]$	Probability of variables event
$R$	Realization
$S_a, S_h$	Facies categories
$S_o$	Oil saturation

SW	Water saturation
T	Reservoir temperature, °C
u	A vector indicating the location in a two or three dimensional space
x, y	Values of random variables X and Y
X,Y	Random variables
z	Data value in original unit

### **Greek Letters**

$\lambda$	Average weight
$\phi$	Porosity
$\rho$	Correlation between different variables

# Introduction

---

Ranking of realizations is considered as an important step before flow simulation can be performed. The idea of ranking was first published in 1992 in the context of reservoir modeling (Ballin et al, 1992). The idea is to use simple criteria to rank realizations and then conduct the full flow simulation on only a few selected realizations, e.g., the P10, P50 and P90 realizations.

An important problem in reservoir management is the uncertainty quantification in the reservoir flow response for improved reservoir exploitation. Uncertainty is always present in the reservoir studies due to the reservoir formation heterogeneity and sparse well data. The uncertainty assessment can be obtained by generating a large number of realizations using geostatistical tools. These realizations are then ranked to provide a reliable basis for flow simulation.

There are some significant advantages to the ranking of the realizations. The main advantage is the minimization of the number of flow simulations, and thus, less computational demand, and more accurate management decisions for the same CPU and professional time. Usually a large number of realizations are generated using geostatistical tools. These are then used in more detailed analysis to assess the production performance. A good ranking measure reduces the number of realizations required to achieve a designated level of precision in the uncertainty assessment (Deutsch, 2003). Good ranking criteria correctly identify the high (P90) and low (P10) realizations.

The production performance parameters include oil production rate ( $OP_{rate}$ ) and amount of steam used relative to oil production or steam-oil-ratio (SOR) (McLennan and Deutsch, 2005). SAGD production performance is affected by the geological heterogeneity of the reservoir. The connectivity and spatial distribution of facies, porosity, permeability and water saturation affect the production performance.

There are a number of ranking techniques that have been developed over years. Chapter two discusses these techniques in more details. This thesis considers local connected hydrocarbon volume as the ranking measure and investigates the correlation between the ranking measure and the SAGD production performance parameters.

## **1.1 Description of the Problem**

A large number of realizations are required to capture the limit cases that could be encountered. Extreme cases should be processed to ensure that production decision and strategies are not unduly affected by an unusually good or bad simulated realization (McLennan and Deutsch, 2004). A large number of realizations may be created quickly using the modern geostatistical tools; however, processing all these realizations in the simulator for decision making is costly and time consuming. The goal is to reduce the number of realizations subjected to detailed analysis. Due to computer limitations, it is only possible to perform flow simulation on a limited number of realizations (Deutsch, 2003).



Reducing this large number can be achieved through a ranking methodology that helps selecting the realizations for detailed simulation. The ranked realizations are then selected to help choose a base case and the extreme cases.

This research focuses on developing a ranking method for the SAGD application. Properties of the SAGD reservoir including porosity, permeability and water saturation were generated by geostatistical tools.

## **1.2 Significance of the Research**

The reason for choosing the SAGD case is the importance of the technique to the Alberta oil industry. The data used to characterize the SAGD reservoir are synthetic, see Chapter 3. The data include the geological and petrophysical properties. Although the data are synthetic, they are built within realistic ranges of the properties. Techniques developed in this research can be used for better and more efficient decision making and improved economical outcome.

## **1.3 Research Motivation**

The motivation of this study stemmed from the difficulties resulting from using conventional ranking measures. The performance parameters are considered to be dependent variables and are expensive to calculate. The ranking measures are considered to be independent variables and are easy to calculate. Characterization of oil and gas reservoirs requires geostatistical techniques that can identify the uncertainty associated with reservoir properties through generating multiple realizations of these properties. There could be hundreds or even thousands of realizations for each

property; this makes the problem more complicated. The ranking of realizations is the reasonable solution to reduce the number of realizations for more detailed flow simulations.

The SAGD success depends on the efficient connectivity of the steam chamber. This project will review the static methods such as connectivity, conductivity, net pore volume and specific well location to identify the uncertainty in  $OP_{rate}$  and SOR. In this project, the validity of the static measures will be evaluated by conducting flow simulations using all the realizations. The realizations will then be ranked from the highest to lowest COP (i.e the lowest to highest CSOR). The ranking methodology will be based on the correlation between the static ranking measures to the performance parameters that can be evaluated from reservoir simulations.

## **1.4 Overall Approach**

The overall approach of this research is to develop a ranking method that can reduce the number of realizations to be used in flow simulations by identifying the realizations that result in the P10, P50 and P90 of the reservoir productivity. The success of this ranking methodology will lead to saving time and improved reservoir management. Ranking based on connected hydrocarbon volume (CHV) is considered in this thesis.

The basic idea in this ranking methodology is to achieve high correlation between CHV and the reservoir performance parameters. Weak correlations are considered undesirable; realizations that rank low but perform well or vice versa must be investigated and the technique must be refined.

## 1.5 Research Outline

The thesis has been divided into seven chapters. The description of the simulation model to be used in the flow simulator, CMG, is shown in Appendix A.

- A literature review of the ranking measures is presented in Chapter 2. Also an overview of the SAGD process, the flow simulation used to produce the ranking parameters, geological models and geostatistical tools used in this work are presented in Chapter 2.
- Chapter 3 discusses the data generation by using the geostatistical codes.
- Chapter 4 demonstrates the ranking methodology implementation.
- Chapter 5 discusses ranking from detailed flow simulations and compares them with the same using the ranking methodology.
- Chapter 6 illustrates the modifications to the ranking method to improve the correlation between the outcomes of the ranking method and the reservoir performance parameters.
- Finally, the conclusions of the thesis and recommendations for future research are presented in Chapter 7.

# Literature Review and Background

---

## 2.1 Literature Review

### 2.1.1 Introduction

Much research has been carried out regarding the ranking of realizations. This literature review focuses on geostatistical measures that have been used for ranking the realizations. It highlights the strengths and limitations of the previously used ranking measures.

Most oil and gas reservoirs are associated with significant uncertainty. Accurate prediction of hydrocarbon recovery is an important challenge. Modern decision making requires an assessment of this uncertainty. For this reason, geostatistical techniques are being increasingly used for reservoir modeling. These techniques provide an estimate of reservoir properties as well as a measure of uncertainty.

Multiple equally probable realizations of the facies and petrophysical properties are generated by using the geostatistical tools. One problem arising from generating several realizations is the time required to simulate all these realizations. Randomly choosing a limited number of geological realizations will not accurately represent uncertainty. Ranking is also required when a significant variation in the variables is present. For example in SAGD reservoir case, the use of geostatistical modeling is to characterize and quantify the uncertainty in production performance resulting from geological uncertainty.

### 2.1.2 Ranking Methodologies

Ranking is a step that is required before flow simulation can be performed efficiently. The idea of ranking realizations was first published in 1992 in the context of stochastic reservoir modeling (Ballin et al, 1992). Two ranking categories were introduced in most of the studies. The first is static ranking and the second is dynamic ranking. Some researchers reviewed these categories including Deutsch and Srinivasan (1996), McLennan and Deutsch (2005) and Zanon et al (2005). Others used dynamic ranking measures in their studies including Ates et al (2003), da Cruz et al (2003), Wang and Kovscek (2002), McCarthy (1993), Saad et al (1996), Norrena and Deutsch (2002), and Idrobo et al (2002).

### 2.1.3 Static Measures

Static measures are the simplest to use for ranking realizations. They include the calculation of parameters such as connectivity, conductivity, and tortuosity. McLennan and Deutsch (2005) classified these measures into four categories: (1) volumetric which includes measures of the original oil in place (OOIP) and the net oil in place ( $OIP_{NET}$ ), (2) statistical measures that include average porosity, permeability and fluid saturation, (3) global connectivity that includes the calculation of the fraction for globally connected cells as well as calculation of average tortuosity, and (4) local connectivity that includes the fraction of locally connected cells. McLennan and Deutsch (2005) stated that ranking methods used for conventional reservoirs cannot be applicable to the SAGD recovery and other *in situ* recovery methods because the SAGD process depends on the efficient connection of the steam chamber to the surrounding reservoir.

Deutsch and Srinivasan (1996) used the static ranking measures. The work was divided into three categories: (1) simple statistics, (2) 3-D measures of connectivity, and (3) connectivity of specific well locations. A unique prediction of which static models produce similar flow results was one of their goals.

A ranking guide for SAGD was published by Deutsch and McLennan (2005). They used volume parameters as the ranking measure and these were correlated to steam-oil-ratio (SOR) and oil production rate ( $OP_{rate}$ ) from flow simulations.

All the above static measures use a global connectivity parameter which cannot be applied to the SAGD reservoirs. Only local connectivity measures can be used for SAGD, which is the focus of this thesis.

#### **2.1.4 Dynamic Measures**

Dynamic measures include:

- Random-Walk algorithms which measure the dynamic continuity or connectivity between the injector and producer wells; it calls for the solution of the pressure field (Deutsch and Srinivasan, 1996; McCarthy, 1993).
- Time-to-Flight algorithm which measures the travel time of a neutral tracer along the streamline (Wang and Kovscek, 2002).
- Tracer measures such as single-phase tracer simulation based on the first moment of tracer production data. Vertical tracer profiling (VTP) is used by

injecting or collecting tracer samples at different locations along the wellbore (Saad et al, 1996).

- Streamline Simulation such as swept volume calculation measure (Ates, et al, 2003; Wang and Kovscek, 2002; Idrobo et al, 2000).
- Water flood simulation (Hewett, 1986).

Dynamic ranking measures account for production mechanisms. There are some limitations in using such techniques. One limitation is that dynamic ranking tends to exceedingly depend on the simplifying flow-physics approximations rather than the underlying geological heterogeneity and uncertainty.

Deutsch and Srinivasan (1996) used rapid ranking measures to rank realizations. These measures are based on approximate flow simulations for simple processes. They included random-walk measures used to calculate the dynamic continuity between the injector and the producer well locations. These techniques always call for the solution to pressure field and require steam injection rate. The distribution time or lengths between the wells were tracked in order to measure the connectivity. The primary parameters used for correlation were breakthrough time, ultimate recovery, final rate, oil rate and intermediate recovery.

McCarthy (1993) used the random-walk as a ranking measure. His work showed how the random-walk method can provide an efficient and accurate alternative to the costly fine-scale finite difference computation for upscaling and image selection in reservoir

characterization. Different realizations of permeability distribution were also used in his work. The images had the following characteristics:

- (i) They produced large-scale variations obtained from surface mapping.
- (ii) They produced known data in grid blocks where data were available.
- (iii) They showed the same spatial variability as the data at scales relevant for flow simulations.

There are two limitations associated with using this method. The first is how to define fine enough grid images of the reservoir which is coarse enough that allows realistic fluid flow simulation. The second is to select proper few images that can represent all the reservoir area.

Saad et al (1996) used 3D interwell tracer measure for ranking realizations. This ranking method was based on the first moment of the tracer production data. Three types of two-phase flow simulations were performed. Two of these were based on stream tube and front tracking simulation while ignoring the gravity or pressure updates. New tracer test called vertical tracer profiling (VTP) was also used to rank the realizations. They conducted test by injecting and collecting tracer samples at different locations along the wellbore. In this work, no capillary pressure effect was considered. 100 realizations were ranked based on cumulative oil recovery, pore volume or average permeability of each realization, tracer breakthrough time, maximum tracer concentration, and mean swept pore volume from tracer production data.



The results obtained from the single-phase tracer simulation were compared with the ranking based on more accurate two-phase flow simulation of the water flood recovery process. Since the tracer breakthrough time is a function of the fastest flow path between the injector and the producer, no correlation was observed between the two methods. The reason is the higher permeability realizations have less oil due to early breakthrough and lower volumetric swept efficiency (Saad and Maroongroge, 1996). To improve the correlation, it was recommended to run the simulation for larger pore volumes.

Ates et al (2003) developed a ranking measure based on the streamline time-of-flight connectivity that was generated from a streamline simulation. The idea was to find the optimal level of vertical upscaling for a finite difference simulation. A direct measure of the volumetric sweep efficiency was evaluated by the time of flight that reflects the fluid front propagation at various times and also the one that reflects the connectivity at certain times. The swept volume simply represents the reservoir volume that corresponds to a time of flight less than or equal to a given time of interest. The time-of-flight connectivity rigorously accounts for the interaction between the flow field and the underlying heterogeneity. A direct measure of the volumetric sweep efficiency influenced by the heterogeneity as well as the well configuration was performed by the connectivity in the time-of-flight approach.

Wang and Kovscek (2002) also used the streamline measure for ranking the reservoir realizations with regard to the production history. History matching was performed by the unit mobility ratio of the streamline geometries. Most history matching techniques require a large number of flow simulations and are therefore computationally intensive (Wang and Kovscek, 2002). A rapid approach has been developed to rank a large suite of

realizations and select rationally a subset that honors the observed production data. A correlation between streamline properties and the corresponding flow simulation results was their objective.

Idrobo et al (2000) discussed the use of connectivity based on the streamline time-of-flight approach as a ranking method. The analysis of the results shows that volumetric sweep efficiency is highly correlated to the oil recovery process.

Another study for ranking was conducted by Norrena and Deutsch (2002) through selecting the optimal well location technique for fine-tuning with simulation. Their work included several steps: (1) construct an objective function that quantifies the performance of a well plan, (2) propose an initial well plan, (3) quantify the performance of the initial well plan, (4) perform random perturbation, (5) apply the simulation decision rule and accept or reject the perturbation, (6) repeat the fifth and sixth steps until the well plan optimizes the objective function. Their work was applied to a SAGD case, and their objective was to choose the optimal vertical location for a well pair located in the middle of the model.

## **2.2 Research Background**

This part presents an overview background of the models used in this research, a brief description of the SAGD technique, the flow simulation process, geological description of oil sands in Alberta, the geostatistics models, and finally the ranking approach.

Prediction of the reservoir performance is a challenging task for all petroleum companies. This challenge is due to the geological heterogeneity that exists in all reservoir properties. The heterogeneity cannot be characterized in a deterministic way leading to uncertainty. Prediction of the uncertainty can be quantified using the probability distribution of the properties in the geological site. The probability distribution requires the variable distribution to be known. The variable distribution can be generated using geostatistical models.

### **2.2.1 SAGD Technique**

SAGD is one of the most relevant *in situ* heavy oil recovery techniques in northern Alberta owing to the huge amount of oil reserves accessible with this technique. This technique which was first invented by Roger Butler in 1970, who explained the concept and the heat transfer mechanism.

SAGD is a conventional thermal recovery technique that works on the basis of the thermal reduction of the oil viscosity as the cold heavy oil is almost immobile because of high viscosity. Two parallel horizontal wells with vertical spacing of about 5 m are drilled in the formation as shown in Figure 2-1. The upper well is a steam injection well where steam heats the formation to increase the temperature and reduce viscosity of the oil. The lower well is the production well from which the heated oil can be drained and then pumped to the surface.

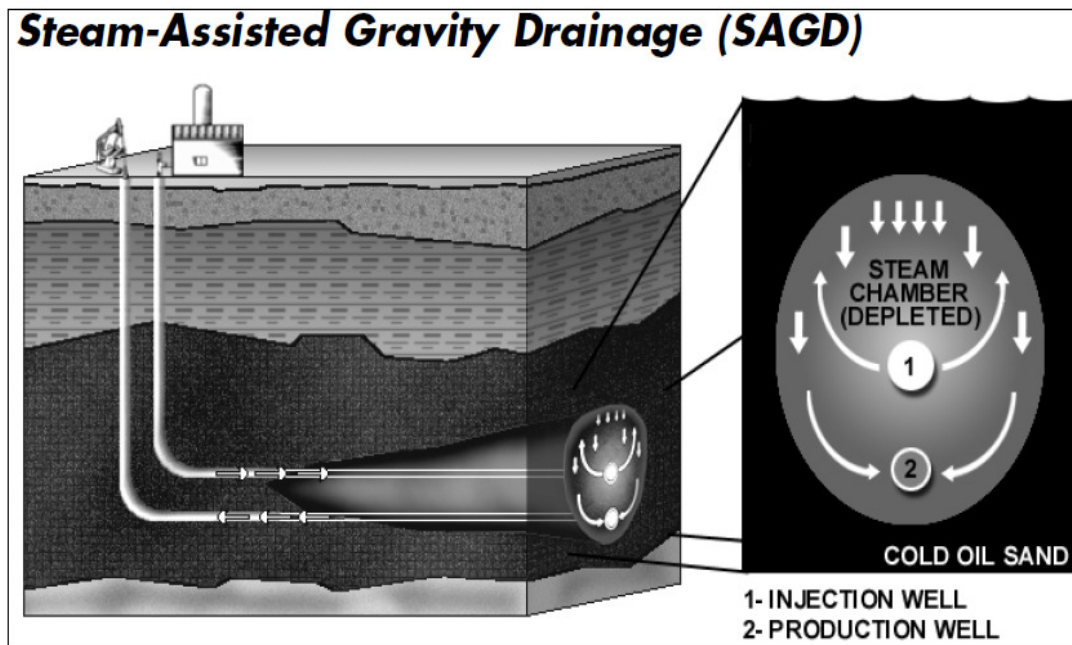
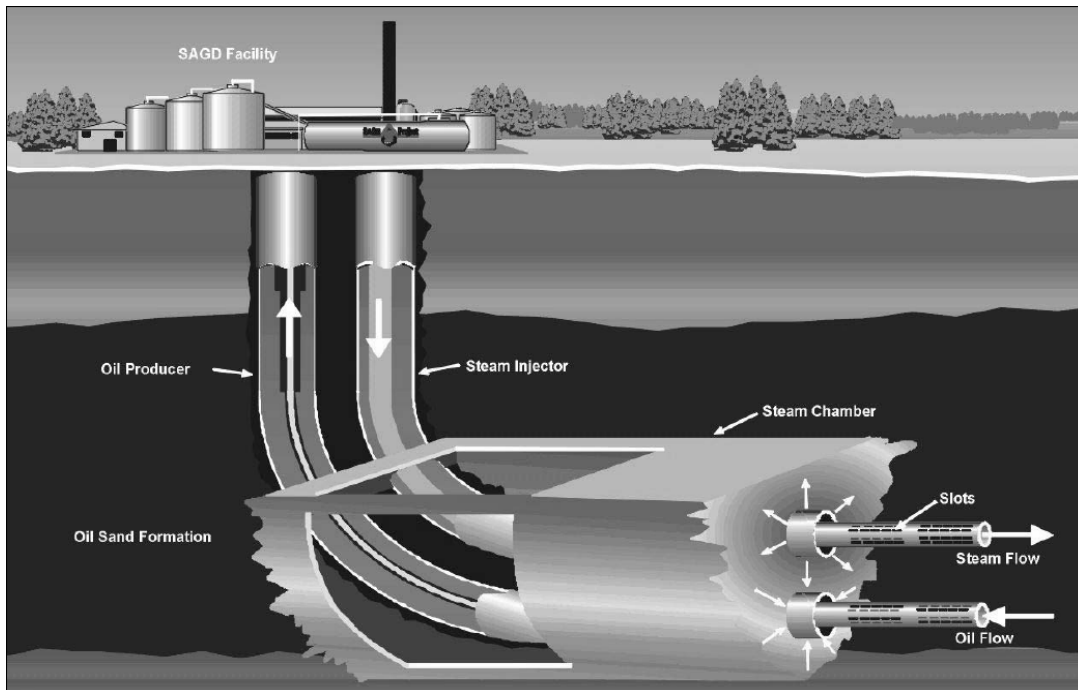


Figure 2-1: SAGD parallel wells (National Energy Board, 2004)

The producer well is located a few meters above the bottom of the pay. In practice, the horizontal wells have a length range from 500-1000 m. SAGD depends on the combustion of natural gas that is used to generate steam. The initial heating or preheating of the cold oil (heavy oil or tar) is very important to form the steam chamber. The heat is transferred by conduction, convection and by latent heat of steam to the formation through injector and producer during the preheating period. The heating is maintained from only the injector after putting the producer to normal operation.

The most expensive part of the SAGD operation is the steam generation. Figure 2-2 shows the steam flow through the injector and as the bitumen is heated up, the oil is pumped through the producer to the surface.



**Figure 2-2: Injection and production processes (National Energy Board, 2004)**

The steam-oil-ratio (SOR) is a measure of the thermal efficiency in SAGD. High SOR results in more natural gas combustion to generate the required steam, which has economic ramifications. Optimizing the steam injection rate to reduce the SOR is imperative in any SAGD project. Steam quality is another important factor that should be kept as high as possible, as low steam quality forms more condensate that flows toward the producer delivering only small amounts of heat to the oil. During the preheating phase, the steam zone is expected to grow laterally. Oil is drained down along the oil/steam interface to the production well.

There are some parameters that influence the SAGD processes. These include reservoir depth, length of the horizontal drilling, vertical spacing between the well pair, steam injection rate, steam temperature, steam pressure and the pressure drop between the

well pair. The success of a SAGD project depends on controlling these parameters to minimize the CSOR and maximize the COP.

### **2.2.2 Flow Simulation**

Flow simulation is the reservoir flow analysis after defining the boundary conditions that closely match the operational and reservoir conditions. Performing flow simulation helps to optimize the well design and the operational conditions. Reservoir performance predictions through flow simulation help to support reservoir management decisions.

CMG–STARS simulator is a widely used simulator in Alberta and around the world. CMG–STARS includes several features such as chemical/polymer flooding, steam injection and thermal options. It is mainly developed to model multiphase flow, *in situ* combustion and steam flooding in complex geological formations.

### **2.2.3 Geological Description of Alberta Oil Sands**

Since this study is applicable to oil sands, it is relevant to briefly describe the oil sand deposits in Alberta. Three main regions of Alberta's natural resources have been discovered which are the Athabasca, Cold Lake and Peace River as shown in Figure 2-3. The majority of the oil sand deposits in these three regions are located at the lower Cretaceous strata.



**Figure 2-3: Geographical map of the oil sands deposits in Alberta (National Energy Board, 2000)**

It has been debated that the geological formations of Alberta were first formed millions of years ago through runoff of sand and mud from the Rocky Mountains in the west and Precambrian shield in the east of Alberta as shown in Figure 2-4. However, The Peace River deposit comprises bitumen-rich sands from the Aptian-Albian Gething Formation, Ostracode Zone, and Bluesky Formation, which overlay Paleozoic and older Mesozoic strata. Stratigraphic and Sedimentology data indicates these sediments were deposited as the Boreal Sea inundated the area from the north (National Energy Board, 2000). Figure 2-5 shows a stratigraphic succession for northeastern Alberta.

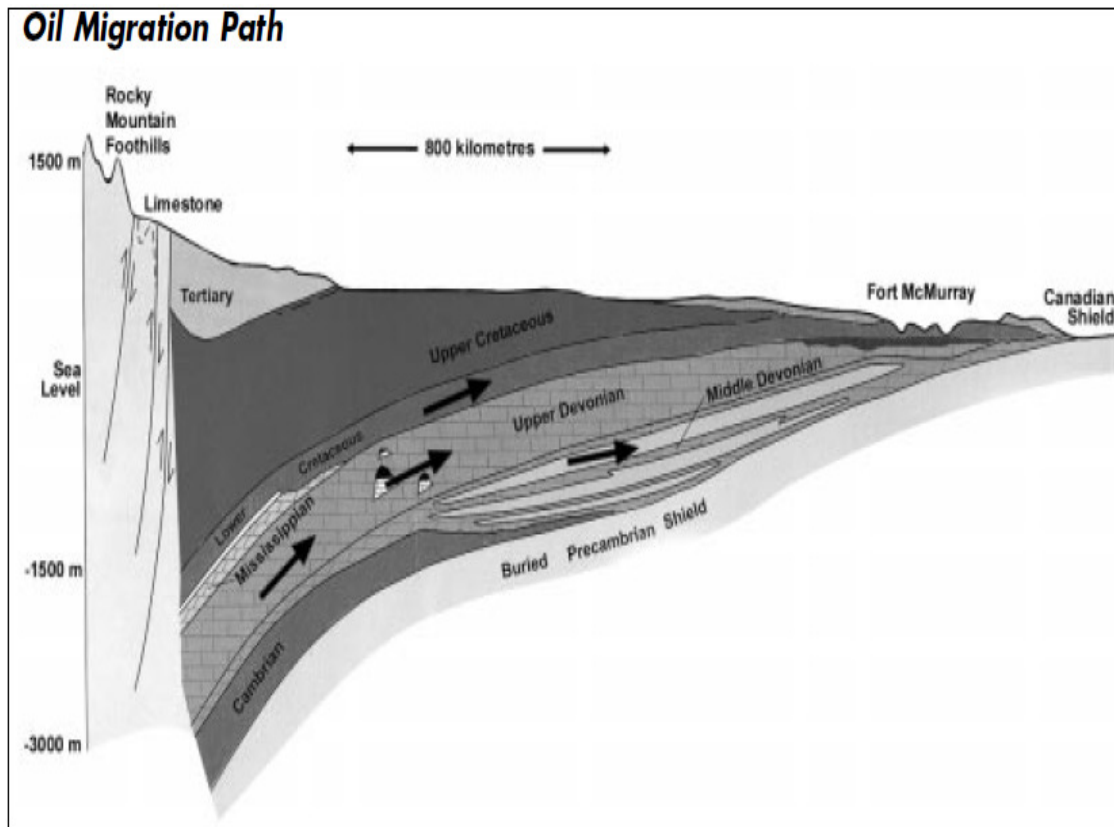


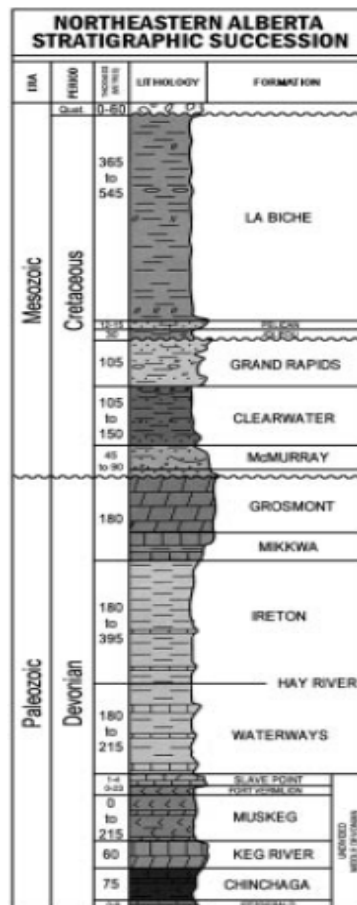
**Figure 2-4: The oil migration from Rocky Mountains to McMurray (National Energy Board, 2004)**

The area of this region has been estimated to be more than 6 million hectares. The Athabasca formation including Grand Rapids formation are buried at upper depth ranges of 200-400 m and lower depth ranges of 270-470 m, Wabiskaw or McMurray formation are buried at Mineable depth ranges of 0-120 m and *In situ* with depth ranges of 80-750 m. The Cold Lake formations including Grand Rapids, Clearwater and McMurray are buried at depth ranges from 275-525 m, 370-500 m and 420-600 m, respectively (see Table 2-1). The Athabasca oil sands are composed of approximately 70% sand and clay, 10% water and from 0 to 18% heavy oil or bitumen (Deutsch and McLennan, 2003). Figure 2-6 shows the properties of the oil sand formations.



**Table 2-1: Geological features of Cold Lake in Alberta (National Energy Board, 2000)**

	Area <sup>1</sup> (hectares)	Net Pay (metres)	Porosity (percent)	Water Saturation (percent)	Bitumen Saturation (percent)	Percent Bitumen by Weight	API Gravity (degrees)
Carbonate Deposits	26 000 - 1 190 000	5 - 29	14 - 27	25 - 48	52 - 75	3.5 - 8.0	8 - 23
McMurray Oil Sands	20 - 4 239 000	0.5 - 50	25 - 31	14 - 49	51 - 86	6 - 13	6 - 13
Grand Rapids Oil Sands	20 - 334 000	0.2 - 10	23 - 37	14 - 55	45 - 86	5 - 15	10 - 12

**Figure 2-5: Northeastern Alberta stratigraphic succession (National Energy Board, 2004)**

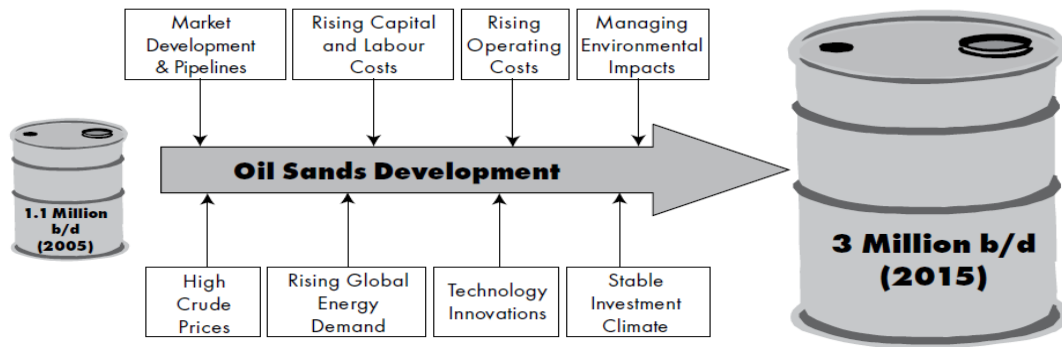


Figure 2-6: Factors influencing oil sands projects (National Energy Board, 2006)

#### 2.2.4 Geostatistics

Geostatistics is the study of spatiality and prediction of the probability distribution of a given property. Deutsch and Journel (1998) stated that geostatistics offers a collection of deterministic and statistical tools aimed at understanding and modeling spatial variability.

Geostatistics was originally applied to mining applications but has evolved as the method of choice for numerical models of environmental, mineral, and petroleum developments (Ricardo, 1999). Geostatistics is distinct from statistics in three respects: (1) geostatistics considers the source of the geological data, (2) geostatistics enables the analysis of spatial correlation between the geological data, (3) in geostatistics data at different scales are used and integrated (Deutsch, 2002).

There are some mathematical theories that are used in geostatistics including Bayes law, Laplace and Gaussian theorems. This part will provide a background for both Bayes law and Gaussian theorems.

Thomas Bayes (1702-1761) established a mathematical model using probability inference known as Bayes law. It was related to the conditional probability of some events. For example, if there are two events A and B then the probability can be calculated by the following equation:

$$P(A|B) = \frac{P(B|A) * P(A)}{P(B)} \quad 2-1$$

where:

P (A) is the marginal probability of Event A,

P (B) is the marginal probability of Event B,

P (A|B) is the conditional probability of Event A given Event B,

P (B|A) is the conditional probability of Event B given Event A.

Carl Friedrich Gauss (1777-1855) established the most widely used model known as Gaussian distribution. Historically it was called the law of error; it is also called the normal distribution. The Gaussian distribution is a continuous function in which the data clusters around the mean and the variance. The Gaussian curve is bell shaped at mean equal zero and variance equal to one as shown in Figures 2-7 and 2-8.

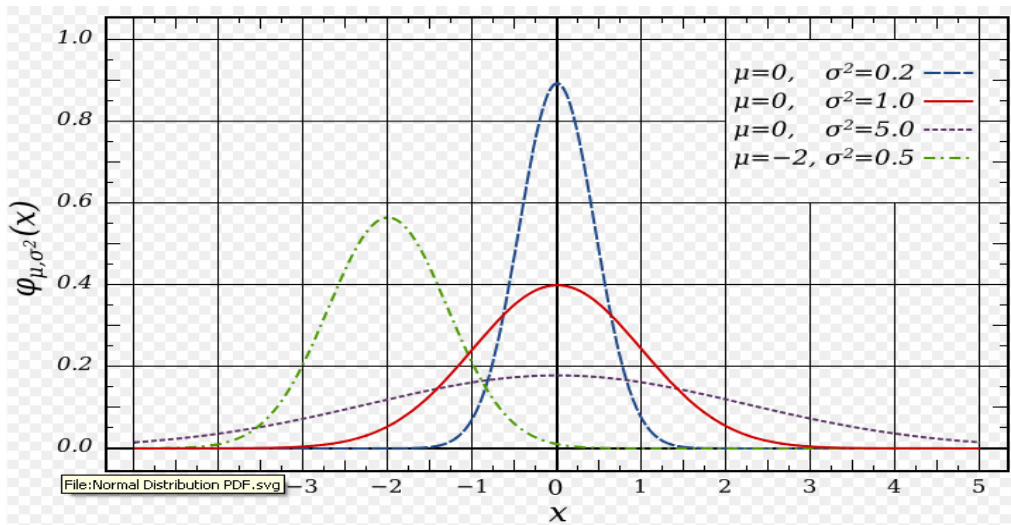


**Figure 2-7: An example of Probability Density Function (PDF)**

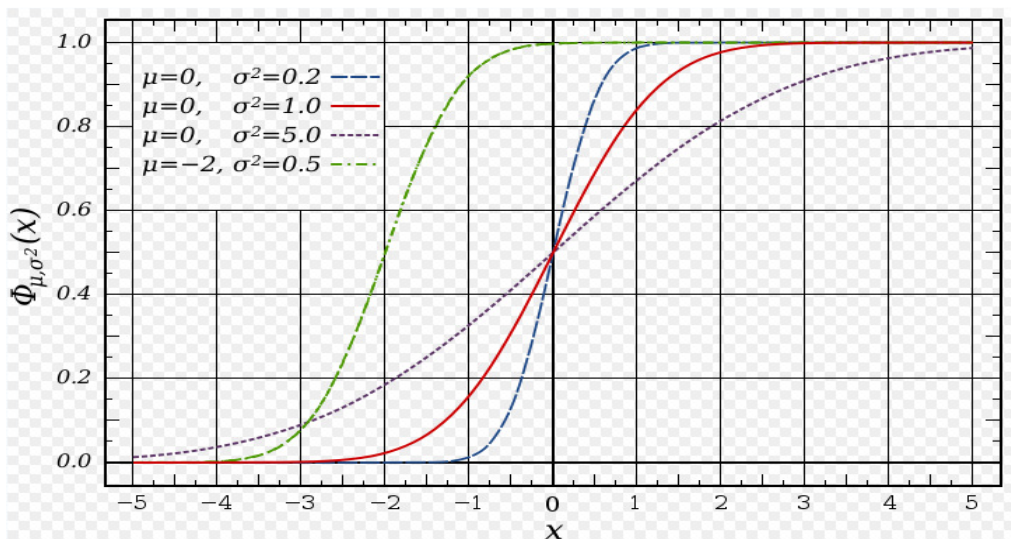


**Figure 2-8: An example of Cumulative Distribution Function (CDF)**

The probability distribution function (PDF) and cumulative distribution function (CDF) of the Gaussian distribution with mean of zero and variance of one is given by the following equation:

$$F(x) = Ce^{\frac{-(x-m)^2}{2\sigma^2}} \quad 2-1$$

where:

$$C = \frac{1}{\sqrt{2\pi\sigma^2}} \quad 2-2$$

Historically, Kolmogorov (1903-1987), who was a Russian mathematician, developed a powerful theory considered as the foundation of Probability theory and the modern Geostatistics theory. Geostatistics was first introduced in 1960 by Professor Georges Matheron (1930-2000) in France and by Krige and Sichel in South Africa. Nowadays, Geostatistical techniques are widely used in many several applications.

In Petroleum engineering, the application of Geostatistics started in 1980 by using the conditional simulation. These techniques, i.e. geostatistical tools, provide a probabilistic estimation of the reservoir properties as well as a measure of the uncertainty associated with these properties.

### 2.2.5 Ranking Realizations

Ranking is a step that is required before flow characterization can be efficiently performed. Normally ranking is conducted when numerous realizations have been produced to analyze a reservoir. Due to the large number of the realizations, detailed flow simulation of all the realizations is impractical. Therefore, it is recommended to rank the realizations and to reduce the number of realizations for detailed reservoir simulation. The ranking measure is a parameter that is well correlated with SAGD

performance parameters (Deutsch and McLennan, 2004). The first part of this chapter presented a literature review on the most commonly used ranking techniques. Chapter 4 will introduce the proposed ranking method along with the implementation details.

# Input Data Generation

---

## 3.1 Geostatistical Models

The geostatistical models used to generate the data in this thesis are presented in the following parts of this chapter. All models are available in GSLIB, geostatistical software library (Deutsch and Journel, 1998).

### 3.1.1 Data Generation

Synthetic data were used in this research. The data were generated using geostatistical tools. Porosity, permeability and fluid saturation were considered as reservoir properties along with reservoir lithofacies. Two facies were considered: sandstone and shale. 100 realizations of reservoir properties were generated and ranked.

Monte Carlo simulation (MCS) was used to generate the reference distribution. The reference values are chosen to be within the actual SAGD reservoir ranges. 100 realizations of porosity, permeability and water saturation in both sandstone and shale were generated using sequential Gaussian simulation (SGS). The output results of these realizations will be in Gaussian units. Back transformation was performed to convert the data from Gaussian units to the original units for all the properties. The geological facies (sandstone & shale) were generated using the sequential indicator simulation (SIM). The properties were then merged with the geological facies for use in ranking and flow simulations as will be elaborated in Chapters 4 and 5. The following is an overview (see Figure 3-1).

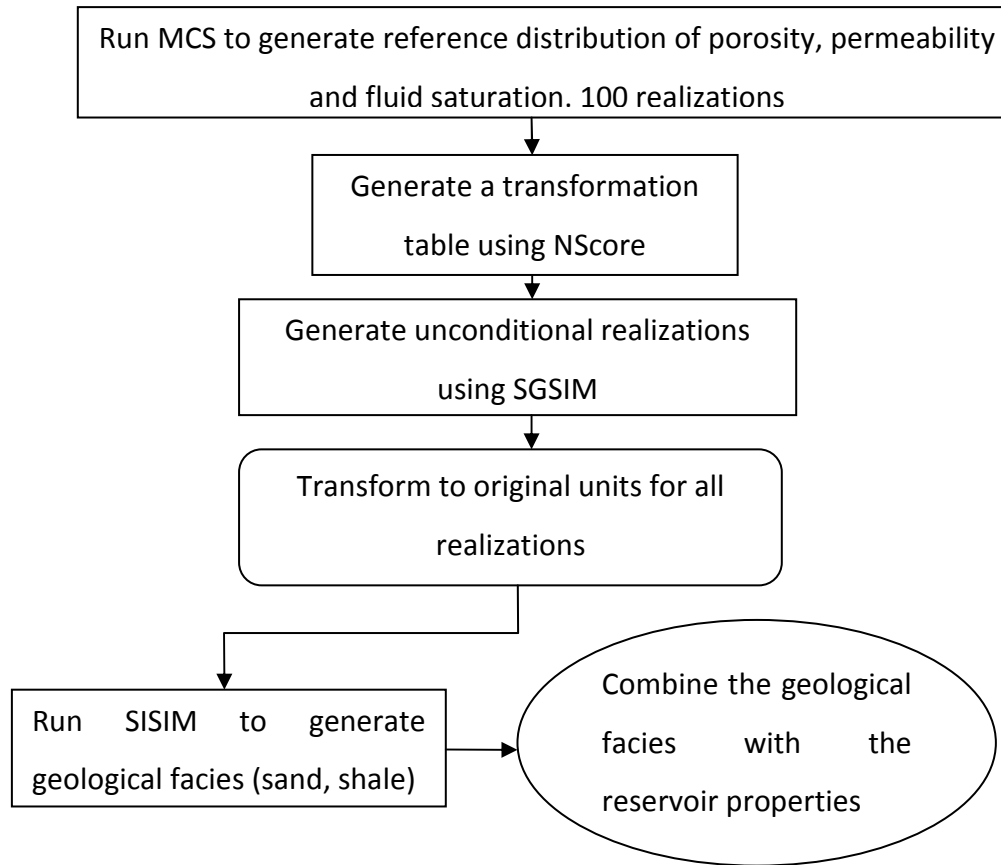


**Figure 3-1: Workflow diagram for generating data**

The above steps will be discussed in more details in the following sections.

### **3.1.2 Monte Carlo Simulation**

Monte Carlo simulation (MCS) is a stochastic method that involves using random numbers. Normally MCS is used to sample the probability distribution of all reservoir properties. It is a method that is especially useful in studying systems with a large number of coupled degrees of freedom (Deutsch and Journel, 1998).



In this work, 100 realizations of reservoir properties were generated using MCS. The reference distribution for these properties considered realistic values for the mean and variance. The results of the reference distribution were used with normal score transformation to generate a transformation table for all the variables.

Table 3-1 below shows the average value of the mean and variance for all reservoir properties. These average values were used to generate the distribution of each variable. The variables used in the data generation include porosity, permeability, and water saturation in both sandstone and shale. The parameter file of MCS was used to produce reference distribution of 100 realizations as shown in Figure 3-2.

**Table 3-1: Mean and variance values for different variables**

	Porosity Sandstone (%)	Porosity Shale (%)	Permeability Sandstone (mD)	Permeability Shale (mD)	Water Sat Sandstone (%)	Water Sat Shale (%)
Mean	31	15	3000	0.0001	25	5
Variance	1	5	1000	1	4	1

```

cat<<EOF>run-templ
cat<<END>mcs.par
START OF PARAMETERS:
mcs-VARI-COL.out      -file for output realizations
7000                  -number of realizations
RNS                   -random number seed
1                     -number of distributions (max of 512)
C1      C2      C3      -Dist 1:  dist type plus parameters

Distribution type: 0=constant      (the value)
                  1=uniform      (minimum and maximum)
                  2=triangular   (minimum, mode, maximum)
                  3=normal       (mean and standard deviation)
                  4=lognormal    (mean and standard deviation)
END
echo mcs.par | mcs
rm mcs.par
EOF

MaxRun=100
RunNo=1
CAT1=ShPoro
DISTTYPE=3
VALUE1=0.15
VALUE2=0.05
CAT2=SaPoro
DISTTYPE=3
VALUE1=0.31
VALUE2=0.01
CAT3=ShPerm
DISTTYPE=4
VALUE1=50
VALUE2=100
CAT4=SaPerm
DISTTYPE=4
VALUE1=3000
VALUE2=1000
RandomNo=68113
COUNT=0
for RunNo in `seq 1 ${MaxRun}` ; do
    let "SEED=$RandomNo+1397"
    let "COUNT=$COUNT+1"
    sed -e "s/COL/$RunNo/g" -e "s/C1/$DISTTYPE/g" -e "s/C2/$VALUE1/g" \
        -e "s/C3/$VALUE2/g" -e "s/VARI/$CAT1/g" \
        -e "s/COL/$COUNT/g" -e "s/RNS/$SEED/g" run-templ > runem
    bash runem ; rm runem
done

```

**Figure 3-2: The parameter file of MCS with mean and variance for each property in each geological facies**

### 3.1.3 Normal Score Transformation (NScore)

The matching of original units to Gaussian units is based on a quantile-to-quantile transformation. The data, regardless of the units, are converted to Gaussian units with the mean of zero and the variance of one. NScore is a universal and straight forward technique.

The quantile transformation requires a cumulative distribution function (CDF) of the original Z-values. CDF can then be plotted. The cumulative probability comes from the proportional data. A code called Normal Score Transformation was used to map the properties from their original units to Gaussian values.

The Z-data are transformed to the normal distribution  $F(y)$  by:

$$y = F_Y^{-1}(F_Z(Z)) \quad 3-1$$

where:

$y$  = corresponding normal score transformation value,

$z$  = data value in original unit,

$F_Y$  = function of normal score value

$F_Z$  = function of original values

The normal score transformation can be approached by linking the two CDFs in a process called quintile-to-quintile transformation.

Back transformation to original z-data (the inverse of NScore) can be achieved by:

$$Z = F_Z^{-1}(F(y)) \quad 3-2$$

In this thesis, the back transformation program was applied to all reservoir variables. Figure 3-3 shows the NScore procedure. Figure 3-4 illustrates an example of normal score for porosity in sandstone.

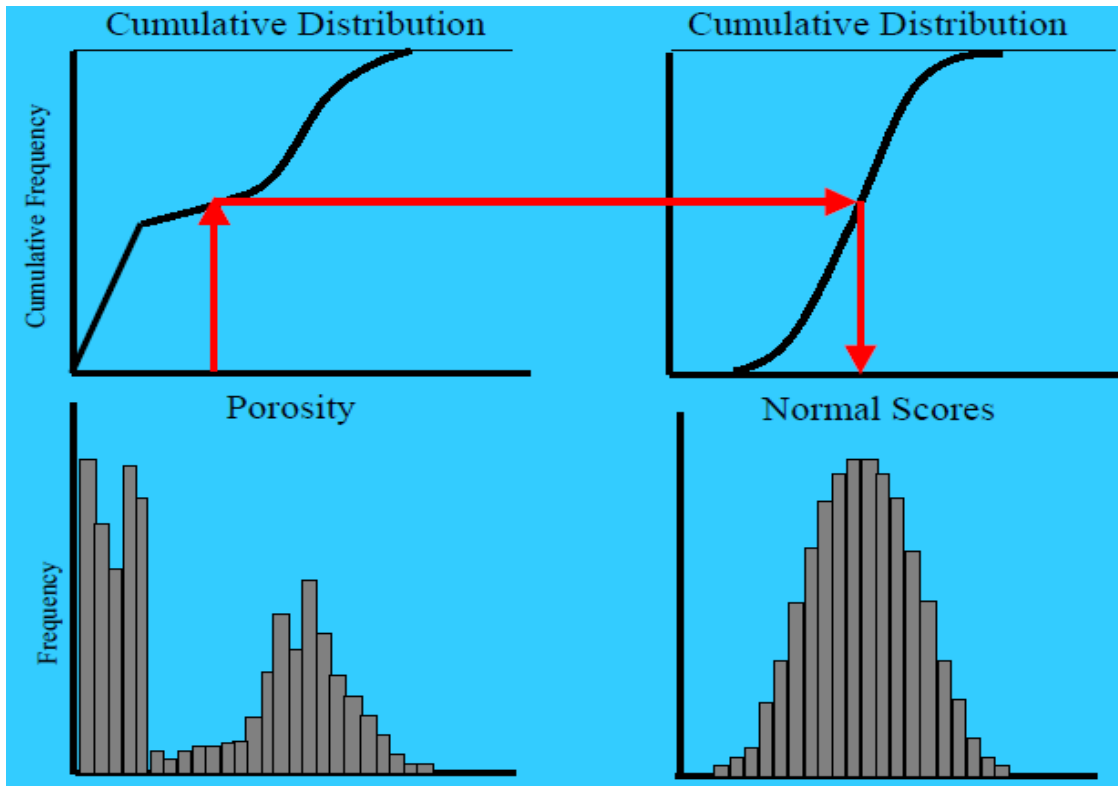
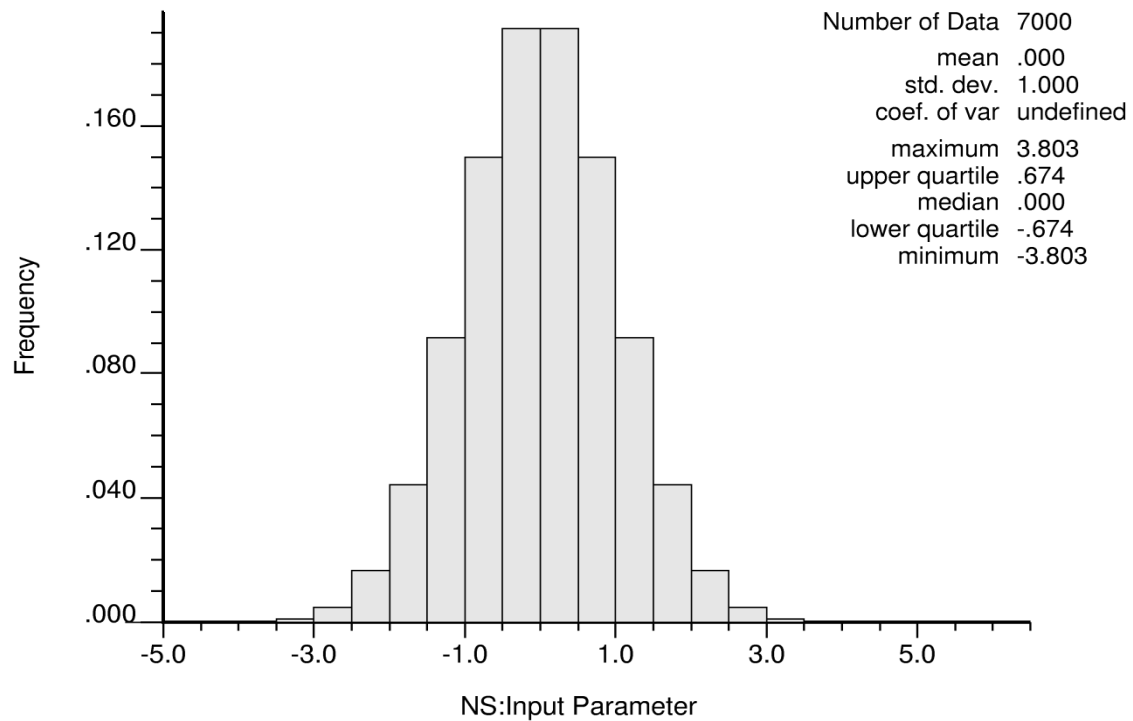


Figure 3-3: Normal Score Transformation ([www.statios.com/Resources/08-sgsim.pdf](http://www.statios.com/Resources/08-sgsim.pdf))



**Figure 3-4: Example of NScore transformation for sand porosity (R-5)**

### 3.1.4 Sequential Gaussian Simulation (SGS)

Sequential Gaussian simulation (SGS) is one of the geostatistical tools that is used to simulate the available data. It is a simple and straight forward technique, and widely used because of its simplicity and flexibility. The theory of SGS has been documented in several references. According to Isaaks (1990), SGS is a common method used to create multiple equiprobable numerical models based on a set of conditioned data as infinite number of values can be created from the distribution at each location.

There are some issues with the implementation of SGS that need to be understood. These include: (1) maximum number of conditioned data is required to produce the best

possible estimation at the unsampled locations, (2) The influence of the secondary data on the results should also be understood, (3) simulation of random numbers is used to avoid artifacts. Random numbers are added to remove the effect of missing variance.

One advantage of SGS is the elimination of the smoothing effect which is resulted from kriging. Smoothing effect makes the estimated kriged variance too small. The simulated maps of all the produced realizations can assess the uncertainty and show reasonable representation of the local variability patterns. SGS requires the data to be in standard Gaussian space (normal distribution). To produce the Gaussian distribution, a normal score transformation must be performed. The simulated data by SGS should be then back-transformed to their original unit.

Deutsch in his class notes (MIN 612) discussed the principles of the SGS in more details. The steps of applying this technique are as follows:

- Transform the original data to normal score.
- Establish the required parameter's mean and variance.
- Simulate number of locations in Gaussian unit at a time with increasing conditioning application of Bayes law.
- Back-transform to the original unit or original distribution.
- Repeat the above steps to produce more realizations.

To produce more realizations, we can use the Bayes law theory as follows:

$$F_{z_i}, i = Z, \dots, N | Z_1 (Z_i, i = 2, \dots, N). F_{z_1} (Z_1)$$

\_\_\_\_\_

$$F_{Z_N} \Big|_{Z_1, Z_2, \dots, Z_{N-1}} (Z_N) * F_{N-1} \Big|_{Z_1, \dots, Z_{N-2}} (Z_{N-1}) \dots F_{Z_2} \Big|_{Z_1} (Z_2) * F_{Z_1} (Z_1)$$

The parameter file used to generate SGS for different variables is shown in Figure 3-5. Figures 3-6 through 3-11 show maps of different variables for different realization using SGS.

```

cat<<EOF>run-temp3
cat<<END>sgsim.par
START OF PARAMETERS:
NO FILE
0 0 0 0 0
-998 1.0e21
0
sgs.trn
0
histsmth.out
3 0
0.01 0.40
1 0.0
1 40
3
sgs.dbg
sgs-VARI-RCOL.out
1
100 1 2
100 1 2
1 0.5 1.0
RNS
2 20
30
1
1 3
3
100.0 68.0 2.0
0.0 0.0 0.0
101 101 11
0 0.6 1.0
SECONDARY VALUE
1
1 0.1
1 0.9 90.0 0.0 0.0
68.0 11.0 1.0
1 0.1
2 0.9 90.0 0.0 0.0
68.0 11.0 1.0

```

**Figure 3-5: The parameter file for sequential Gaussian simulation**

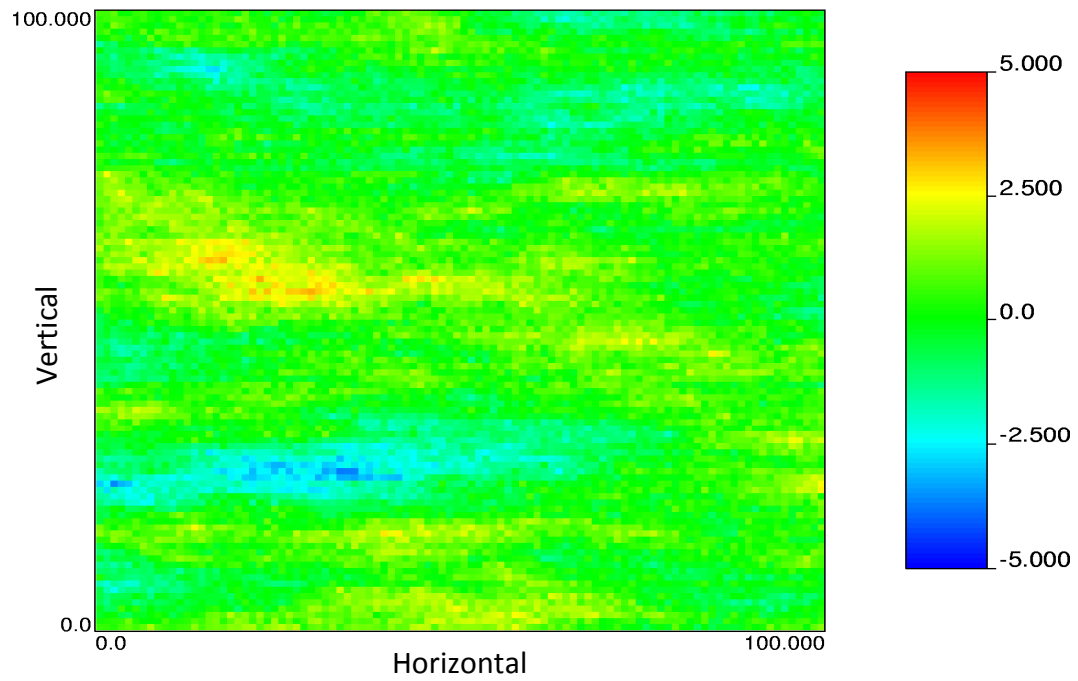


**Figure 3-6: Sample sand permeability map simulated by SGS (R-5)**

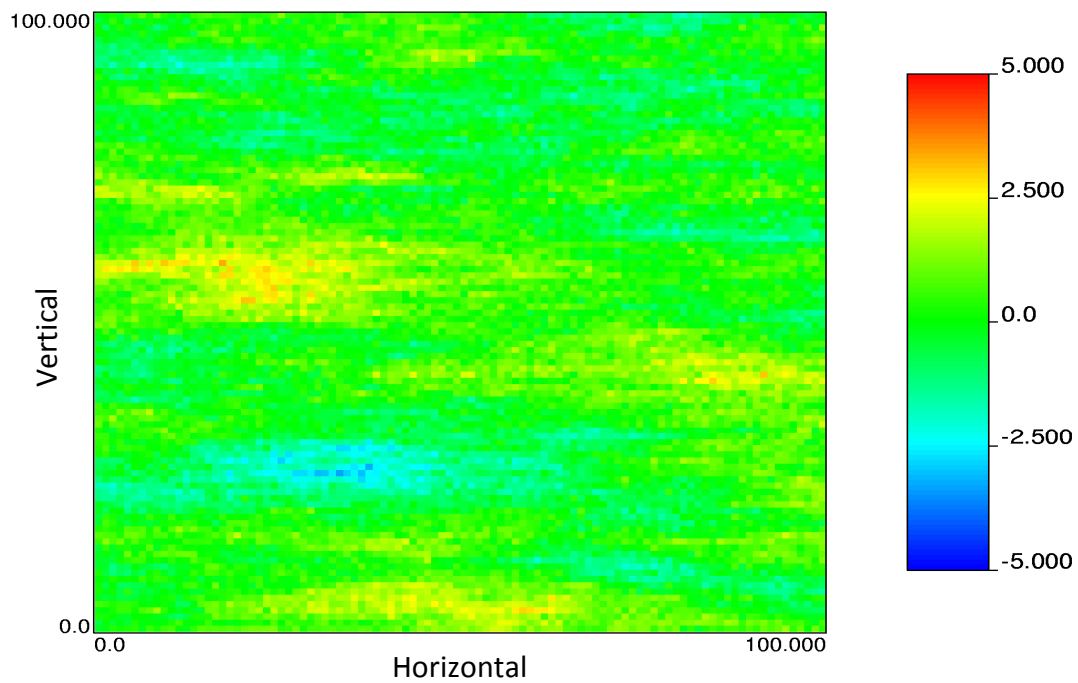


**Figure 3-7: Sample shale porosity map simulated by SGS (R-5)**



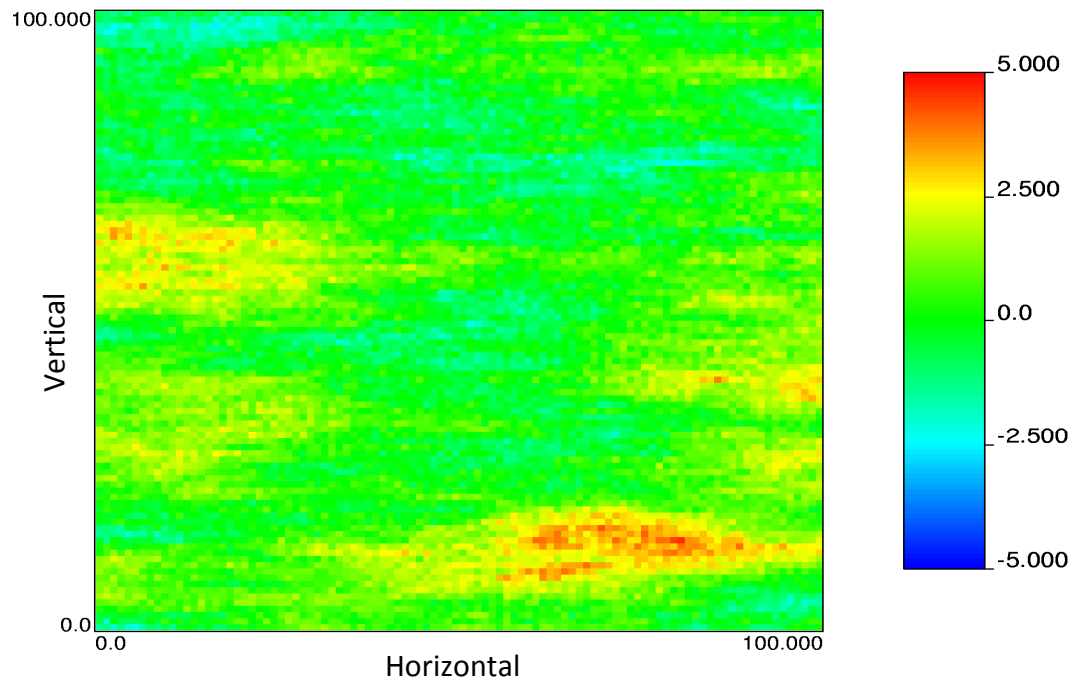


**Figure 3-8: Sample water saturation map in sand simulated by SGS (R-5)**

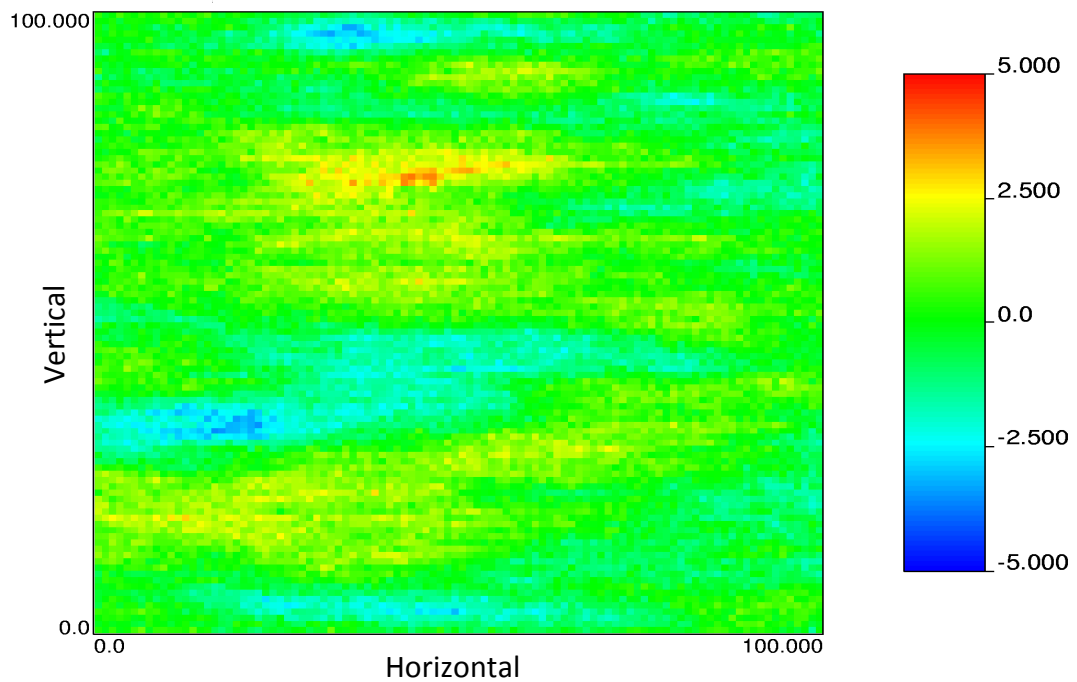


**Figure 3-9: Sample shale permeability map simulated by SGS (R-5)**

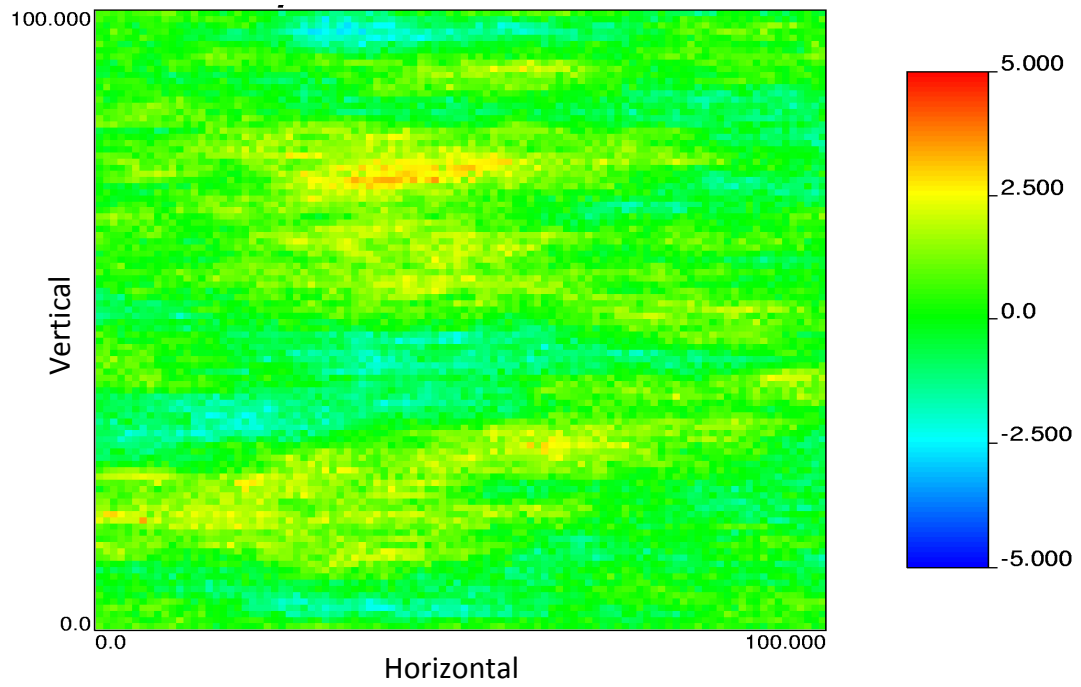


**Figure 3-10: Sample shale porosity map simulated by SGS (R-5)**

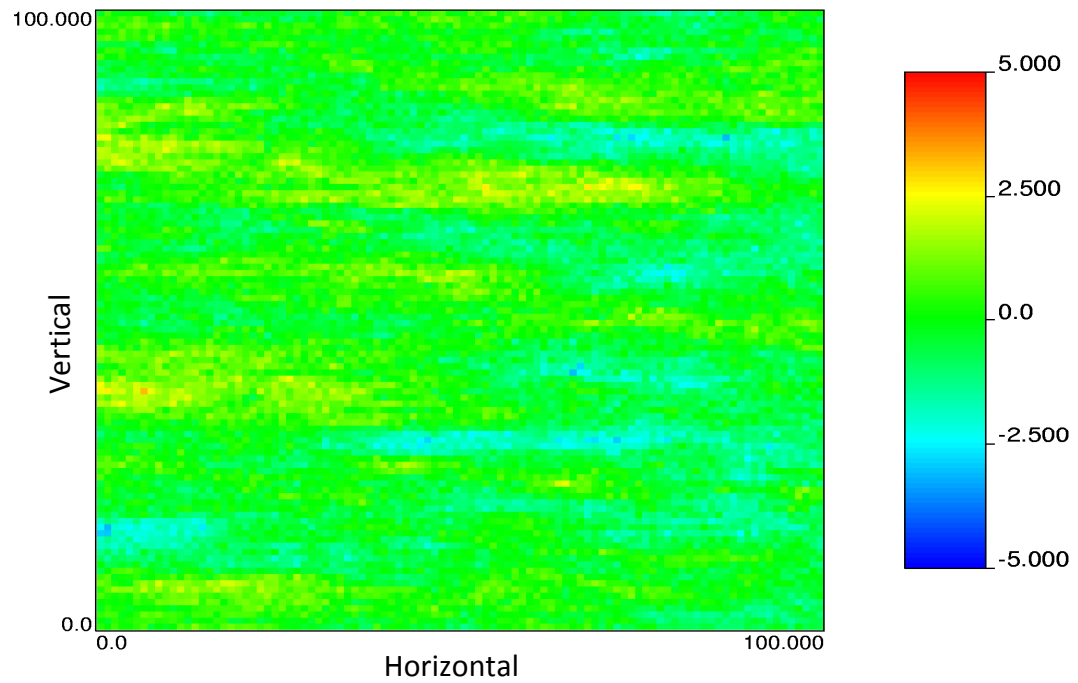


**Figure 3-11: Sample water saturation map in shale simulated by SGS (R-5)**

### 3.1.5 Back Transformation

Back transformation is a tool used to transform the distributions from Gaussian unit to the original units. Back transformation cannot be applied to the mean and variance; the transformation is applied only to quintiles. The outcome is the realizations of the properties in their original units.

In Gaussian space, the values and distributions are Gaussian, all conditional expectations are linear, and all conditional variances are homeostatic. When transferring to original units, mean, variance and the probability distribution are calculated.

Back transformation to the original z-data can be achieved by:

$$Z = F_Z^{-1}(F(y)) \quad 3-3$$

For multiple realizations, back transformation can be drawn from:

$$Z^l = F_Z^{-1}(G(\sigma_k G^{-1}(P^l) + y)) \quad 3-4$$

For  $l = 1, \dots, L$

This procedure was applied to all variables simulated by SGS. A parameter file named *backtr.par* is available in GSLIB that was used, see Figure 3-18. Figures 3-19 through 3-23

show the histogram of back transformation for different variables and different realizations.

```
cat<<EOF>run-temp
cat<<END>backtr.par
START OF PARAMETERS:
sgs-VARI-RCOL.out          -file with data
1                          - column with Gaussian variable
-998   1.0e21              - trimming limits
backtr-VARI-RCOL.out       -file for output
nscore-VARI-COL.trn        -file with input transformation table
0.01   0.40               -minimum and maximum data value
1      0.0                 -lower tail option and parameter
1      40.0                -upper tail option and parameter

END
echo backtr.par | backtr
rm backtr.par
EOF

MaxRun=100
RunNo=1
Face=SaPoro
Face=ShPoro
Face=SaPerm
Face=ShPerm
Face=SaWSat
Face=ShWSat
for RunNo in `seq 1 ${MaxRun}` ; do
    sed -e "s/COL/$RunNo/g" -e "s/VARI/$Face/g" run-temp > runem
    bash runem ; rm runem
```

**Figure 3-12: The parameter file of back transformation from Gaussian unit to original unit**

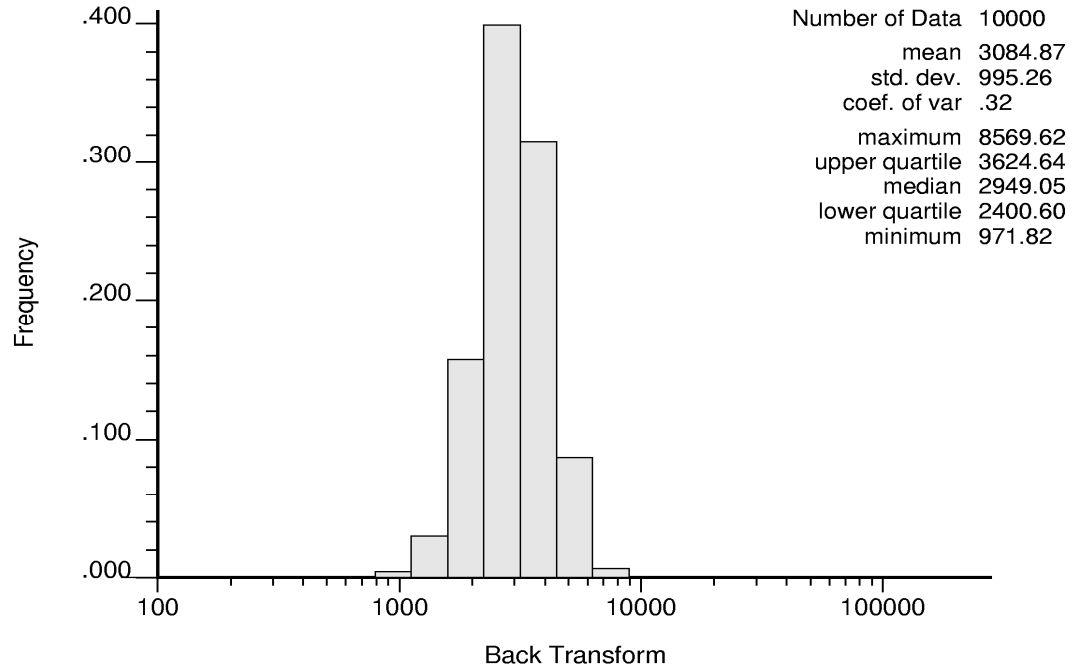


**Figure 3-13: Sample histogram of the back transformation of the sand permeability (R-5)**

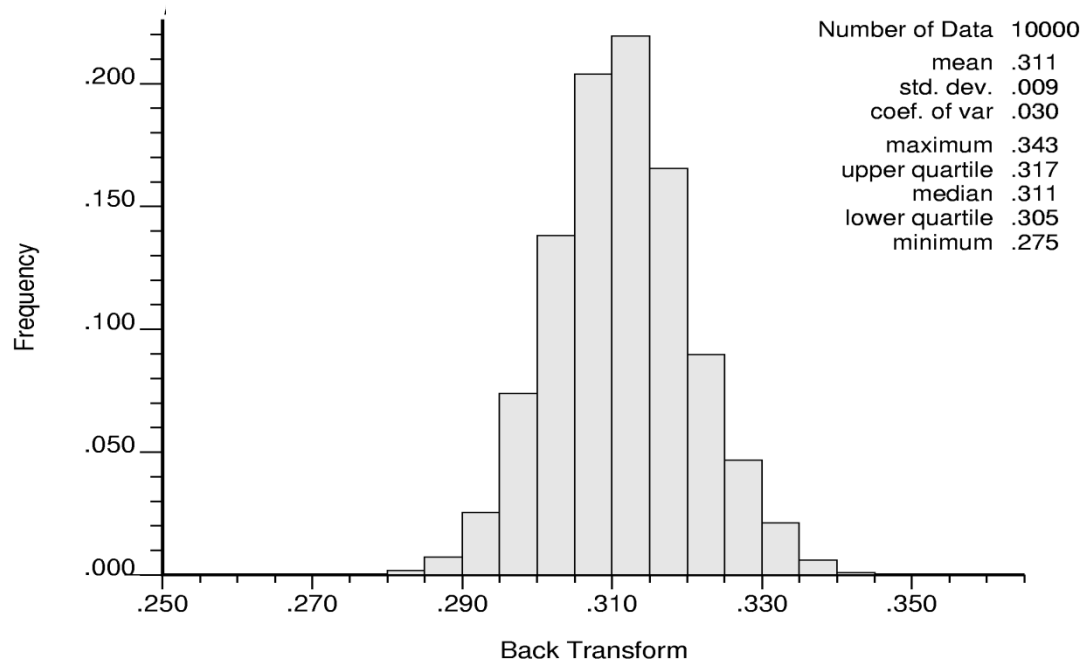


**Figure 3-14: Sample histogram of the back transformation of the sand porosity (R-5)**

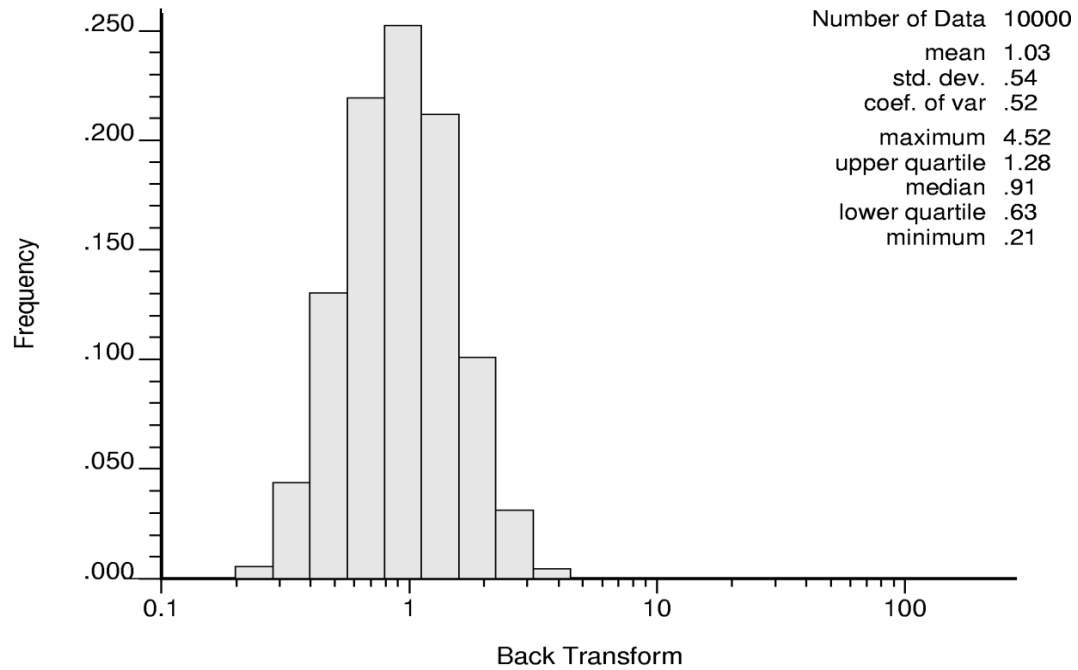


**Figure 3-15: Sample histogram of the back transformation of the shale permeability (R-5)**

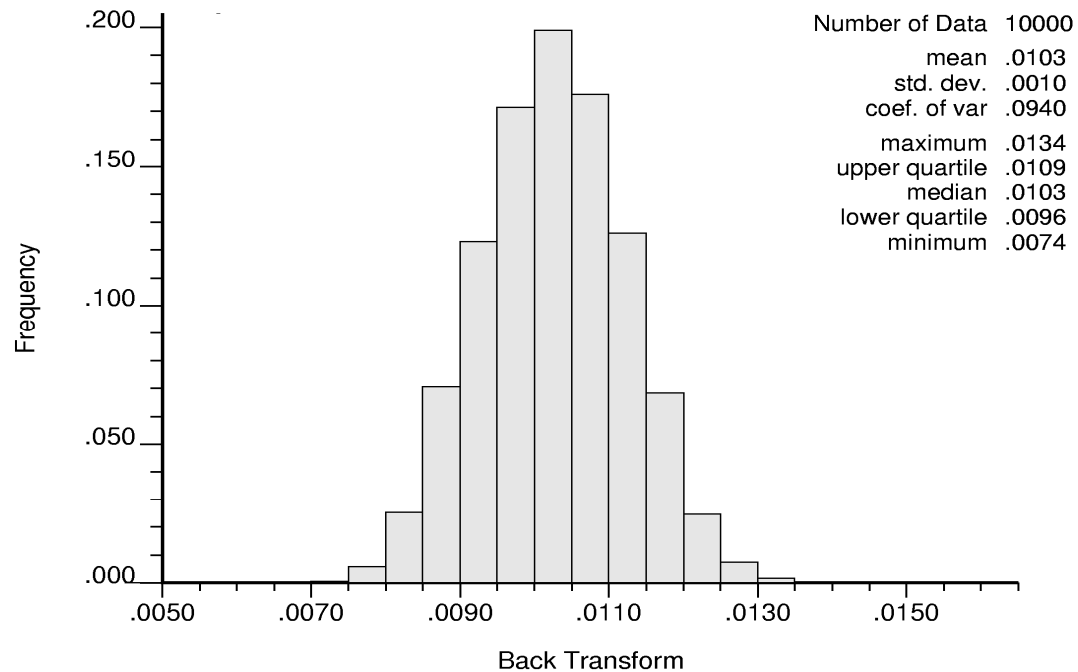


**Figure 3-16: Sample histogram of the back transformation of the shale porosity (R-5)**

### 3.1.6 Sequential Indicator Simulation (SIS)

The sequential indicator simulation (SIS) is a geostatistical tool used to simulate categorical variables with indicator data obtained from a CDF. The theory of simulating the categorical variables was discussed in more details in GSLIB. SIS is widely used for diagnostically controlled facies because the results have high variability and yet correct anisotropy and variogram measures of spatial correlation (Deutsch and Journel, 1998). The distribution of facies controls the distribution of reservoir properties; as such the facies distribution is an important aspect and should be given more attention. Facies are important especially in reservoir modeling where petrophysical properties such as porosity and permeability are highly correlated to facies types. Only one trend model is needed when there are two facies types; the proportion or probability of the second facies is one minus the proportion of the first (Deutsch, 2002).

Consider  $K$  as the number of categories

$$S_k, k = 1, \dots, K$$

where only one  $K$  will take the  $u$  location

If  $i(u; s_k)$  is the indicator variable, then

$$i(u; s_k) = \{ 1 \text{ if the location } u_j \text{ in category } S_k, 0 \text{ otherwise} \}$$

Sequential indicator simulation will randomly visit each grid node and assign facies code to the grid nodes in accord with the following steps:

- Find the closest data and the previously simulated grid nodes.

- Construct the conditional distribution by kriging; probability of each facies at the current location will be calculated.
- Draw the simulated facies distribution from the set of probabilities.
- Generate multiple realizations by repeating the above steps and considering different random number seeds.

To generate the categorical facies for multiple realizations, the calculation of the local varying proportion between the facies is required. This is achieved by increasing the proportion of one categorical facies with respect to the other as realization number increases. In this thesis, two categorical variables are considered. These are sandstone and shale with the base proportion of 95% for sand. The shale proportion is increased in increments of 0.025 as the realization number increases. For example, if the proportions between sand and shale in Realization #5 are 94% and 6%, respectively, then the incremental increase in shale proportion results 82.25% of sand and 17.75% of shale for Realization #52. This procedure allows producing multiple realizations in different categorical maps with different facies distribution as shown in Figures 3-17 and 3-18. The parameter file used to generate geological facies is shown in Figure 3-19.



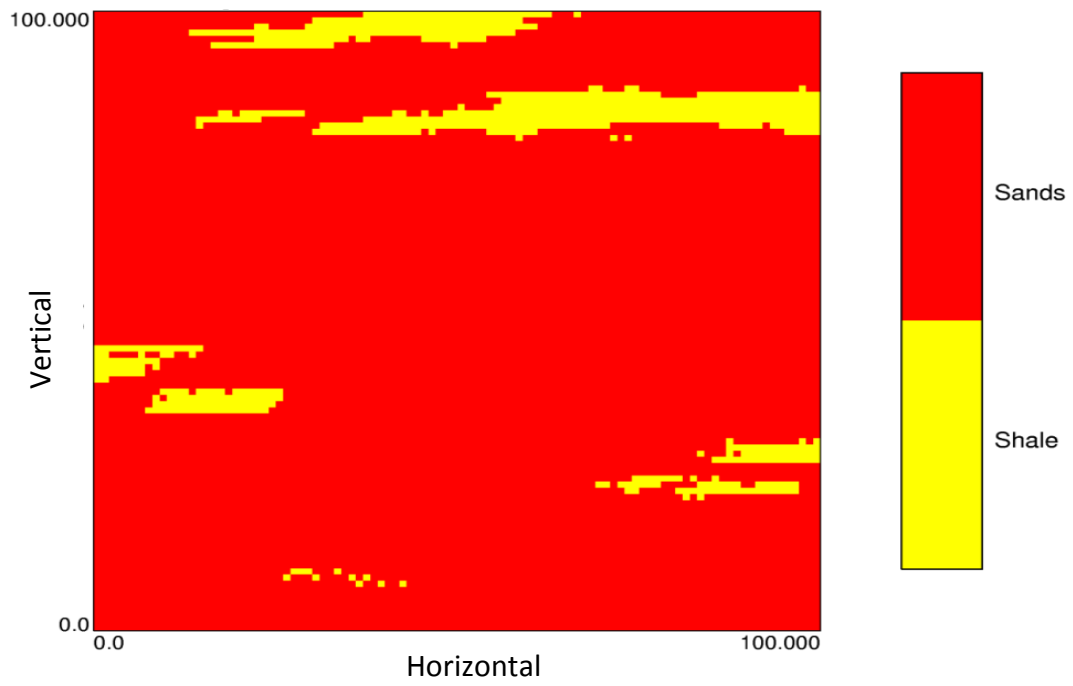


Figure 3-17: Sample facies map for R-5

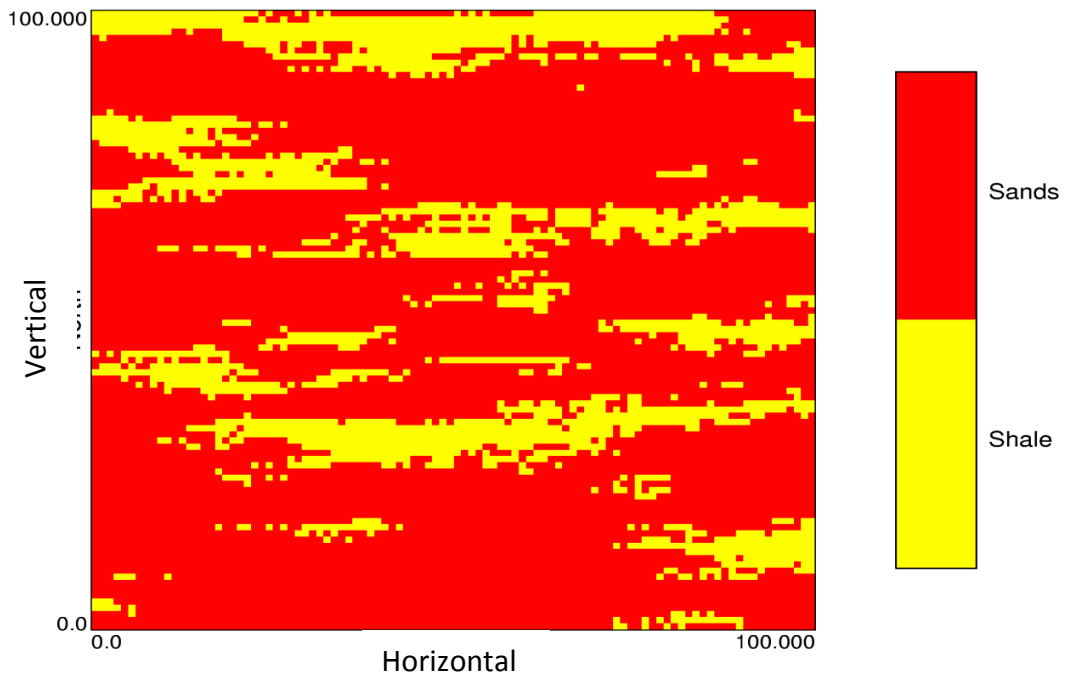


Figure 3-18: Sample facies map for R-52

```

cat<<EOF>run-temp55
cat<<END>sisim.par
START OF PARAMETERS:
0
2
1      2
PRO1 PRO2
NOFILE
0 0 0 0
direct.ik
1 2
0
0.61 0.54 0.56 0.53 0.29
-1.0e21 1.0e21
0.0 30.0
1 0.0
1 1.0
1 30.0
cluster.dat
3 0
3
sisim.dbg
sisim-RCOL.out
1
100 1 2
100 1 2
1 0.5 1
RNS
12
12
1
1
1 3
0
100.0 70.0 2.0
0.0 0.0 0.0
101 101 11
0 2.5
0
1 PRO1
1 PRO2 90.0 0.0 0.0
      70.0 12.0 2.0
1 PRO1
1 PRO2 90.0 0.0 0.0
      70.0 12.0 2.0

ProV1=`echo $ProV1 | awk '{print $1 + 0.0025}'`
ProV2=`echo $ProV2 | awk '{print $1 - 0.0025}'`

```

-1=continuous(cdf), 0=categorical(pdf)  
 -number thresholds/categories  
   thresholds / categories  
 - global cdf / pdf  
 -file with data  
   columns for X,Y,Z, and variable  
 -file with soft indicator input  
   columns for X,Y,Z, and indicators  
 - Markov-Bayes simulation (0=no,1=yes)  
   calibration B(z) values  
   trimming limits  
 -minimum and maximum data value  
   lower tail option and parameter  
   middle option and parameter  
   upper tail option and parameter  
   file with tabulated values  
   columns for variable, weight  
 -debugging level: 0,1,2,3  
 -file for debugging output  
 -file for simulation output  
 -number of realizations  
 -nx,xmn,xsiz  
 -ny,ymn,ysiz  
 -nz,zmn,zsiz  
 -random number seed  
 -maximum original data for each kriging  
 -maximum previous nodes for each kriging  
 -maximum soft indicator nodes for kriging  
 -assign data to nodes? (0=no,1=yes)  
 -multiple grid search? (0=no,1=yes),num  
 -maximum per octant (0=not used)  
 -maximum search radii  
 -angles for search ellipsoid  
 -size of covariance lookup table  
 -0=full IK, 1=median approx. (cutoff)  
 -0=SK, 1=OK  
 -Two nst, nugget effect  
   it,cc,ang1,ang2,ang3  
   a\_hmax, a\_hmin, a\_vert  
 -Two nst, nugget effect  
   it,cc,ang1,ang2,ang3  
   a\_hmax, a\_hmin, a\_vert

Figure 3-19: Parameter file of SIS

### 3.1.7 Merging of the Realizations

A complete picture of what subsurface may look like can be achieved by combining the geological facies with the realizations of the reservoir properties. Merging can be achieved through using the *meregmod.par* in GSLIB. The idea is to combine the categorical variables (sand and shale) simulated by SIS with the reservoir properties simulated by SGS. The results are maps of the combined variables as shown in Figures 3-20 and 3-21.

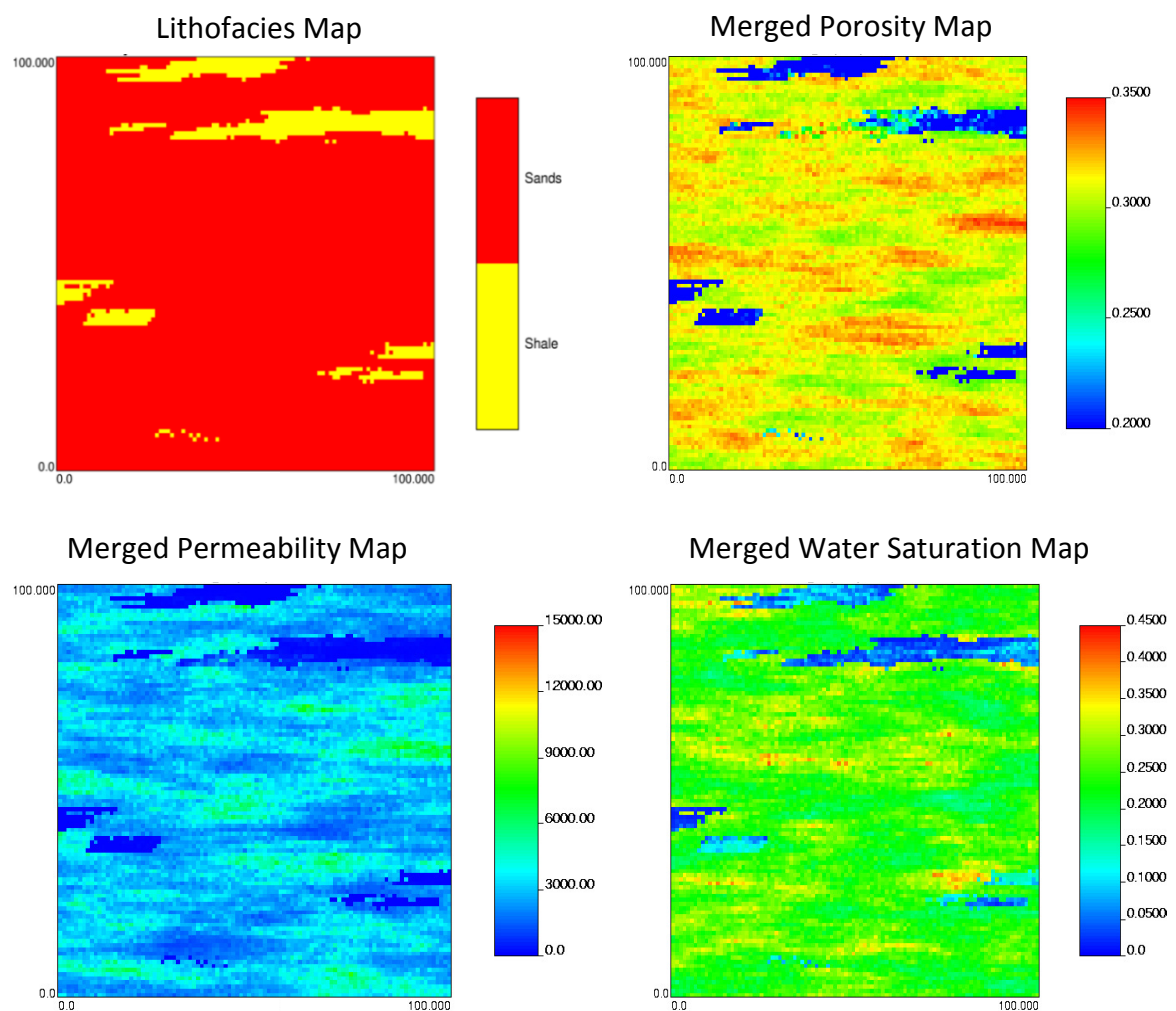
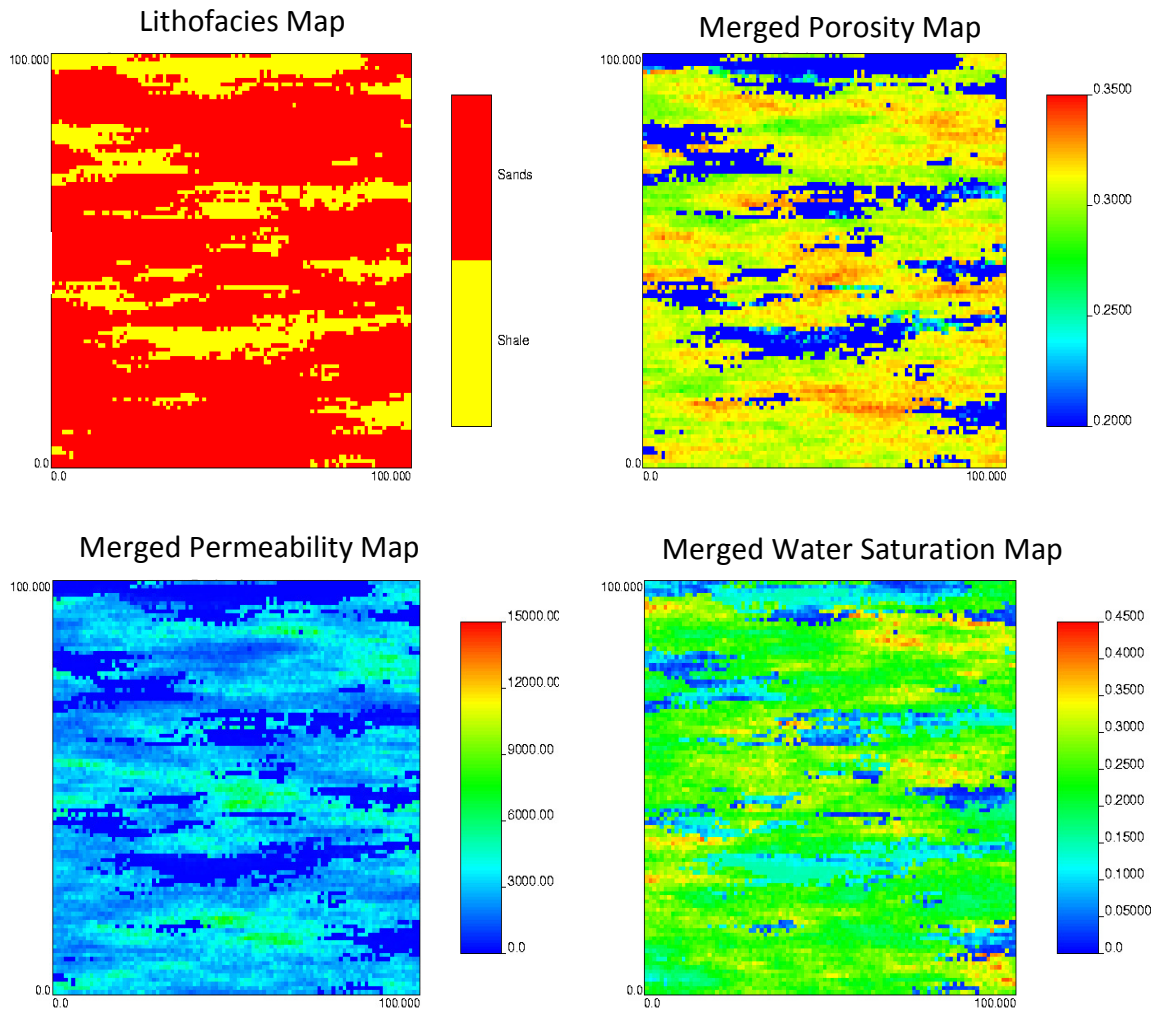


Figure 3-20: Sample maps of merged geological facies with reservoir properties (R-5)



**Figure 3-21: Sample maps of merged geological facies with reservoir properties (R-52)**

### 3.2 Generating Realizations

Generating a small number of realizations, for example 10 realizations, is not enough to adequately quantify the uncertainty and will not give accurate results. Usually 100 realizations need to be generated to adequately evaluate the high and low values of the performance parameters. In this thesis, 100 realizations of porosity, permeability, water saturation and lithofacies (sand and shale) were generated. These realizations were then ranked by the proposed ranking methodology as will be discussed in Chapter 4. Figure 3-22 shows examples of generated realizations imported to the simulator for validation of the developed ranking methodology as will be discussed in Chapter 5.

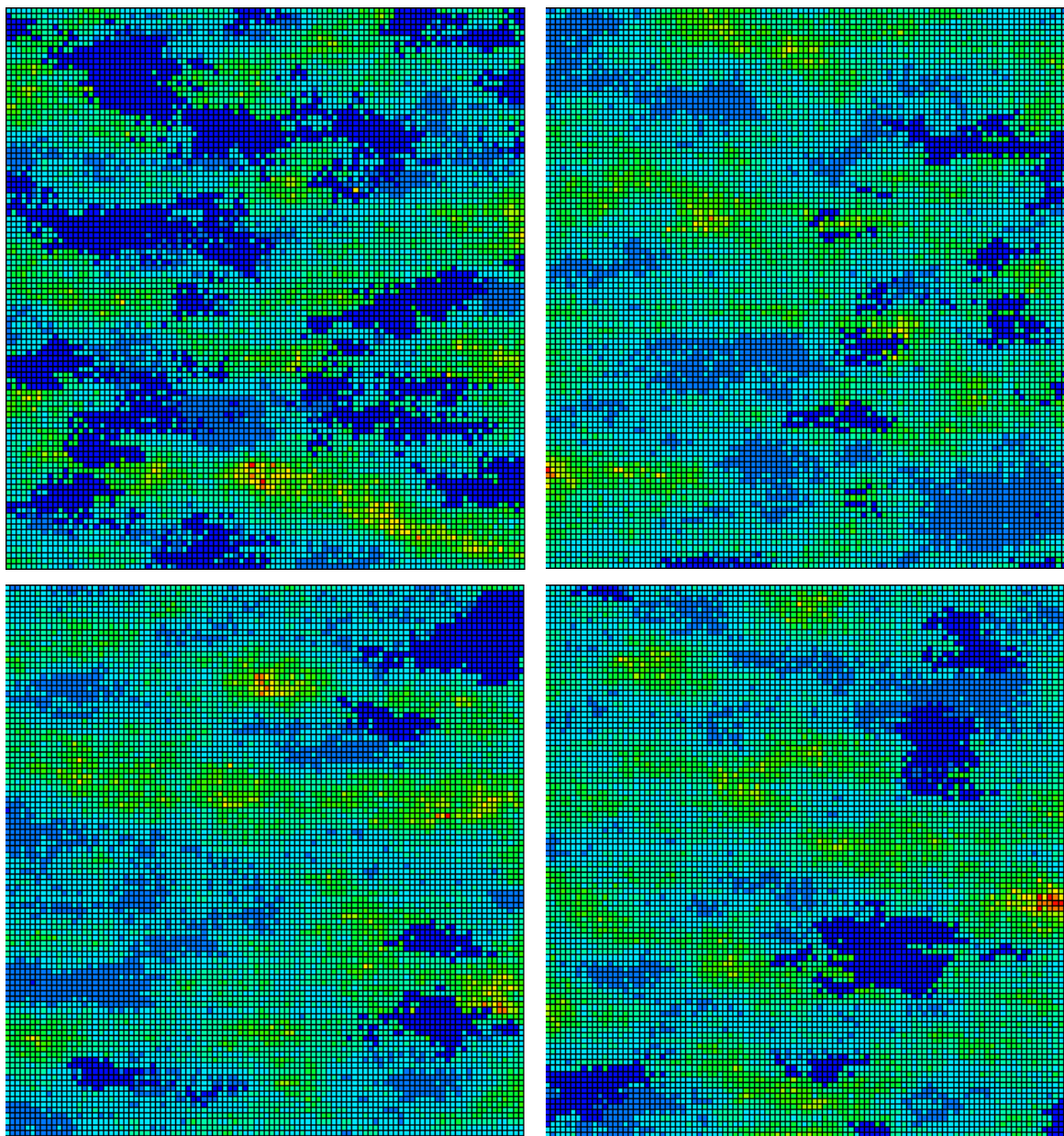


Figure 3-22: Sample merged generated realizations for use in flow simulation

# The Ranking Methodology

---

## 4.1 Introduction

As mentioned earlier, the ranking of realizations is an important step before flow simulation. The goal of ranking is to reduce the large number of realizations to a few for further processing by a flow simulator.

The proposed ranking methodology is based on using a static measure as discussed in Chapter 2 by measuring the local connected hydrocarbon volume (CHV) within a local window. The CHV is defined as the amount of hydrocarbon in the reservoir that is connected to the producer and can be produced. The local window is the reservoir dimensions considered to calculate the connected hydrocarbon; it is started from the producer and takes the two directions along the x-axis of the producer as shown in Figure 4-1. It also includes the location of the production well from which direct lines of sight are drawn to enable assessing the connectivity of the hydrocarbon within this window. The lines of sight are used to add the net cells that are directly connected to the producer as shown in Figure 4-2.

## 4.2 Ranking Methodology

In the proposed ranking method, realizations are ranked from the highest to lowest CHV. Two constraints are considered in the calculation of CHV: (1) limiting the connectivity calculation to within a maximum distance from the well, (2) calculating only the net cells directly connected to the production well. The net cells are those that belong to the list of net facies that are controlled by the properties cutoff. A code was

developed to evaluate the CHV within the window. CHV is evaluated using the following equation:

$$CHV = \frac{1}{L} \sum_{l=1}^L \sum_{j=1}^N i(u_j) * \phi_j (1 - Sw_j) \quad 4-1$$

The local connectivity is a relatively new ranking measure. However, it is considered as a straightforward method compared with the global connectivity measure. The indicator of connectivity is the net cells connected to the producer. A net cell is considered as connected cell only when  $i(u_j) = 1$  regardless of its direct connectivity above or below the same row of the cells. These net cells are part of the net facies and should be greater than the property cutoff. The cutoff is a value of reservoir property below which the cell is considered as non-net. For example, if the value of the permeability cutoff is 150 mD, any cell with permeability below 150 mD will not be counted in the calculation of CHV and will be considered as non-connected net cell. In this study the cutoff for the porosity, permeability and water saturation are considered 0.75, 50 mD and 0.05, respectively.

The window size is an important function and must be chosen carefully. The window is considered normal to the horizontal well axis as shown in Figure 4-1.

In figure 4-2, the SAGD producer is represented by a dot point from which the connectivity calculation is started. The gray color shows the non-net cells, the green indicates the net cells but not connected and the red color represents the net cells

considered as connected bitumen cells. All net cells that are directly connected to the producer and are calculated by the line-of-sight will be added to the net cells calculated within the window size as shown in Figure 4-2.

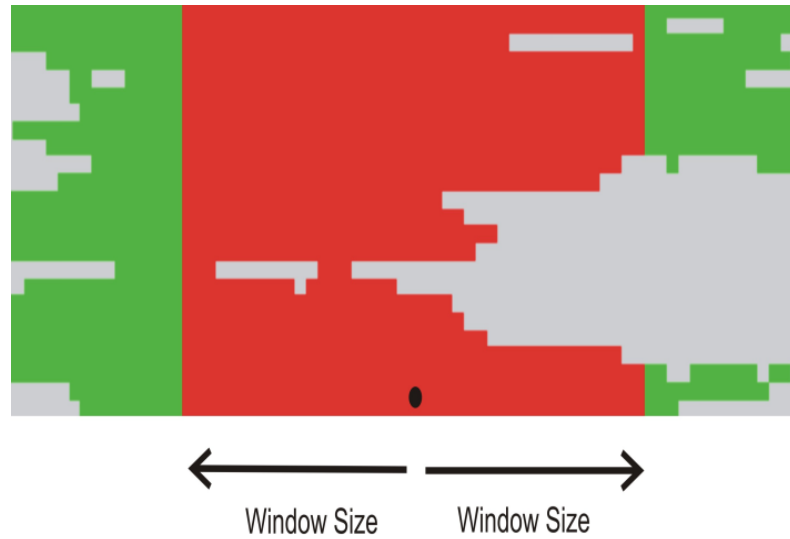


Figure 4-1: Example of window size

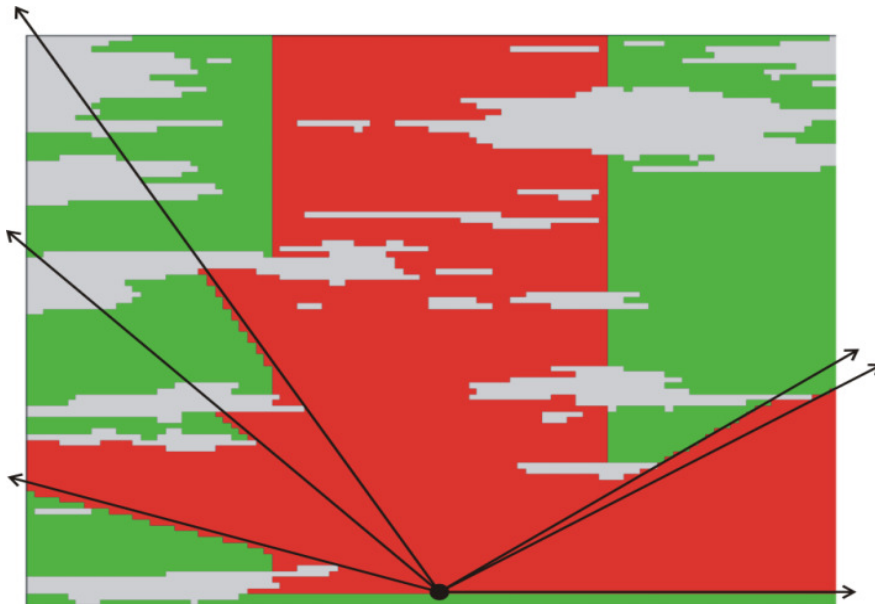


Figure 4-2: Directions of line of sight



If the well trajectory is not considered, the calculations will be performed in all X and Y grids. In this case, calculations will search for the thickest connected interval and consider them as net cells. It is better to use fixed well trajectory if the well location is known.

To evaluate the sensitivity of the results to the window sizes, a variation of window sizes in the range of 20-50 m was considered. The methodology was applied and results were ranked to check the highest and lowest performance cases. All the results from this methodology with more discussion are presented in Chapter 5. The parameter file built for ranking is shown in Figure 4-3.

```

Parameters for CHV
*****
cat<<EOF>run-templ
START OF PARAMETERS:
cat<<END>CHV_CP.par
sisim-RCOL.out
merge-Poro-RCOL.out
merge-WatSat-RCOL.out
merge-Perm-RCOL.out
1
chv3d-RCOL.out
chv2d-RCOL.out
chv1d-RCOL.out
1
100 0.5 1.0
1 0.5 1.0
100 0.5 1.0
20 1
1 2
0.05
0.75
200
1 1
1
2
1 50
1
R-COL.dat

END
echo CHV_CP.par | CHV_CP
rm CHV_CP.par
EOF

MaxRun=100
RunNo=1
Face1=Poro
Face2=WatSat
Face3=Perm
for RunNo in `seq 1 ${MaxRun}` ; do
    sed -e "s/COL/${RunNo}/g" -e "s/VAR1/${Face1}/g" -e "s/VAR2/${Face2}/g" \
        -e "s/VAR3/${Face3}/g" run-templ > runem
    bash runem ; rm runem
done

```

Figure 4-3: Parameter file for connected hydrocarbon volume (CHV)

# Validation of the Ranking Methodology

---

This thesis used several geostatistical models to generate the data. These data were imported to CMG simulator to evaluate the reservoir performance parameters including cumulative steam-oil-ratio (CSOR) and cumulative oil produced (COP). The realizations are then ranked from the highest to the lowest COP. This is equivalent to ranking from the minimum to the maximum CSOR. The results obtained from CMG and ranking method are then compared to validate the proposed ranking method.

## 5.1 Flow Simulation

Reservoir performance parameters for the SAGD example are considered in this research to be correlated with the CHV in the proposed ranking methodology. Modeling SAGD processes requires a thermal pseudo-compositional reservoir simulator. In this thesis, CMG-STARS simulator was utilized for doing the simulation.

Cartesian grid was used with a 2D grid net consisting of 100, 1, 100 grid blocks and grid lengths of 1 m, 100 m and 1 m in I, J and K directions, respectively. Two horizontal and parallel wells with distance of 5 m between them were considered. Heavy oil model with two components of water and oil was used. No gas cap zone or aquifer was considered. The reservoir is heterogeneous with properties including porosity, permeability and water saturation. The initial reservoir pressure is 4 MPa and the initial reservoir temperature is 18 °C. The heat loss was assumed to be at the overburden where no flow boundary was considered. The perforations of both injector and producer were

assumed to be in the J direction. Well radius was 0.11 m and the simulation time was 10 years. Table 5-1 summarizes the input variables used in CMG-STARs along with their values. Figures 5-1, 5-2, 5-3 and 5-4 show the rock type data, relative permeability plot, permeability map and porosity map, respectively.

**Table 5-1: Variables with their values used to simulate SAGD case (CMG)**

<b>Input variable</b>	<b>Value</b>	<b>unit</b>
Initial reservoir pressure	4000	kPa
Reservoir thickness	20	m
Formation compressibility	7E-06	1/kPa
Rock compressibility	9.6E-6	1/kPa
Volumetric heat capacity	2.347E+6	J/m <sup>3</sup> °C
Reservoir rock thermal conductivity	6.6E5	J/m °C
Oil thermal conductivity	1.15E+4	J/m °C
Water thermal conductivity	5.35E+4	J/m °C
Gas thermal conductivity	140	J/m °C
Reservoir top	600	m
Oil viscosity at 12 °C	2.0E+5	cp
Initial reservoir temperature	18	°C
<b>Injector Constraints</b>		
Bottom hole pressure (BHP)	2500	kPa
Surface water rate (STW)	75	m <sup>3</sup> /day
Injection fluid	Steam	
Steam temperature	224	°C
Steam quality	0.9	
<b>Producer Constraints</b>		
Surface liquid rate	100	m <sup>3</sup> /day
Steam rate	0.5	m <sup>3</sup> /day

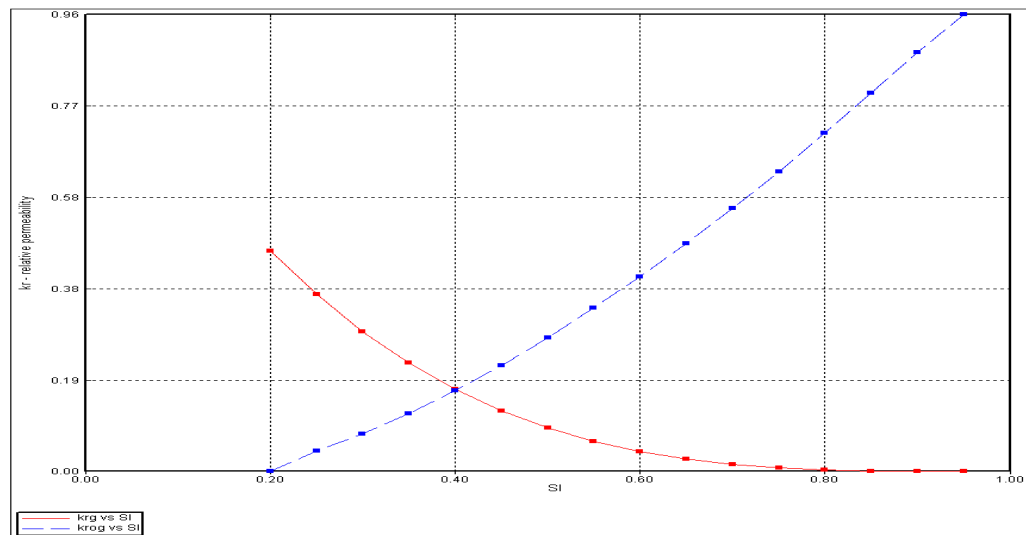


Figure 5-1: Curve of relative permeability to oil and gas

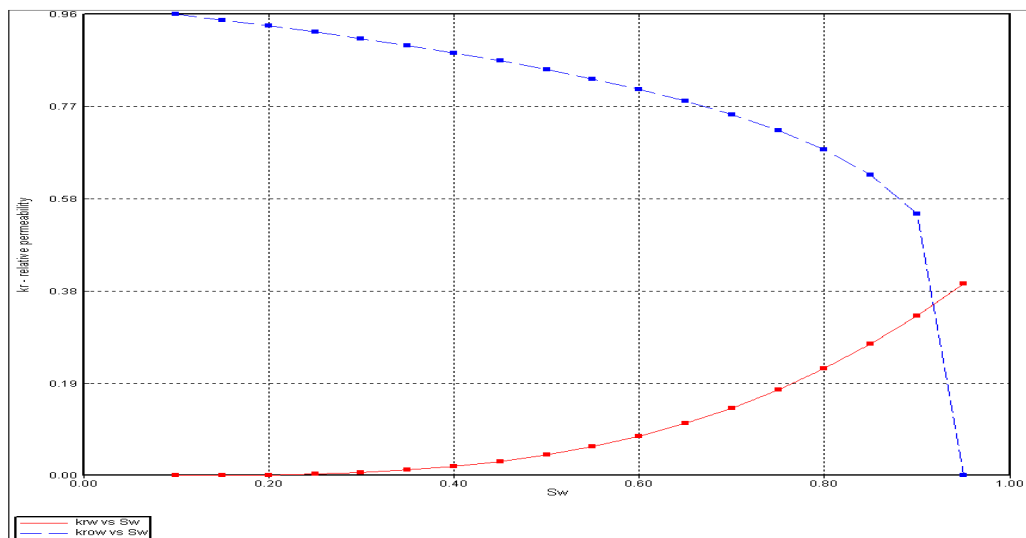


Figure 5-2: Curve of relative permeability to oil and water

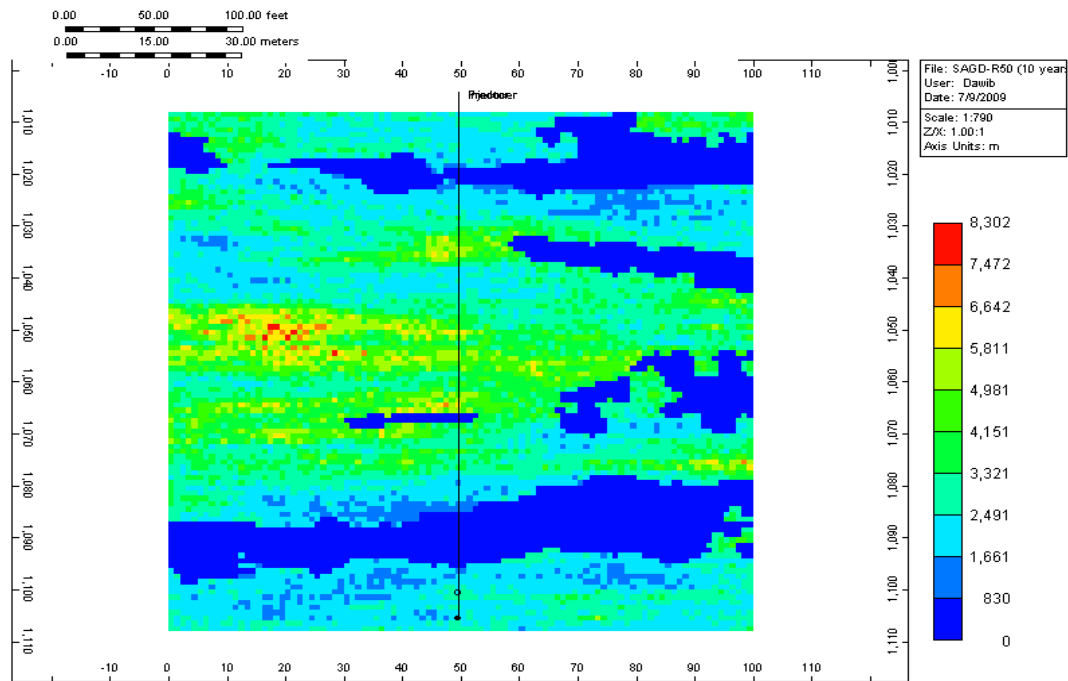


Figure 5-3: Permeability map as imported to CMG (R-50)

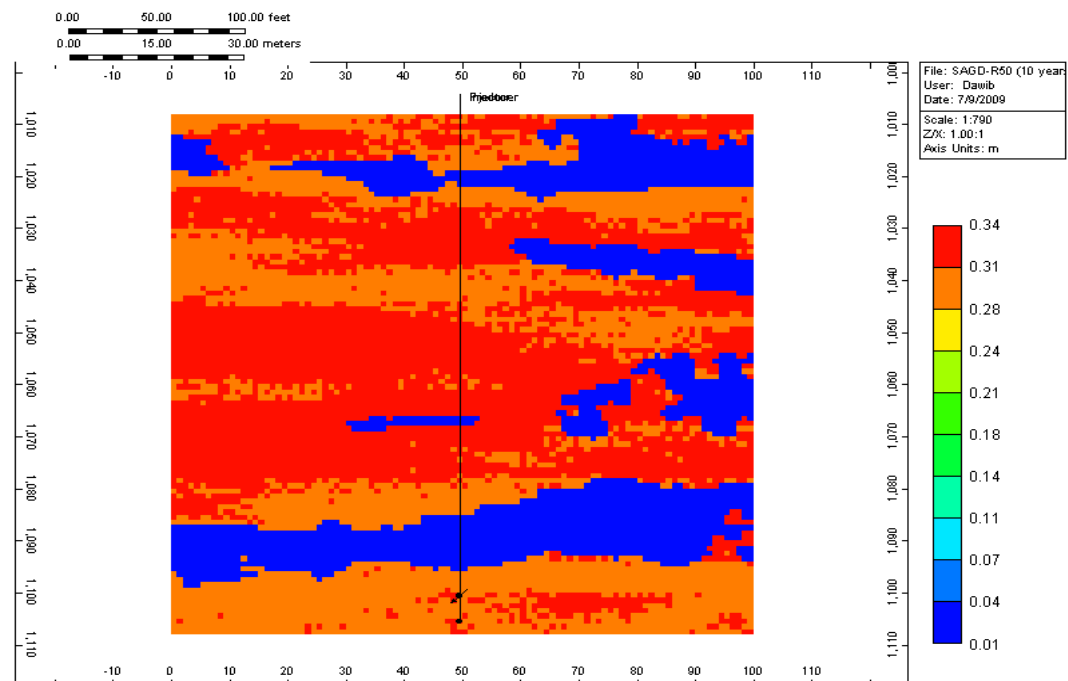


Figure 5-4: Porosity map as imported to CMG (R-50)

## 5.2 Results from Flow Simulation

Flow simulations were carried out for all realizations for a period of 10 years. Results from the CMG simulator were carefully reviewed to understand the flow behavior for each realization. Reservoir properties especially the permeability play significant role in the flow behavior. The detailed results in this chapter are presented only for realizations (here referred as R) R-6, R-50 and R-52 which indicate different flow behavior due to different properties distributions. Figure 5-5 shows the oil volume per unit area for R-50.

A wide span of shale at the bottom of the reservoir should stop any oil from flowing downward to the producer; this is clearly observed in Figure 5-6 after 10 years of production, where only oil under the shale layer was produced. Figure 5-7 shows the temperature changes during the preheating and production. Figure 5-8 plots the CSOR and COP for ten years; it also shows the daily oil production (OP). Negative correlation of OOIP with the number of realizations was observed as shown in Figure 5-9. This signifies the decreasing OOIP with the increasing realization number. For example, R-5 has OOIP of about 200,000 m<sup>3</sup> whereas R-52 has OOIP of about 170,000 m<sup>3</sup>. This is true since shale proportion is higher in R-52 than in R-5. Figure 5-10 shows the histogram of OOIP, the upper quantile is about 196,600 m<sup>3</sup>, whereas the lower quantile is nearly 170,800 m<sup>3</sup>.

The parameters of interest in these results are CSOR and COP; those two parameters will be compared with CHV from the proposed ranking method. Figures 5-11 and 5-13 show the plots of CSOR and COP with the number of realizations, respectively. COSR plot shows an increasing trend with the increasing realization number, whereas COP shows a decrease with the increasing realization number. It is clear that realizations with

high shale content require more steam injection to produce the same amount of oil. Figures 5-12 and 5-14 are the histogram of CSOR and COP, respectively. The first plot has upper quantile of 4.79 and the lower quantile is 3.4, whereas the second plot has upper quantile of about 71,800 m<sup>3</sup> and lower quantile of 48,400 m<sup>3</sup>. There are some realizations that have wider quantile ranges depending on the facies distribution.

Another factor that influences the values of CSORs and COPs is the producer well location. If the producer well is located a few meters below a shale zone, the production is adversely affected and CSOR increases due to the reduced oil production. In other words, selection of the producer well location far from any shale layer boosts well productivity. High correlation between CSOR and COP was observed as shown in Figure 5-15.

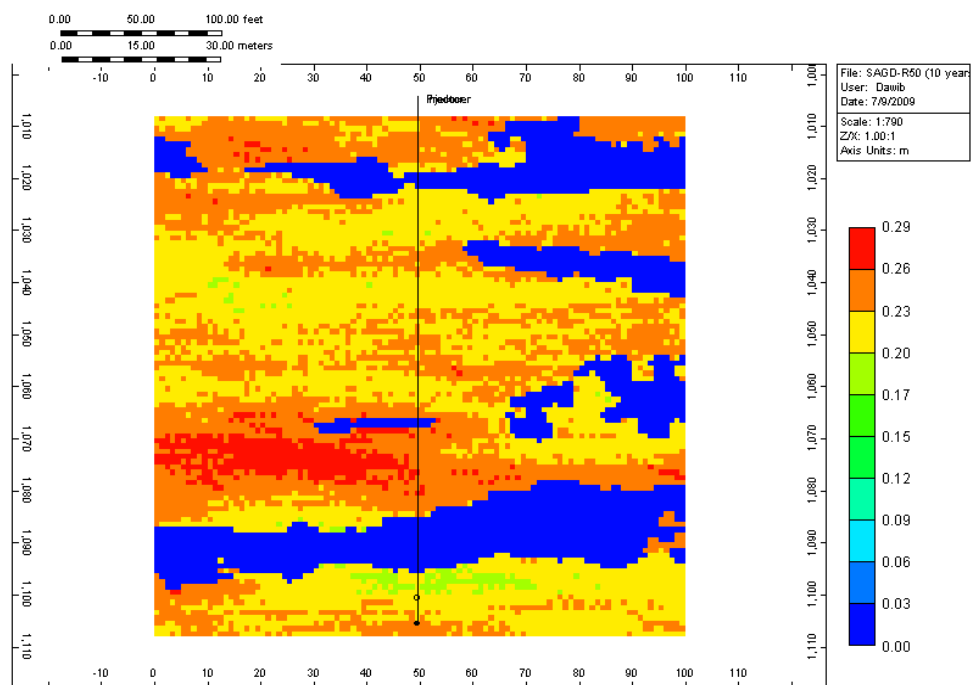


**Figure 5-5: The oil volume per unit area before drainage (R-50)**

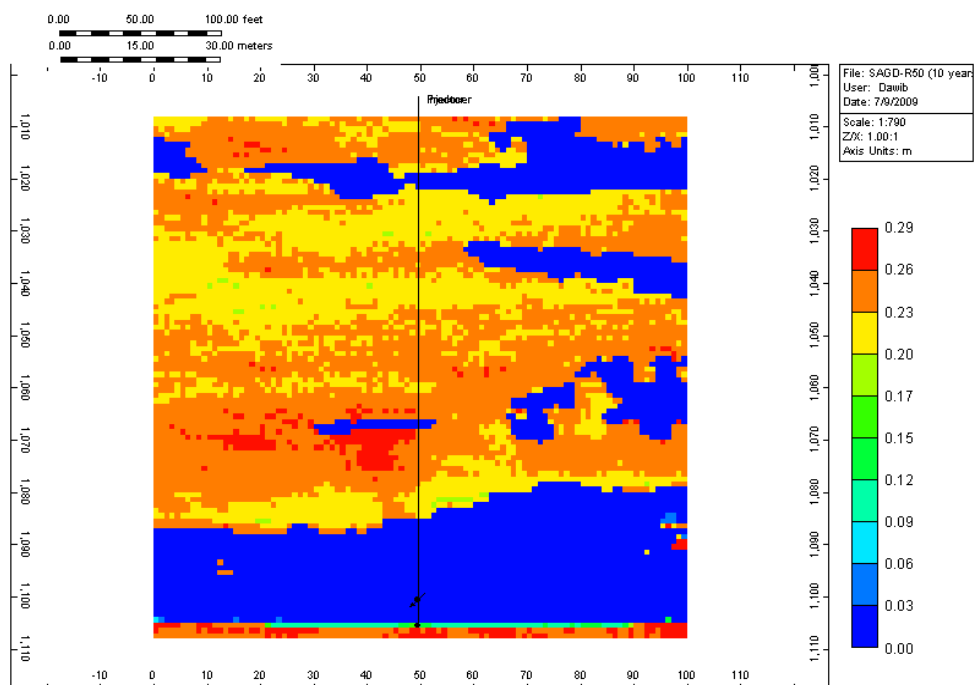


**Figure 5-6: Oil volume per unit area after 10 years of drainage (R-50)**



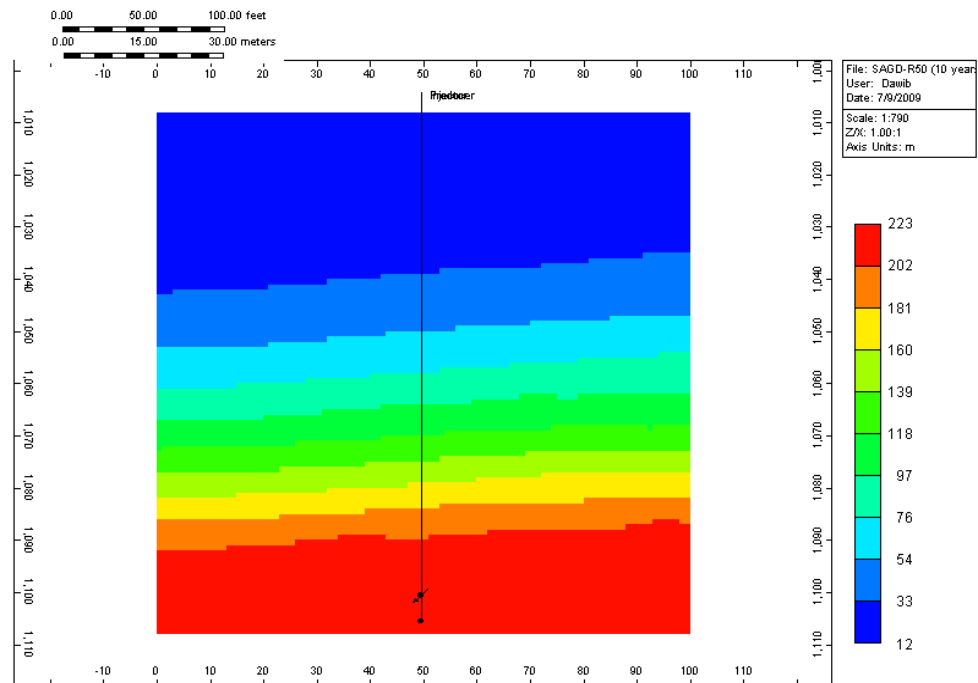


Figure 5-7: Temperature distribution after 10 years (R-50)

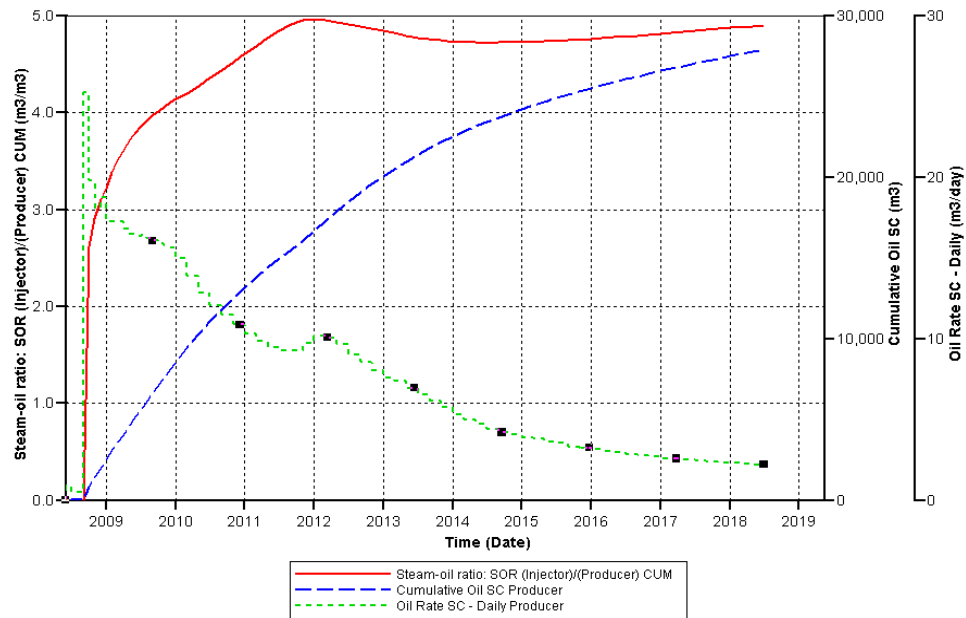


Figure 5-8: CSOR, COP and daily OP for R-50

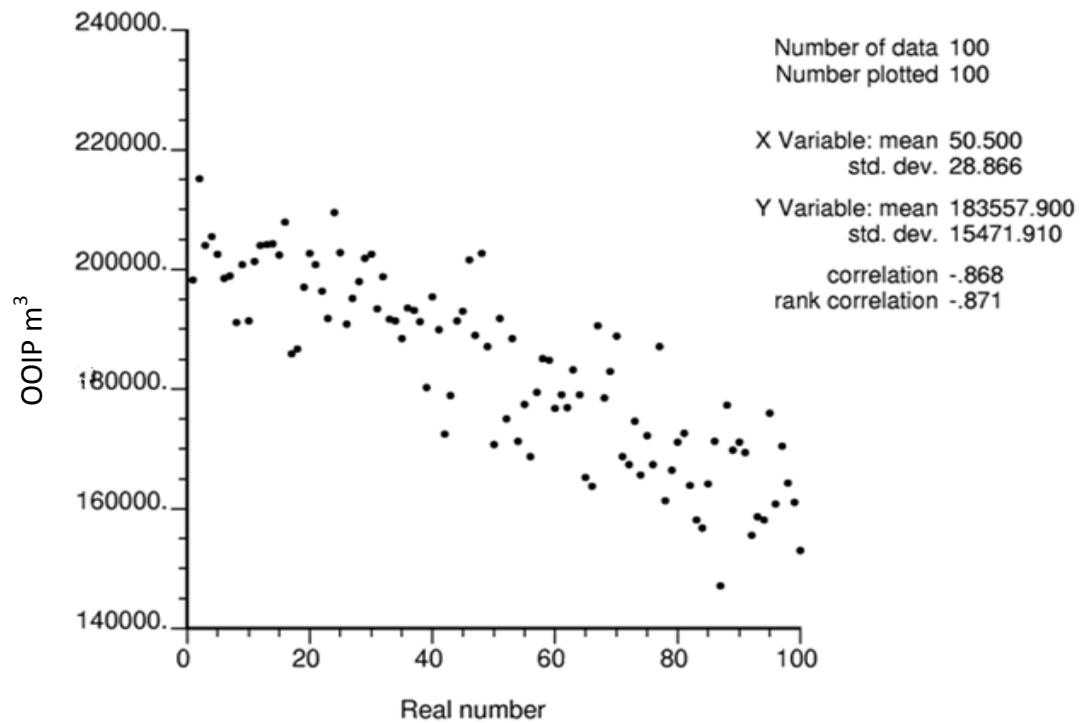


Figure 5-9: Plot of OOIP vs. realization number (CMG results)

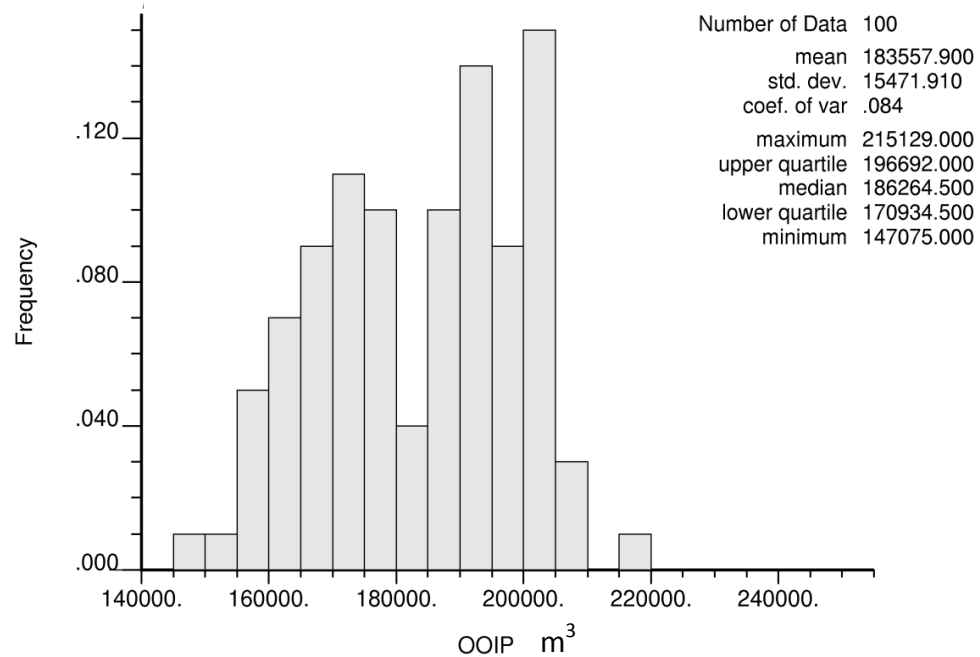


Figure 5-10: Histogram plot of OOIP (CMG results)

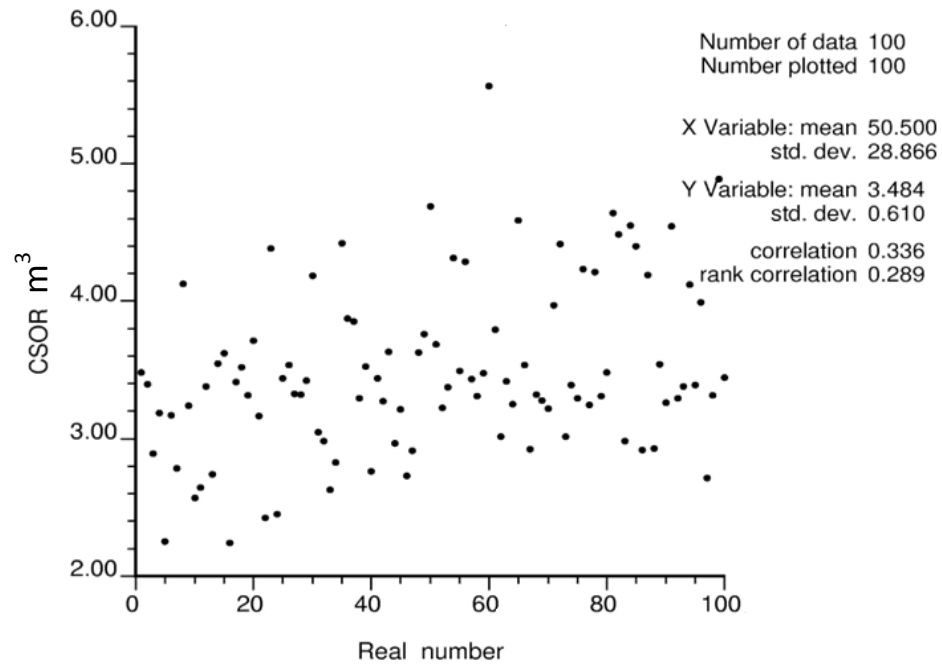


Figure 5-11: Plot of CSOR vs. realizations number (CMG results)

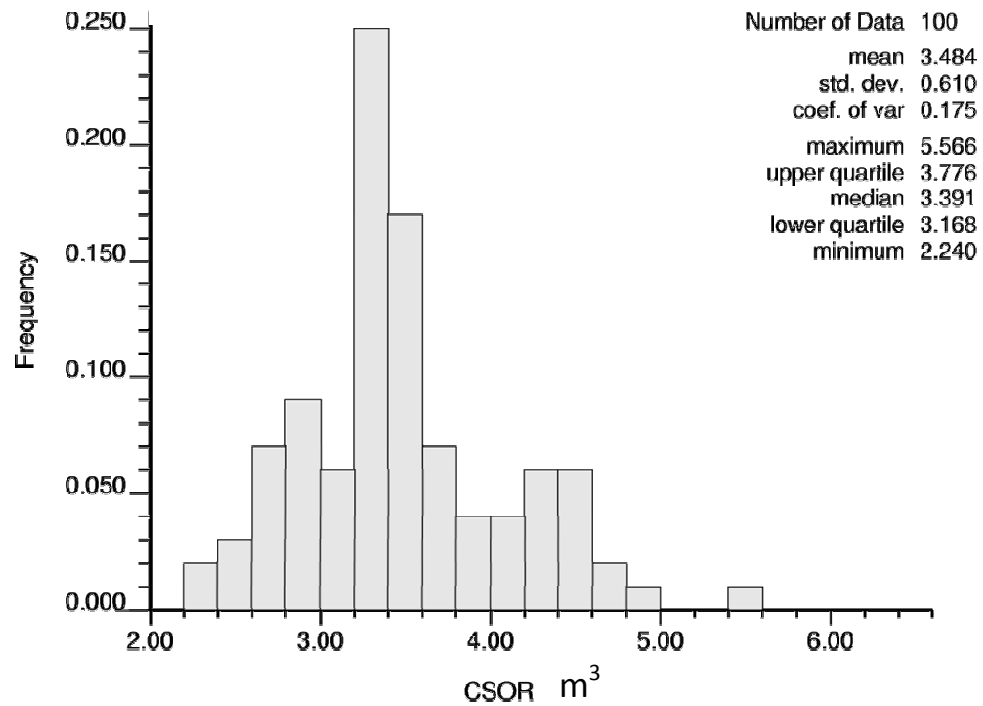


Figure 5-12: Histogram plot of CSOR (CMG results)

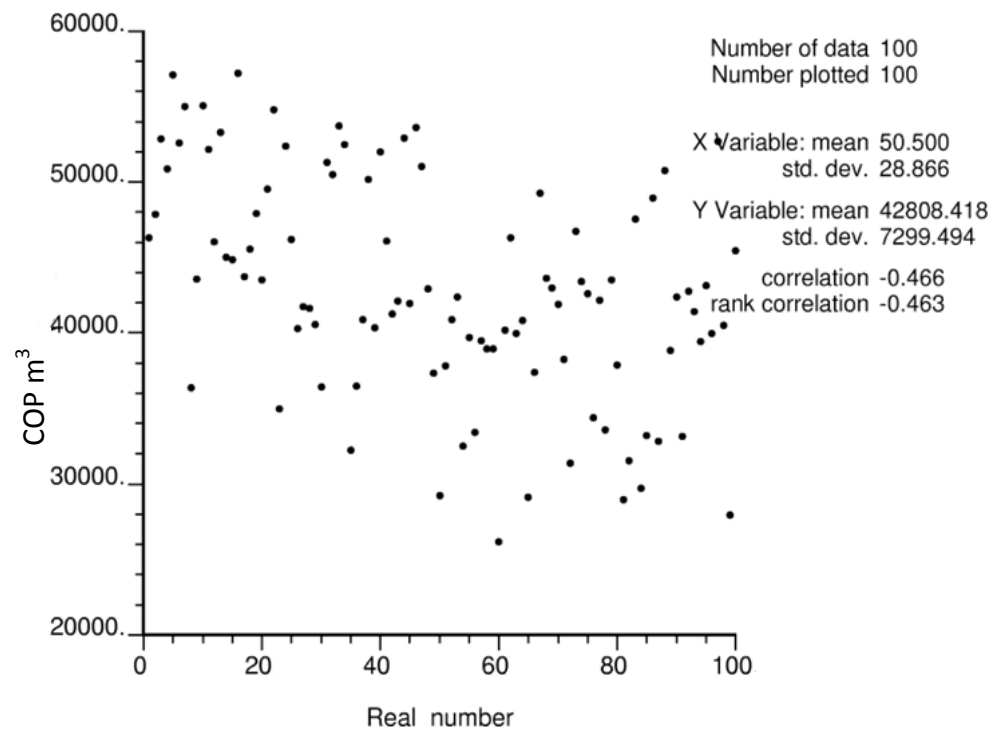


Figure 5-13: Plot of COP vs. realizations number (CMG results)

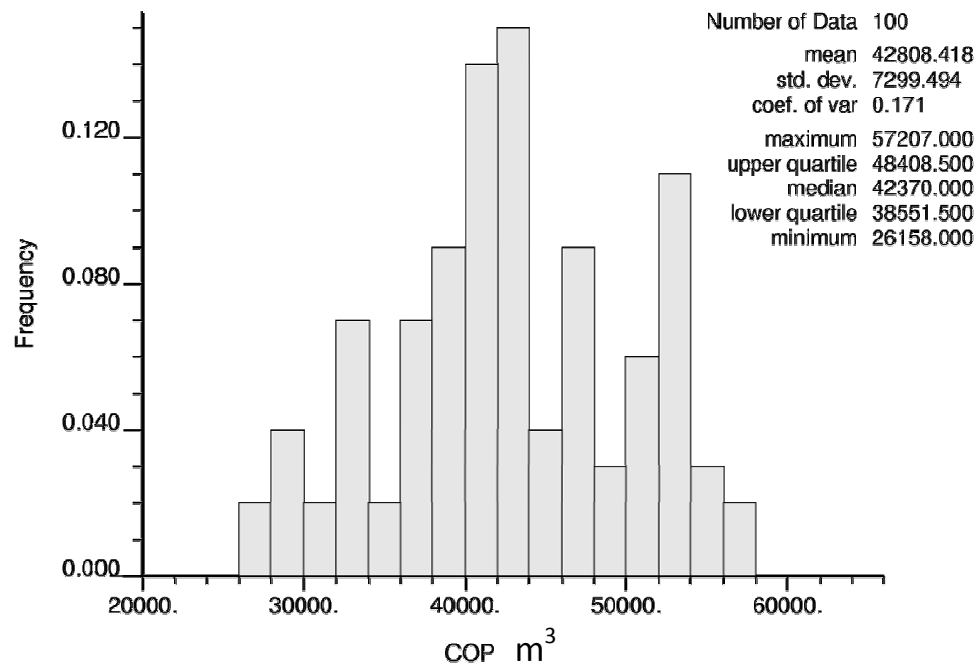
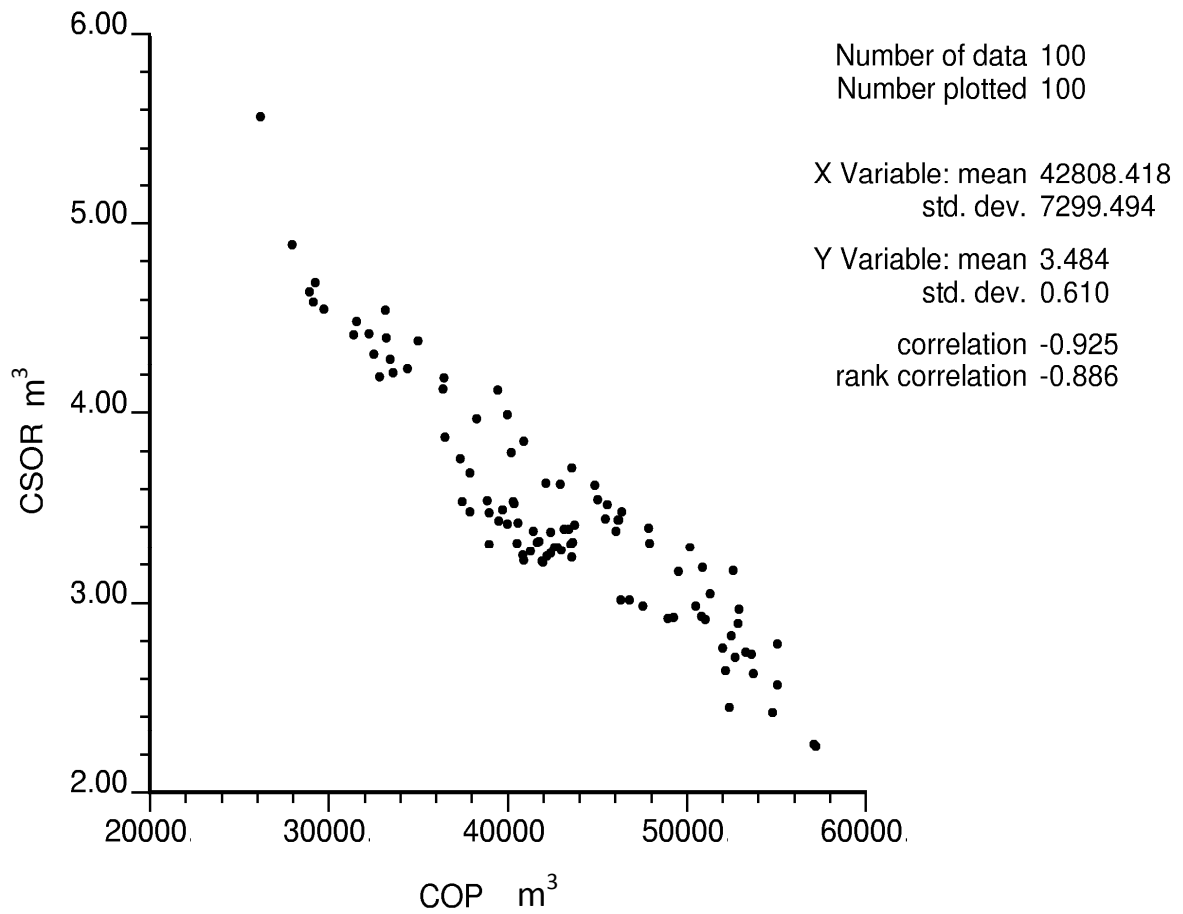


Figure 5-14: Histogram plot of COP (CMG results)



**Figure 5-15: Correlation between CSOR and COP (CMG results)**

### 5.3 Ranking using Flow Simulation Results

Realizations were ranked using CSOR and COP as the ranking parameters. Table 5-2 summarizes the first 15 ranked realizations that resulted from CMG simulator for the above-mentioned parameters.

**Table 5-2: The first 15 ranked realization based on CSOR & COP (CMG results)**

NO	Ranked Realizations	SCSOR $\text{m}^3/\text{m}^3$	Ranked Realizations	COP $\text{m}^3$	Ranked Realizations	OOIP $\text{m}^3$
1	16	2.66541	16	87317.4	2	215129
2	29	2.82186	29	81430.8	24	209583
3	24	2.94511	24	79702	16	207952
4	11	2.94796	11	79549	4	205533
5	5	2.97186	5	78244.2	14	204312
6	89	3.11353	6	78193	13	204107
7	22	3.15431	46	77481.4	12	204054
8	52	3.20687	57	76999.5	3	203972
9	7	3.22428	22	75953.4	25	202847
10	10	3.23335	15	75919.2	48	202695
11	46	3.25547	49	75716.2	20	202620
12	4	3.2807	69	75498.9	5	202575
13	3	3.28866	61	75444.8	30	202558
14	42	3.29179	10	74975.1	15	202453
15	6	3.29829	30	74922.7	29	201876

#### 5.4 Results from the Ranking Methodology

In this part, realizations were ranked from the highest to the lowest CHV. Different window sizes (WS) were used to check the WS effects. Figure 5-16 shows a map of the calculated CHV for R-50. This plot can be compared with the plot of Figure 5-6. Figures 5-17, 5-18 and 5-19 show the CHV for different realizations at WS of 50, 40, 30 and 20 m, respectively. It is evident that choosing the window size is very important. For example, in Figure 5-6 the CHV calculated at WS= 50 m relates to the entire domain despite the shale above the producer; at WS= 20 m, however, the sand zones below and above the shale were not connected.

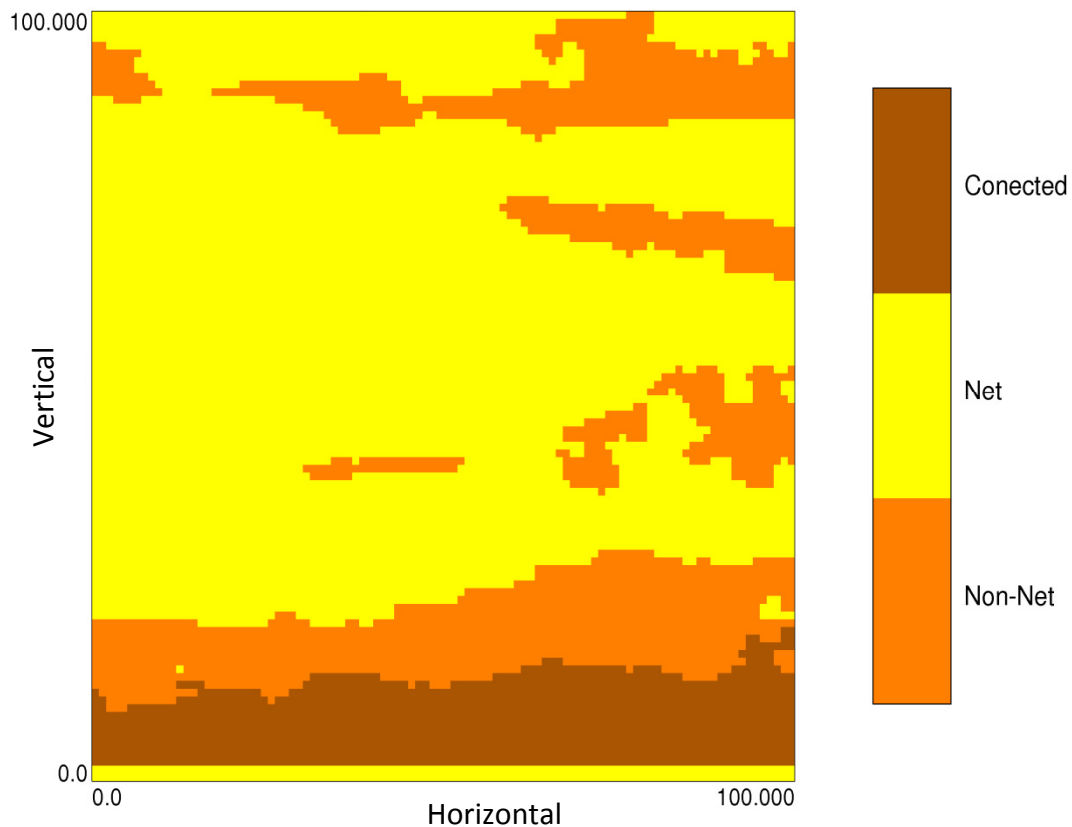


Figure 5-16: Map for calculated CHV to compare with Figure 5-12 (R-50)

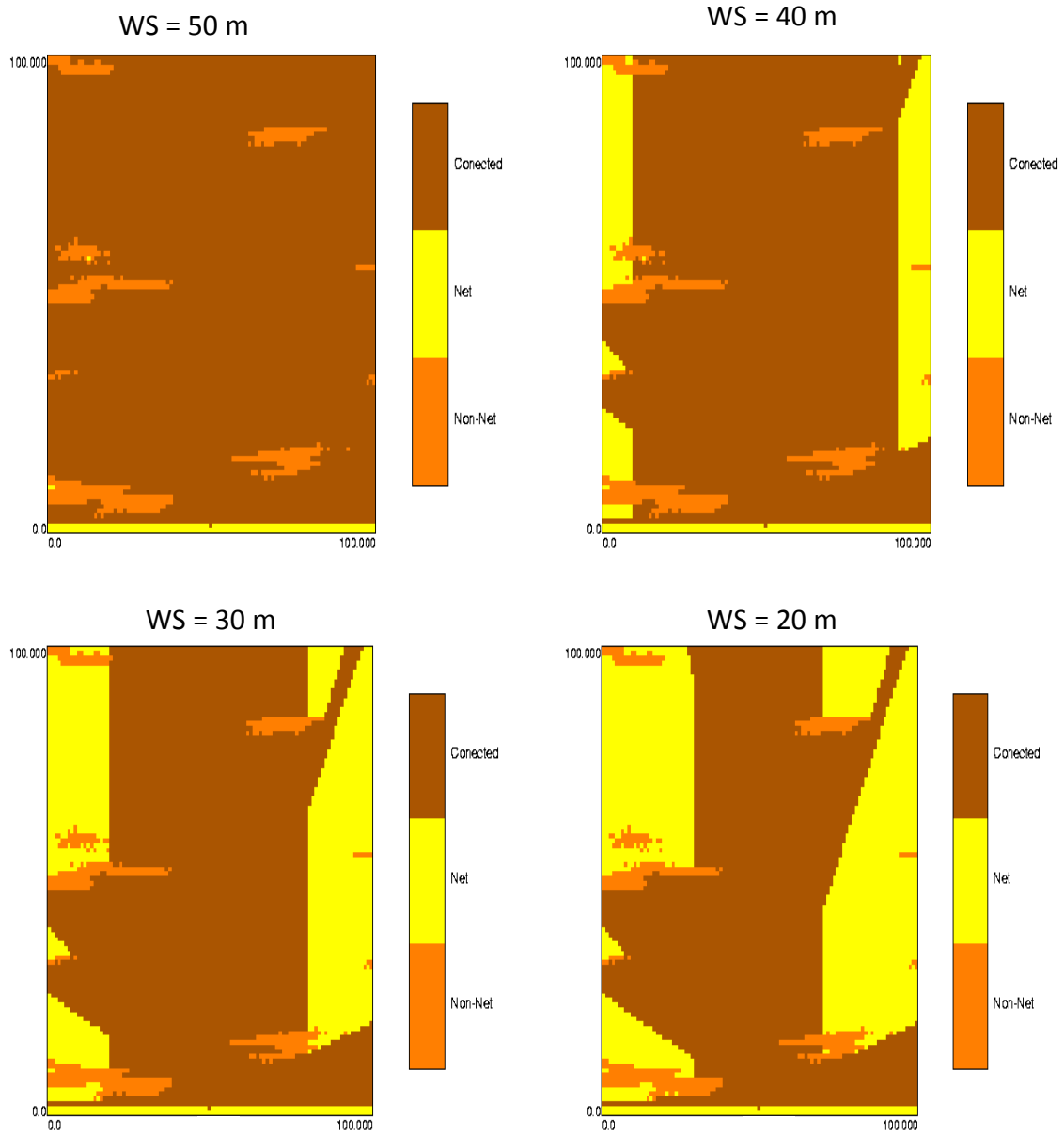


Figure 5-17: Maps of CHV at different window sizes (R-4)



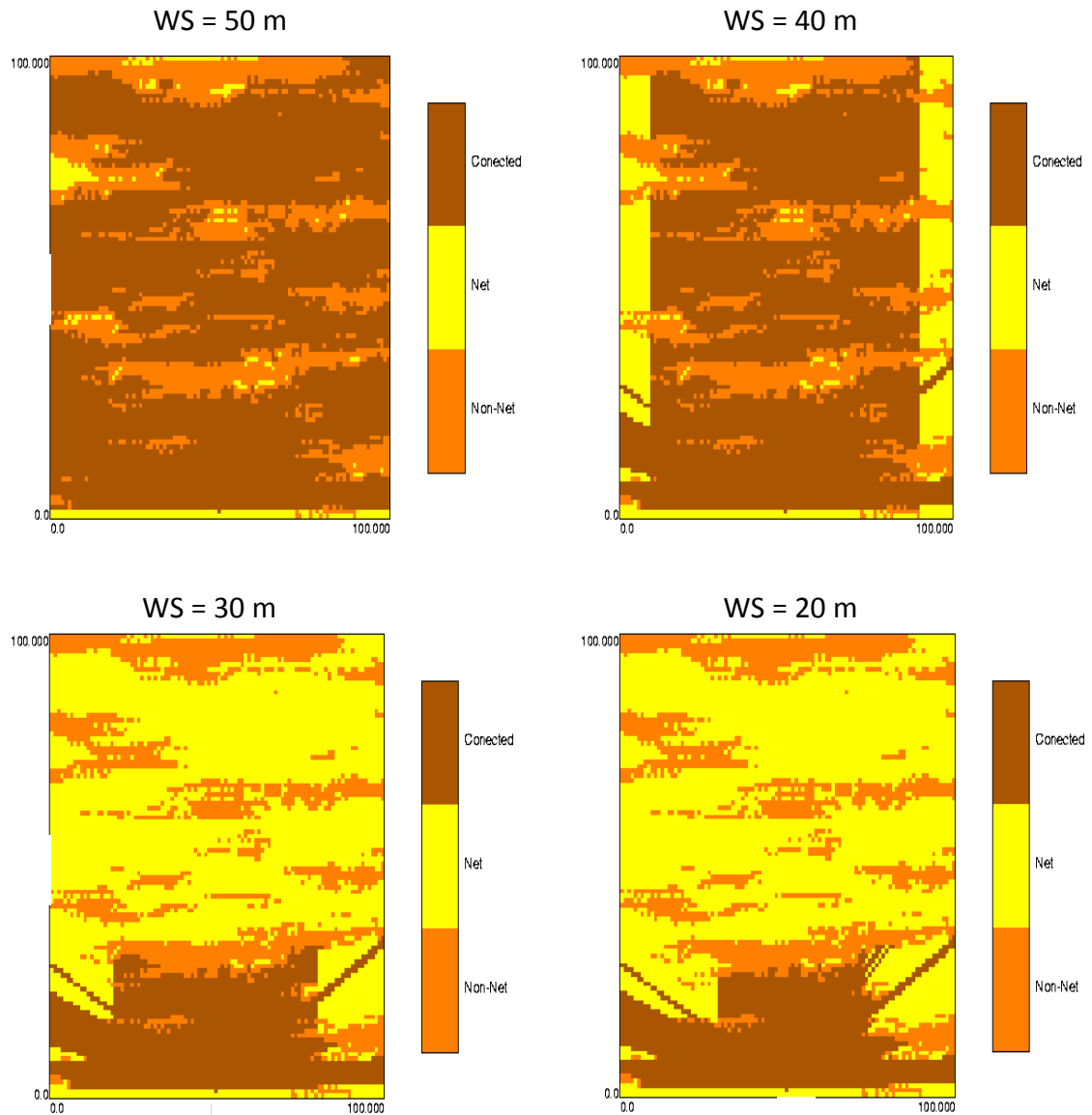


Figure 5-18: Maps of CHV at different window sizes (R-52)

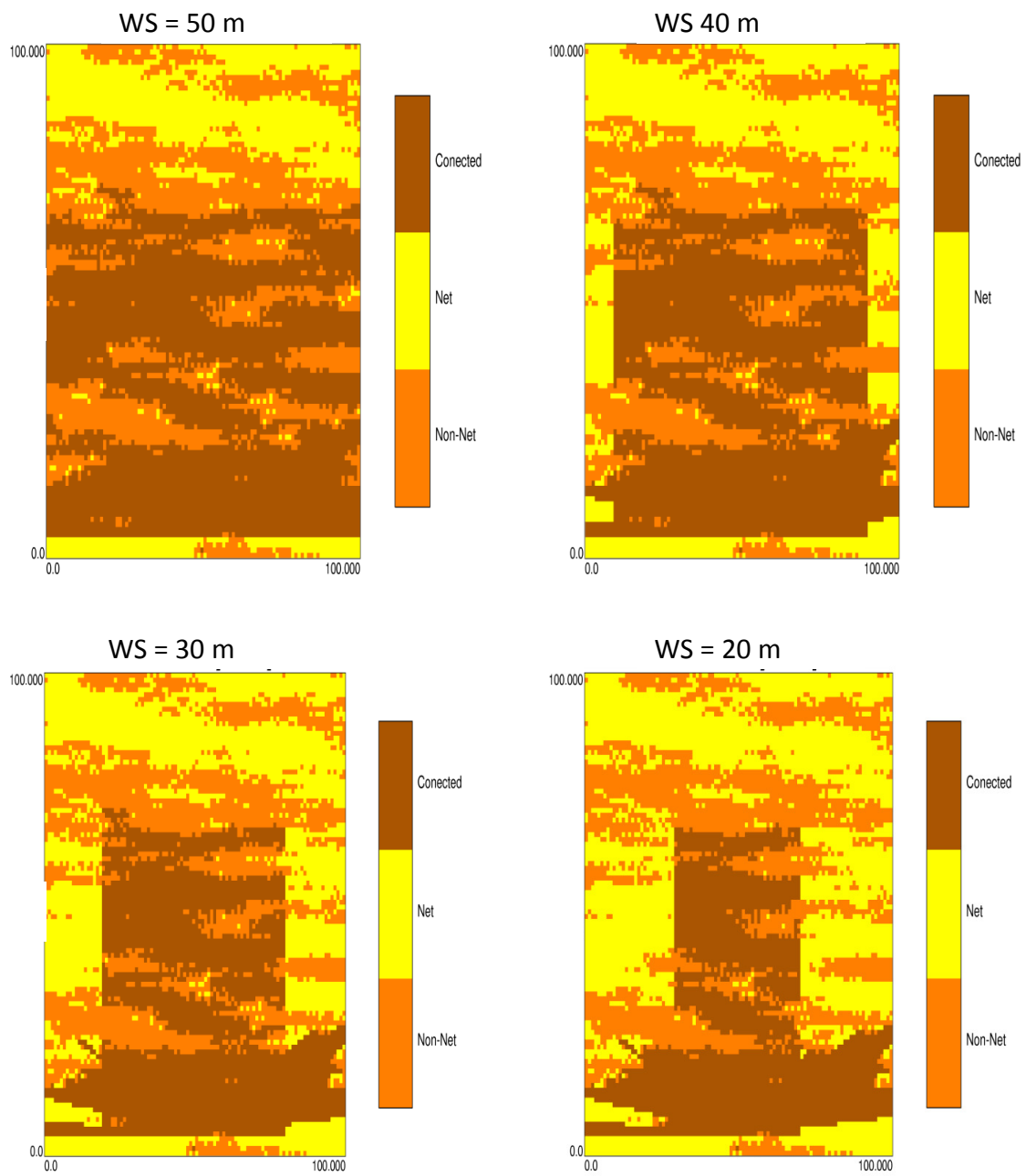


Figure 5-19: Maps of CHV at different window sizes (R-84)

Table 5–3 below summarizes the first 15 ranked realizations at different WSs. For example, R–2 ranked 1st for both WS = 50 and 40 m. It comes 2nd when WS = 30 m and 5th when WS = 20 m. Table 5–4 summarizes the number of net cells, connected net cells and CHV at different window sizes and different realizations.

**Table 5-3: The first 20 ranked realizations for different window sizes**

NO	Window Size =50 m		Window Size =40 m		Window Size =30 m		Window Size =20 m	
	Ranked Realzs	CHV m <sup>3</sup>	Ranked Realzs	CHV m <sup>3</sup>	Ranked Realzs	CHV m <sup>3</sup>	Ranked Realzs	CHV m <sup>3</sup>
1	2	2201.3	2	1999.5	7	1825.2	7	1706.4
2	4	2149.2	7	1961.1	2	1797.8	5	1632.5
3	24	2143.3	24	1960.1	24	1787.3	24	1615.8
4	6	2110.3	5	1913.8	5	1731.1	16	1600.9
5	5	2107.5	16	1903.4	16	1719.5	2	1590.5
6	16	2105.1	25	1885.8	21	1689.7	3	1441.2
7	7	2100.6	21	1872.1	25	1648.3	22	1384.6
8	14	2097.9	14	1865.0	14	1631.4	25	1366.7
9	3	2094.4	4	1847.3	3	1612.0	14	1363.4
10	25	2081.5	3	1845.6	22	1569.1	4	1320.3
11	9	2080.7	9	1820.9	4	1561.9	27	1310.3
12	15	2077.8	6	1814.6	9	1546.6	19	1294.5
13	20	2077.7	12	1799.8	27	1542.5	9	1277.1
14	48	2077.3	48	1785.7	6	1515.4	21	1269.5
15	12	2073.2	27	1785.1	19	1510.3	13	1221.1

**Table 5-4: Net cells, connected net cells and CHV for different realizations**

	Realization No. 4				Realization No. 54			
Window Sizes (m)	50	40	30	20	50	40	30	20
Net Cells	9458	9458	9458	9458	7604	7604	7604	7604
Connected Net Cells	9255	7938	6694	5660	7014	5517	4037	656
CHV (m <sup>3</sup> )	2149.24	1847.33	1561.99	1320.39	1635.59	1283.96	936.01	152.76

From the sensitivity analysis it has been observed that the correlation between OOIP and CHV decreases as WS decreases. For example, the correlation at WS = 50 m is 0.942 while at WS = 30 m it is 0.858. Thus, further results will be shown only for a WS of 50 m.

The goal is to achieve an acceptable consistency between the performance parameters and the ranking methodology. However, Figure 5-20 shows not a so remarkable correlation between CSOR and COP with CHV. To improve the correlation, various types of modifications were investigated, as well be discussed in Chapter 6.

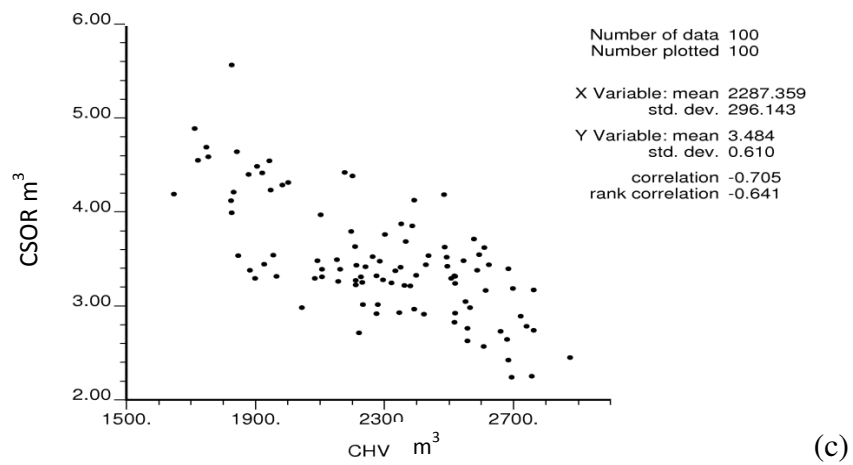
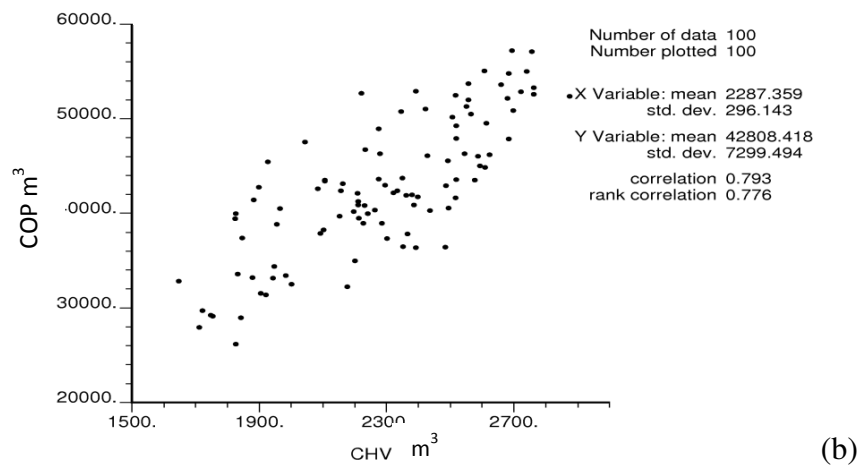
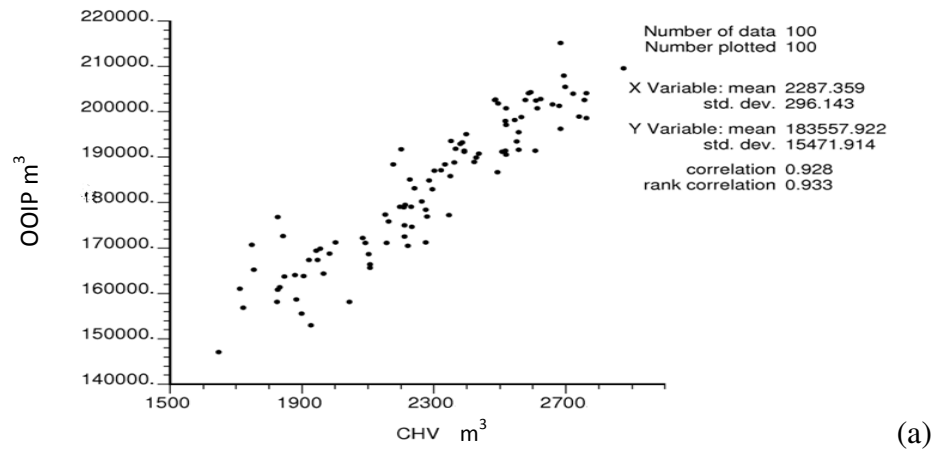


Figure 5-20: Plot of (a) OOIP , (b) COP, (c) CSOR vs. CHV at WS= 50

# Modification of the Ranking Method

---

## 6.1 The Need for the Modification

It is rare to find a relatively homogeneous reservoir with uniform or regular shape. For example, the actual reservoir permeability varies in non-uniform distribution due to the reservoir heterogeneity. In addition to the properties, the reservoir thickness is also not uniform. Cardwell et al (1944) stated that actual reservoirs have complicated shapes and non-uniform permeabilities and porosities.

Effective permeability is an important aspect in reservoir characterization and considered as the most significant reservoir property that affects fluid flow through the formation. Several studies have been carried out on effective permeability and its effects on fluid flow through a porous medium. Cardwell et al (1944) conducted their work by calculating average permeability using harmonic and average arithmetic averaging methods. Deutsch (1989) studied experimentally two methods to calculate the block effective permeability in both sandstone and shale. The two methods were power-average and percolation models. Typically a geometric average ( $\omega = 0$ ) is used for vertical permeability and arithmetic average ( $\omega = 1$ ) is used for horizontal permeability (Deutsch, 1989), where  $\omega$  is the average power between -1 and +1. The procedure to calculate the average permeability for the SAGD drainage volume is included in this chapter.

The objective is to improve the correlation between CHV from the ranking methodology and the SAGD performance parameters evaluated from the flow simulations. As mentioned in the last chapter, the correlation between CHV and COP was not remarkable, see Figure 6-1, rendering P10, P50 and P90 selection difficult. The modification to the methodology will be discussed in the remainder of this chapter.

### **6.2 Modification of the Methodology**

The observation from the results indicates that the permeability, especially around the wellbore, plays a great role in fluid flow. To improve the correlation, each realization is divided into 100 horizontal layers and weighted average permeability is evaluated for each layer. The averaging starts from the bottom layer and moves upward. Next, a dimensionless scaling factor (wt) is evaluated. This factor is multiplied by CHV to give the modified CHV (MCHV).

The average weighted permeability is preferably evaluated in layers whose directions conform to the flow directions such as horizontal, vertical or radial.

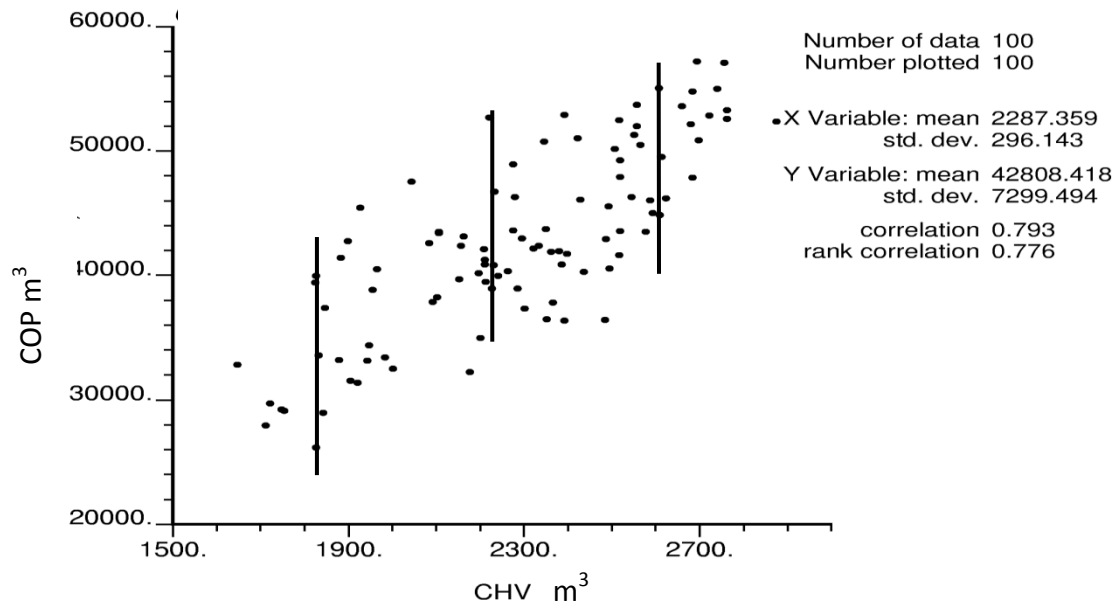


**Figure 6-1: Correlation of CHV with COP**

In the proposed modification, arithmetic averaging is done along the X direction using the following formula:

$$K_{(arithmetic)} = \frac{\sum k_i}{N} \quad 6-1$$

Harmonic averaging calculation is performed along the Z direction using the following formula:

$$K_{(harmonic)} = \frac{N}{\frac{1}{k_i} + \dots + \frac{1}{k_n}} \quad 6-2$$

where:



K is the average calculated permeability,

$k_i$  is the individual permeability for each grid block in each layer,

N is the number of the grid blocks.

In the general case of blocks of porous medium involving variable permeabilities and any type of directional variations, the equivalent permeability lies between a harmonic and an arithmetic average of actual permeabilities (Cardwell et al, 1944).

The idea here is to sum all the calculated arithmetic average in the X direction with the calculated harmonic average in the Z direction to calculate the effective average permeability in all directions according by the following formula:

$$\frac{1}{K_{eff}} = \sum_{layers} wt_i * \frac{1}{k_i} \quad 6-3$$

After calculating the weighted average effective permeability, a dimensionless weighted factor is established and multiplied by the CHV calculated before. The weight factor uses the median permeability value and calculates a factor using to the following equation:

$$F_{(k)} = 1 - e^{\left[\frac{-3K}{K_{net}}\right]} \quad 6-4$$

The final modified connected hydrocarbon volume (CHV modified) is calculated using the following equation:

$$MCHV = F_{(K)} * CHV \quad 6-5$$

The geostatistical ranking algorithm (the code built for ranking) was modified to include the average permeability calculation discussed above.

### 6.3 Results from the Modified Ranking Method

The results obtained from the modified ranking method must be convincing to ensure this method can be used to rank the realizations. This section shows the results from the modified ranking method.

Figure 6-2 is a plot of COP versus MCHV. A significant improvement by the modification can be observed. Figure 6-3 shows a plot of CSOR versus MCHV, which indicated most of the data are located at low CSOR and high CHV. Compared to results from Figure 5-20, the correlation between CSOR and the modified CHV shows an improvement as much as 20%. Plot of CSOR with COP at high correlation is shown in Figure 6-4. An acceptable improvement in the ranking method is observed from the results obtained from the modification.

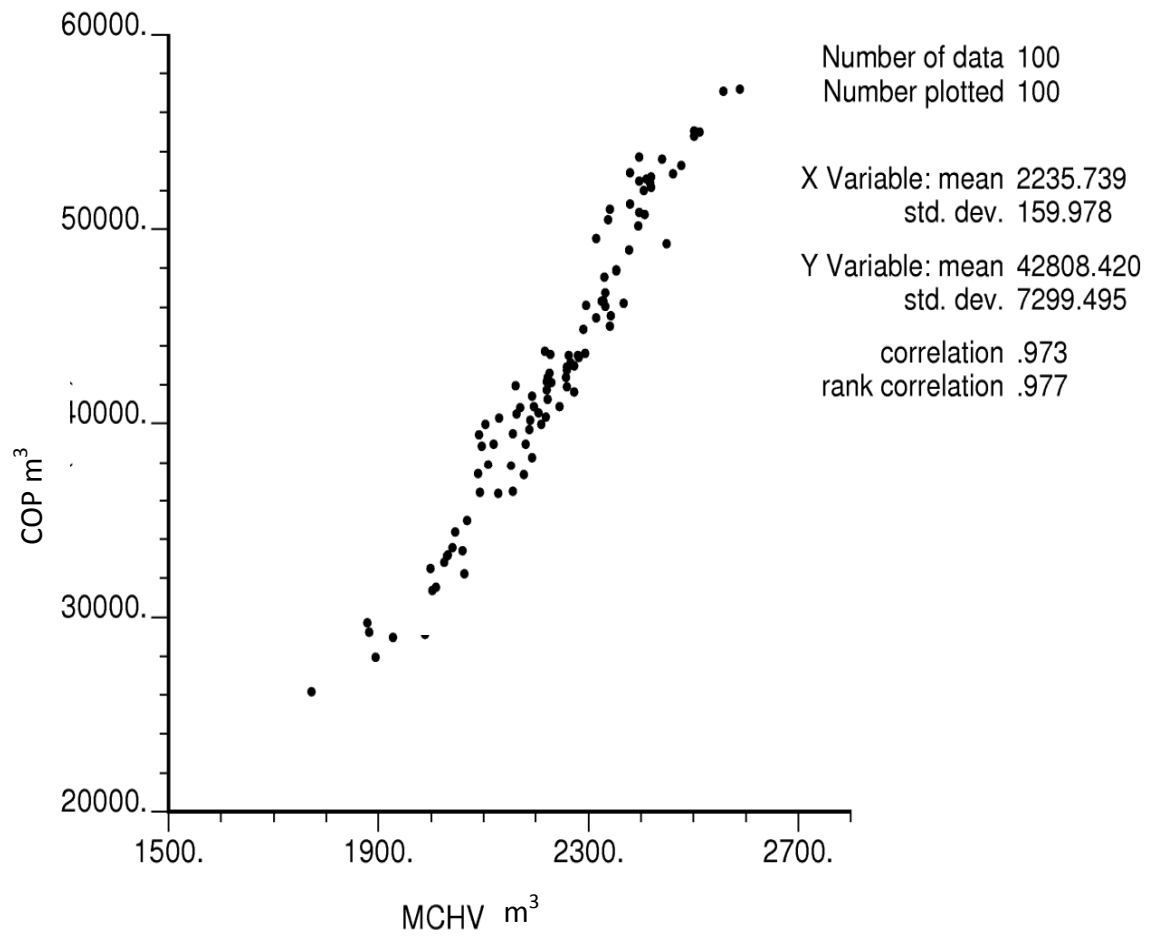
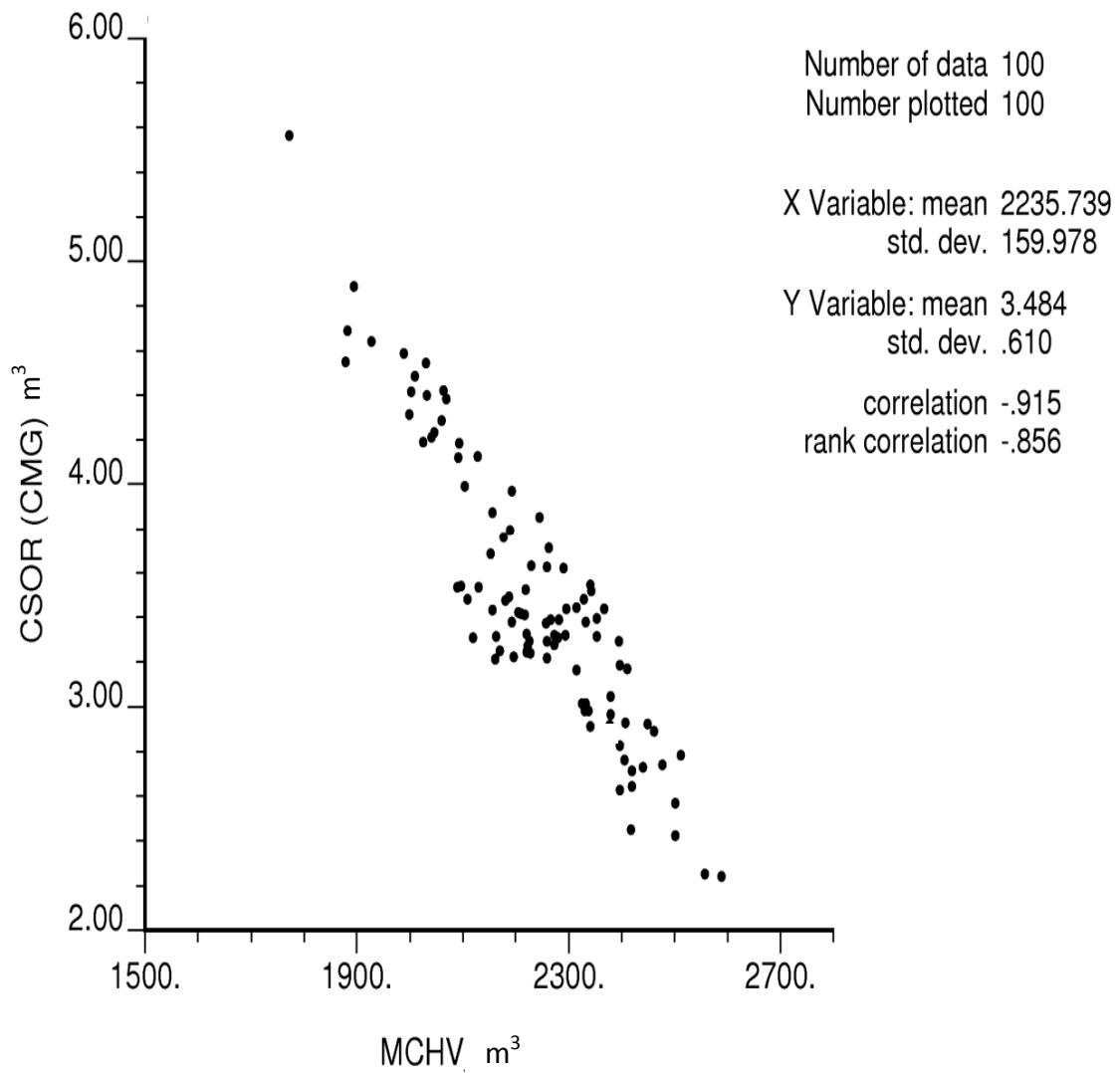


Figure 6-2: Plot of COP with MCHV



**Figure 6-3: Plot of CSOR with MCHV**

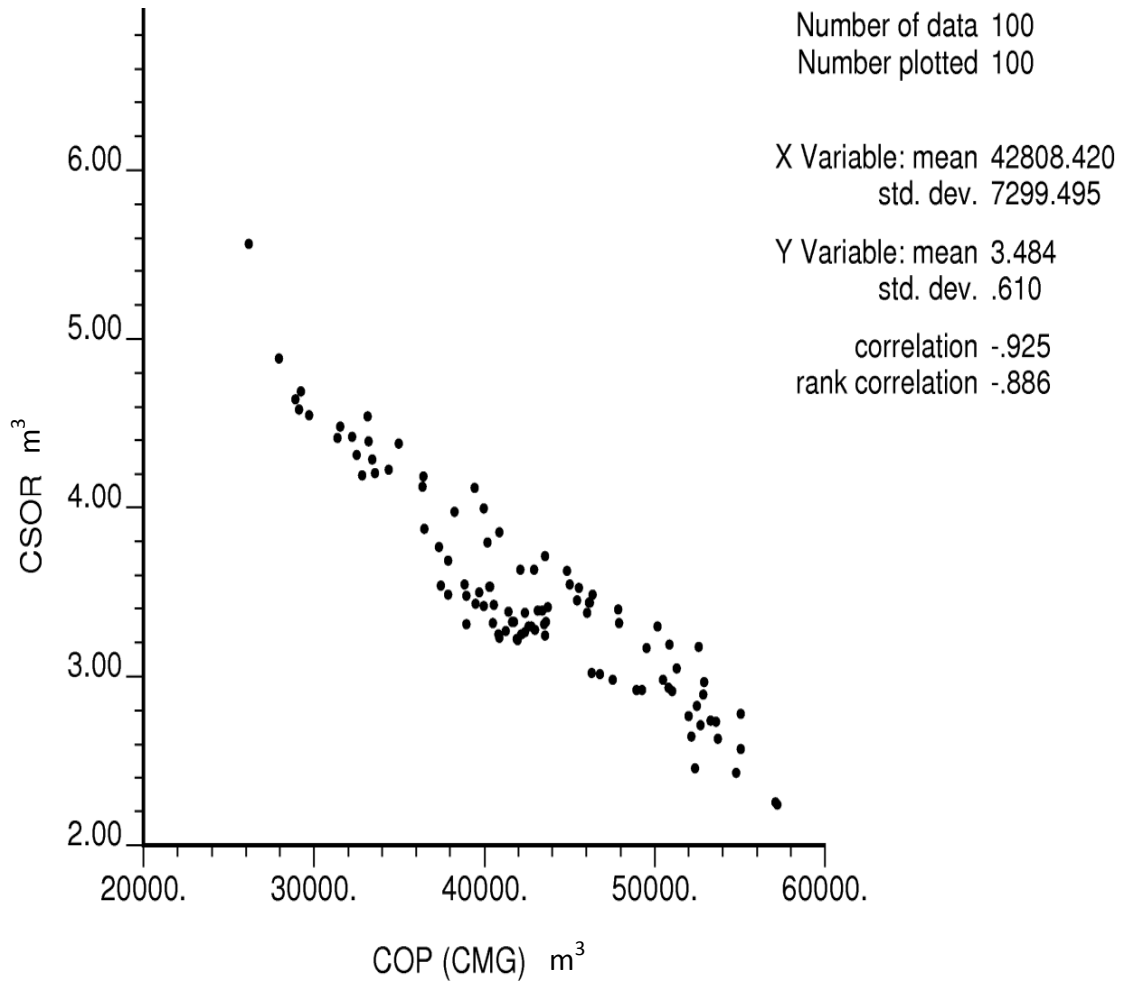


Figure 6-4: Plot of COP with CSOR after MCHV

# Conclusions and Recommendations

---

This thesis developed a geostatistical methodology for ranking multiple realizations to reduce the large number of realizations to a few that can be easily used in flow simulations. The ranking methodology as proposed in this thesis was validated against the results of detailed simulations. A strong correlation was observed between the parameter of the ranking methodology (CHV) and the performance parameters (COP and CSOR), which validates the proposed methodology. The summary and main conclusions of this research are described below.

## 7.1 Summary

Synthetic data were generated for a SAGD reservoir case. 100 realizations were generated for each of the variables, porosity, permeability, and fluid saturation in both sandstone and shale. The realizations were generated using geostatistical tools. All the data were tested, reviewed and imported to the reservoir simulator and the proposed ranking tool.

A geostatistical algorithm was developed and applied to rank a large number of realizations. Non-commercial software, namely GSLIB, was used to generate the realizations.

An important component in the developed ranking methodology is to merge porosity, permeability, water saturation and lithofacies together and produce maps that

represent the distribution of each of the properties in accordance with the geological facies.

In generation of lithofacies realizations, the sand-to-shale volume proportion was designed to increase as much as 0.025% for each increase in realization number. The volume proportion started at 95% for sand and 5% shale; the last realization consisted of 70% sand and 30% shale.

The proposed ranking methodology was applied to a SAGD reservoir case. Modifications may be needed to the methodology for application to other types of reservoirs.

SAGD is *in situ* thermal process which requires utilization of a hydro-thermal simulator in the validation process. The simulations were conducted for 10 years of operation. All the correlations between the CHV and the performance parameters were made at the end of the 10 years period. It would be instructive, however, to examine the correlation at different times in future research.

An important component of the ranking methodology was the cutoff values that were considered for porosity, permeability and water saturation. In that, if the porosity or other properties of a cell were below certain value, they were excluded from the CHV calculations.

The results obtained from the ranking method are important for reservoir characterization, managements, and production performance prediction. In SAGD, COP and CSOR are two important performance parameters that are interrelated and have significant impact on project profitability. Steam-oil-ratio and production rate should be considered as coupled variables.

In this work, the ranking methodology parameter, CHV, was correlated with the SAGD performance parameters. The advantage is that the possible range of hydrocarbon recovery can be evaluated without needing to perform a large number of detailed reservoir simulations.

## **7.2 Conclusions**

This research showed that the CHV was a viable static parameter that could be easily evaluated and is highly correlated to dynamic simulation parameters such as COP and CSOR.

In the unmodified ranking methodology, relatively poor correlations resulted in the middle ranges of CHV. The consequence is that several realization cases with different COP values correspond to a single CHV value. The correlation is much better near the high and low CHV values. Consequently, it is relatively easy to pick the P10 and P90 but difficult to pick the P50.

The modified methodology resulted significant improvements in correlations. In that, a formula was developed for a coefficient of CHV. The coefficient was a function of harmonic and arithmetic averages of permeability. An improvement as much as 20 %



resulted in the correlation between the proposed ranking parameter, CHV, and the performance parameters, COP and CSOR.

The realizations in which a large shale zone surrounded the injector and producer or in which a shale layer spanned across the reservoir boundaries resulted in the least CHV values and as well showed poor COP and CSOR values in the simulations.

### **7.3 Future Work**

The main recommendations for future research can be summarized as follows:

- Although the ranking method was developed for a SAGD reservoir, it may be applied to any reservoir after modifications to the procedure for calculating CHV. The correlation in this research was made with the production performance parameters of SAGD, i.e COP and CSOR. It is recommended to carefully examine the correlation parameter in other applications.
- It is recommended to study the application of the ranking methodologies in history match analysis, where multiple realizations are involved in the study.

## References

Ates, H., Bagar, A., and Mohsen, S., 2003. *Ranking and Upscaling of Geostatistical Reservoir Models Using Streamline Simulation*, Society of Petroleum Engineers (SPE), Paper 81497.

Ballin, P.R., Journel, A.G., and Aziz, K.A., 1992. *Prediction of Uncertainty in Reservoir Performance Forecasting*, JCPT, **31** (4): 52-62.

Butler, R., 1998. *SAGD Comes of Age*, *Journal of Canadian Petroleum Technology*, 37(7): 9-12.

Cardwell, W.T. and Parsons, R. L., 1944. *Average Permeabilities of Heterogeneous Oil Sands*. Los Angeles Meeting, A.I.M.E.

Da, Cruz. and Deutsch, C.V., 2000. *Reservoir Management Decision Making in Presence of Uncertainty*, CCG 2<sup>nd</sup> report.

Da. Cruz, P., Home, R., and Deutsch, C.V., 2003. *Quality Map: A Tool for Ranking Reservoir Uncertainty Quantification and Decision Making*, Society of Petroleum Engineers (SPE), Paper 98168.

Deutsch, C., 2002. *Geostatistical reservoir Modeling*. Oxford University Press, New York.

Deutsch, C.V. and Srinivasan, S., 1996. *Improved Reservoir Management through Ranking Reservoir Models*, Society of Petroleum Engineers (SPE), Paper 35411.

Deutsch, C.V., 1989-1999. *Fortran Programs for Gaussian Back Transformation*, Publicized in Computers and Geosciences.

Deutsch, C.V., 1989-1999. *Fortran Programs for Sequential Gaussian Simulation*, Publicized in Computers and Geosciences.

- Deutsch, C.V., 1993. *Fortran Programs for Merge Multiple GSLIB out Files*, Publicized in Computers and Geosciences.
- Deutsch, C.V., 2003. *Fortran Programs for Conditional Simulation of 3-D Rectangular Grid*, Publicized in Computers and Geosciences.
- Deutsch, C.V., 2007. *Geostatistical Methods for Modeling Earth Sciences Data*, Class Notes, MIN 612, University of Alberta.
- Deutsch, C. V., 2008. *Fortran Programs for Calculate Local Connectivity Within Specified Windows*, Publicized in Computers and Geosciences.
- Deutsch, C. V., 2005. *Some Notes on the Value of Ranking Realizations*, Center for Computational Geostatistics (CCG).
- Deutsch, C. V, Begg, S.H., 2001. *The Use of Ranking to Reduce the Required Number of Realizations*. Society of Petroleum Engineers (SPE), Paper 32456
- Deutsch, C. V., 1992. *Annealing Techniques Applied to Reservoir Modeling and the Integration of Geological and Engineering (Well Test) Data*. PhD Thesis, Stanford University, Stanford, CA. 306 p.
- Deutsch, C. V and Jason A. McLennan., 2003. *Guide to SAGD (Steam Assisted Gravity Drainage) Reservoir Characterization Using Geostatistics*, Centre for Computational Geostatistics, Guidebook Series **3**.
- Deutsch, C.V. and Journel, A.G., 1998. *GSLIB: Geostatistical Software Library and User's Guide*, 2nd Edition, Oxford University Press.
- Deutsch, C.V., 1998. *Fortran Programs for Calculating Connectivity of 3-D Numerical Models and Ranking Multiple Realizations*, Computers and Geosciences, **24** (1): 69-76.

- Fang, J.H. et al, 1992. *Reservoir Characterization vs. Geostatistical and Fractal Simulations*, SPE 25525.
- Gilman, J., Meng, H., Uland, M., Dzurman, P., and Cosic, S., 2005. *Statistical Ranking of Stochastic Geomodels Using Streamline Simulation: A Field Application*, Society of Petroleum Engineers (SPE), Paper 77374.
- Hewett, T.A., 1986. *Fractal Distributions of Reservoir Heterogeneity and Their Influence on Fluid Transport*. SPE paper 15386.
- Idrobo, E.A., et al, 2000. *Swept Volume Calculations and Ranking of Geostatistical Reservoir Models Using Streamline Simulation*, Society of Petroleum Engineers (SPE), Paper 62557.
- Isaaks, E. H. and Srivastava, R.M., 1989. *An Introduction to Applied Geostatistics*. New York, Oxford University Press, 561 p.
- Isaaks, E. H., 1991. *The Application of Monte Carlo Methods to the Analysis of Spatially Correlated Data*. PhD Thesis. Stanford University, 226 p.
- Journel, A.G., 1990. *Geostatistics for Reservoir Characterization*, SPE paper 20750.
- Mccarthy, J.F., 1993. *Reservoir Characterization: Efficient Random-Walk Methods for Upscaling and Image Selection*, Society of Petroleum Engineers (SPE), Paper 25334.
- McLennan, J. and Deutsch, C.V., 2005. *Ranking Geostatistical Realizations by Measures of Connectivity*, Society of Petroleum Engineers (SPE), Paper 98168.
- McLennan, J. and Deutsch, C.V., 2004. *SAGD Reservoir Characterization Using Geostatistics*, Center for Computational Geostatistics (CCG), September.
- National Energy Board, 2006. *Canada's Oil Sands: Opportunities and Challenges to 2015*, An Energy Market Assessment.

National Energy Board, 2004. *Canada's Oil Sands: Opportunities and Challenges to 2015*, An Energy Market Assessment.

National Energy Board, 2000. *Canada's Oil Sands: A supply and Market Outlook to 2015*, An Energy Market Assessment.

Norrena, K, Deutsch. C.V., 2002. *Automatic determination of Well Placement Subject to Geostatistical and economic Constraints*, Society of Petroleum Engineers (SPE), Paper 78996.

Randy, J.M., 1999. *Oil Sands Conditioning, Bitumen Release Mechanisms and New Process Development*, CIM.

Ren, W., Leuanghong, O. and Deutsch, C.V., 2004. *Geostatistical Reservoir Characterization of McMurray Formation by 2-D Modeling*, CCG Report 6.

Saad, N., Maroongroge, V. 1996. *Ranking Geostatistical Using Tracer Production Data*, Society of Petroleum Engineers (SPE), Paper 35494.

Wang, Y. Kovscek., 2002. *Streamline Approach for Ranking Reservoir Models that Incorporates Production History*, Society of Petroleum Engineers (SPE), Paper 77377.

Zanon, S. Zabel, F. and Deutsch, C.V., 2005. *Improvement of Realizations through Ranking for Oil Reservoir Performance Prediction*, Center for Computational Geostatistics (CCG).

## Appendix A      Code of CMG-STARs

RESULTS SIMULATOR STARS 200800

RANGECHECK ON

TITLE1 'Ranking Of Realizations-SAGD'

CASEID '20030610'

\*INUNIT \*SI

\*INTERRUPT \*INTERACTIVE

WPRN GRID 0

WPRN SECTOR 0

WSRF WELL TIME

WSRF GRID TIME

WSRF SECTOR 1

WPRN ITER 1

\*\*NONE

OUTPRN WELL ALL

OUTPRN GRID NONE

OUTPRN RES NONE

OUTPRN ITER NEWTON

OUTSRF GRID HEATCAP MASDENO OBHLOSS PRES SO SW TEMP VISO W X Y Z

OUTSRF SPECIAL SOR 'Injector' 'Producer' CUM

OUTSRF WELL COMPONENT ALL

OUTSRF WELL LAYER ALL

\*XDR \*ON

```

*MAXERROR 20

*SR2PREC *DOUBLE

**$ Distance units: m

RESULTS XOFFSET      0.0000

RESULTS YOFFSET      -750.0000

RESULTS ROTATION      0.0000 **$ (DEGREES)

RESULTS AXES-DIRECTIONS 1.0 -1.0 1.0

**$
*****
***

**$ Definition of fundamental cartesian grid

**$
*****
***

GRID VARI 100 1 100

KDIR UP

DI IVAR

100*1

DJ JVAR

100

DK ALL

10000*1

DTOP

100*1008

**$

**$ Property: NULL Blocks Max: 1 Min: 1

```



\*\*\$ 0 = null block, 1 = active block

NULL CON 1

\*\*\$ Property: Porosity Max: 0.343385 Min: 0.013787

POR ALL

0.29905 0.300229 0.311413 0.30965 0.302267 0.30629 0.31445 0.31206  
 0.325535 0.32043 0.3195 0.32504 0.323414 0.31891 0.32325 0.32214 0.32274  
 0.319551 0.33043 0.332142 0.32427 0.325562 0.319732 0.321768 0.326062  
 0.320678 0.31876 0.32395 0.328404 0.326102 0.31786 0.32575 0.32245  
 0.31954 0.31973 0.325784 0.319854 0.315118 0.325899 0.3169 0.316575  
 0.316368 0.315615 0.31669 0.328236 0.315684 0.31002 0.312843

\*\*\$ Property: Permeability I (md) Max: 9358.01 Min: 0.003077

PERMI ALL

2528.782 2096.906 3054.12 2623.275 3276.257 3401.421 3888.869 3716.816  
 3829.365 3139.361 3768.038 4397.972 3791.172 5246.905 4656.347 4186.623  
 3646.789 3678.011 3575.778 4105.409 5038.104 4369.264 4885.554 4958.98  
 5443.851 6708.16 8035.436 5668.649 5997.21 4620.642 4096.427 5402.628  
 5051.392 3961.439 4235.099 3403.987 4257.354 3221.891 3076.744 3401.531  
 3061.543 4240.431 3593.761 4898.875 5320.883 4806.932 5682.515

PERMJ EQUALSI

PERMK EQUALSI \* 0.5

\*\*\$

\*\*\$ Property: Pinchout Array Max: 1 Min: 1

\*\*\$ 0 = pinched block, 1 = active block

PINCHOUTARRAY CON 1

```

END-GRID
ROCKTYPE 1
  PRPOR 100.
  CPOR 7.E-06
  ROCKCP 2.347E+06
  THCONR 6.6E+05
  THCONW 5.35E+04
  THCONO 1.15E+04
  THCONG 140.
THCONMIX SIMPLE
  HLOSST 7.
  HLOSSTDIF 0.1
**$ Model and number of components
MODEL 2 2 2 1
COMPNAME 'WATER' 'OIL'
CMM
0 0.5
PCRIT
0 0
TCRIT
0 0
KV1
0 0
KV4
0 0

```

KV5

0 0

CPG1

00 841

CPL1

0 1000

HVAPR

0 1346

MOLDEN

0 2020

CP

0 6.84E-7

CT1

0 7.85E-4

CT2

0 0

\*\*nc6 effective viscosities based on Shu correlation

\*\* Temp

VISCTABLE

\*\*\$ temp

6.9 0 8000000

8 0 6527000

10 0 5000000

20 0 1345000

40 0 75686

60	0	8186
80	0	1510
100	0	409.5
120	0	147.5
140	0	65.6
160	0	34.3
180	0	20.3
200	0	13.2
220	0	9.3
240	0	6.9
260	0	5.4
280	0	4.4

\*\* ===== ROCK-FLUID DATA =====

\*ROCKFLUID

RPT 1 LININTERP WATWET

\*\* SW KRW KROW

\*\* ----- 0.050000 0.000000 0.972500 0.000000

SWT

\*\*\$ Sw krw krow Pcow

0.100000	0	0.961400	0.000000
0.150000	0.000354	0.949900	0.000000
0.200000	0.001294	0.937700	0.000000
0.250000	0.003249	0.924800	0.000000
0.300000	0.006636	0.911200	0.000000
0.350000	0.011892	0.896700	0.000000

0.400000	0.019476	0.881300	0.000000
0.450000	0.029859	0.864600	0.000000
0.500000	0.043528	0.846600	0.000000
0.550000	0.060980	0.826900	0.000000
0.600000	0.082726	0.805100	0.000000
0.650000	0.109287	0.780700	0.000000
0.700000	0.141191	0.752700	0.000000
0.750000	0.178977	0.719900	0.000000
0.800000	0.223193	0.679600	0.000000
0.850000	0.274392	0.626700	0.000000
0.900000	0.333138	0.545600	0.000000
0.950000	0.400000	0.000000	0.000000

\*\* SL KRG KROG

\*\* ----- 0.150000 0.570000 0.000000 0.000000

SLT

**\$	Sl	krq	krog	Pcog
0.200000	0.464000	0	0.000000	
0.250000	0.372500	0.043000	0.000000	
0.300000	0.294300	0.079000	0.000000	
0.350000	0.228300	0.121600	0.000000	
0.400000	0.173300	0.169900	0.000000	
0.450000	0.128200	0.223300	0.000000	
0.500000	0.092000	0.281400	0.000000	
0.550000	0.063600	0.343800	0.000000	
0.600000	0.041900	0.410300	0.000000	

```

0.650000 0.025900 0.480500 0.000000
0.700000 0.014800 0.554400 0.000000
0.750000 0.007500 0.631700 0.000000
0.800000 0.003200 0.712300 0.000000
0.850000 0.001000 0.796000 0.000000
0.900000 0.000200 0.882800 0.000000
0.950000 0.000000 0.961400 0.000000
**0.950000 0.000000 0.972500 0.000000
** Temp  Swr  Sorw  Sorg  Krwro  Krocw  Sgr
KRTEMTAB SWR SORW SORG KRWIRO KROCW SGR
**$  TEMP  SWR  SORW  SORG  KRWIRO  KROCW  SGR
      7.  0.15  0.5  0.4  0.4  1.  0
      226.  0.15  0.05  0.05  1.  1.  0
** ===== INITIAL CONDITIONS =====
*INITIAL
*VERTICAL *OFF
INITREGION 1
**$
**$ Property: Gas Saturation  Max: 0  Min: 0
SG CON      0
**$
**$ Property: Pressure (kPa)  Max: 1090  Min: 1090
PRES CON    1090
**$
**$ Property: Temperature (C)  Max: 7  Min: 7

```

```

TEMP CON      7

**$ Property: Oil Mole Fraction(OIL)  Max: 0.97  Min: 0.97

MFRAC_OIL 'OIL' CON      0.97

**$

**$ Property: Gas Mole Fraction(WATER)  Max: 0  Min: 0

MFRAC_GAS 'WATER' CON      0

**$

**$ Property: Water Mole Fraction(WATER)  Max: 1  Min: 1

MFRAC_WAT 'WATER' CON      1

*NUMERICAL

DTMAX 10.0

**NORM PRESS 400 SATUR 0.2 TEMP 30 Y 0.2 X 0.2

** tight

**CONVERGE TOTRES TIGHTER

*ITERMAX 100

UPSTREAM KLEVEL

**NORTH 75

RUN

** Heat up around the wells

DATE 2008 06 01.

DTWELL 0.01

**$

WELL 'Producer'

**OPERATE MIN STEAMTRAP 10. CONT REPEAT

PRODUCER 'Producer'

```

```

OPERATE MAX STL 100. CONT REPEAT
OPERATE MIN BHP 500. CONT REPEAT
OPERATE MAX STEAM 0.5 CONT REPEAT
**$      rad geofac wfrac skin
GEOMETRY J 0.11 0.229 1. 0.
PERF GEO 'Producer'
**$ UBA   ff Status Connection
      50 1 3 1. OPEN  FLOW-TO 'SURFACE'
**$
WELL 'Injector'
INJECTOR MOBWEIGHT EXPLICIT 'Injector'
INCOMP WATER 1. 0.
TINJW 224.
QUAL 0.9
OPERATE MAX BHP 2500. CONT REPEAT
OPERATE MAX STW 75. CONT REPEAT
**$      rad geofac wfrac skin
GEOMETRY J 0.11 0.229 1. 0.
PERF GEO 'Injector'
**$ UBA   ff Status Connection
      50 1 8 1. OPEN  FLOW-FROM 'SURFACE'
**SHUTIN 'Producer'
*SHUTIN 'Injector'
**$
**$ Property: Prop. Heat Transfer Coeff. (J/(day*C))  Max: 3e+010  Min: 3e+010

```



UHTR IJK

50:50 1:1 8:8 3E+011

50:50 1:1 3:3 3E+011

\*\*\$

\*\*\$ Property: Temp. Setpoint for Controller (C) Max: 180 Min: 180

TMPSET IJK

50:50 1:1 8:8 180

50:50 1:1 3:3 180

DATE 2008 07 01.

DATE 2008 08 01.

DATE 2008 09 01.

\*\* Turn off heaters

\*\* Start the steam

\*\*\$

\*\*\$ Property: Prop. Heat Transfer Coeff. (J/(day\*C)) Max: 0 Min: 0

UHTR IJK

50:50 1:1 8:8 0

50:50 1:1 3:3 0

OPEN 'Injector'

\*\*OPEN 'Producer'

DATE 2008 10 01.

DATE 2008 11 01.

DATE 2008 12 01.

DATE 2009 01 01.

DTWELL 0.01

DTMAX 10.0

DATE 2009 02 01.

DATE 2009 03 01.

DATE 2009 04 01.

DATE 2009 05 01.

DATE 2009 06 01.

DATE 2009 07 01.

DATE 2009 08 01.

DATE 2009 09 01.

DATE 2009 10 01.

DATE 2009 11 01.

DATE 2009 12 01.

DATE 2010 01 01.

DATE 2010 03 01.

DATE 2010 05 01.

DATE 2010 07 01.

DATE 2010 09 01.

DATE 2010 11 01.

DATE 2011 01 01.

DATE 2011 03 01.

DATE 2011 05 01.

DATE 2011 07 01.

DATE 2011 09 01.

DATE 2011 11 01.

DATE 2012 01 01.

DATE 2012 03 01.

DATE 2012 05 01.

DATE 2012 07 01.

DATE 2012 09 01.

DATE 2012 11 01.

DATE 2013 01 01.

DATE 2013 03 01.

DATE 2013 05 01.

DATE 2013 07 01.

DATE 2013 09 01.

DATE 2013 11 01.

DATE 2014 01 01.

DATE 2014 03 01.

DATE 2014 05 01.

DATE 2014 07 01.

DATE 2014 09 01.

DATE 2014 11 01.

DATE 2015 01 01.

DATE 2015 03 01.

DATE 2015 05 01.

DATE 2015 07 01.

DATE 2015 09 01.

DATE 2015 11 01.

DATE 2016 01 01.

DATE 2016 03 01.

DATE 2016 05 01.

DATE 2016 07 01.

DATE 2016 09 01.

DATE 2016 11 01.

DATE 2017 01 01.

DATE 2017 03 01.

DATE 2017 05 01.

DATE 2017 07 01.

DATE 2017 09 01.

DATE 2017 11 01.

DATE 2018 01 01.

DATE 2018 03 01.

DATE 2018 05 01.

DATE 2018 07 01.

STOP